AFIT/GE/ENG/92D-22

REMOTE SENSING OF TURBULENCE AND TRANSVERSE ATMOSPHERIC WIND PROFILES USING OPTICAL REFERENCE SOURCES

THESIS

Steven Carl Koeffler
Captain, USAF

AFIT/GE/ENG/92D-22

AFIT/GE/ENG/92D-22

REMOTE SENSING OF TURBULENCE AND TRANSVERSE ATMOSPHERIC WIND PROFILES USING OPTICAL REFERENCE SOURCES

THESIS

Presented to the Faculty of the School of Engineering

of the Air Force Institute of Technology

Air University

In Partial Fulfillment of the

Requirements for the Degree of

Master of Science in Electrical Engineering

Steven Carl Koeffler, B.S.E.E.

Captain, USAF

December 1992

Acknowledgements

I would like to take this opportunity to thank my thesis advisor, Dr. Byron Welsh, for his invaluable guidance during this thesis effort. His sincere interest in this research and gracious assistance were greatly appreciated. I also thank my committee members, Major Steve Rogers and Captain Dennis Ruck, for their helpful comments. Finally, heartfelt thanks to my family, especially my wife, Cheryl, and children, Jason and Melanie, for being a constant source of joy in my life.

Table of Contents

List of Figures

AFIT/GE/ENG/92D-22

Abstract

This thesis examines a remote sensing technique for measuring the atmospheric structure constant (C_n^2) and the transverse atmospheric wind velocity ($\vec{V}$) as a function of altitude by performing temporal and spatial correlations of band pass filtered wave front slope sensor measurements. Two point sources are used to illuminate two pairs of co-located wave front slope sensors. The sources and sensors are arranged to give rise to crossed optical paths. For each pair of wave front slope sensors, the output of the larger sensor is subtracted from the output of the smaller sensor. This band pass filters the smaller sensor's output. The filtered outputs are then correlated. It is shown that the spatial correlation is related to the structure constant by an integral containing C_n^2 and a path weighting function. The path weighting function is sharply peaked at the intersection altitude and decays rapidly to zero. It is also shown that the temporal correlation is related to $\vec{V}$ through an integral containing $\vec{V}$, C_n^2, and a wind path weighting function which is sharply peaked at the intersection altitude and decays rapidly to zero. The vertical resolution of each path weighting function is calculated. Also, signal-to-noise ratios are calculated using generally accepted models for the structure constant and atmospheric wind profiles.

REMOTE SENSING OF TURBULENCE AND TRANSVERSE ATMOSPHERIC WIND PROFILES USING OPTICAL REFERENCE SOURCES

I. Introduction

1.1 Atmospheric Turbulence and Winds

Lightwaves traveling from space to Earth are distorted when they pass through the Earth's atmosphere. This distortion gives rise to the well known twinkling (properly termed scintillation) of stars, and is the limiting factor in astronomers' efforts to obtain high resolution images of celestial objects. In theory, the resolution achievable by an imaging system, called the diffraction limited resolution, is proportional to the size of the system's aperture (5). Yet atmospheric distortion reduces the resolving power of large aperture telescopes to that of a telescope with a 10 to 20 cm aperture (14).

A growing field of study called adaptive optics attempts to restore the telescope's theoretical resolution by compensating for the atmospheric distortions. Generally, adaptive optics systems incorporate deformable mirrors to remove wave front distortions (8). A control system senses the incoming wave front distortion and sends commands to the mirror. The mirror assumes a shape that is the conjugate of the wave front distortions. Thus, distortions are removed when the wavefront reflects off of the mirror.

The efficient design and operation of adaptive optics systems require characterization of the distribution of turbulence along the wave front's propagation path. This distribution can be determined from a parameter called the atmospheric structure constant. The structure constant is discussed further in the next section.

Along similar lines, meteorologists and aviators are interested in knowing the atmospheric wind velocity as a function of altitude. Such information helps increase weather forecasting accuracy and aviation safety (13). Additionally, knowledge of the vertical wind profile is used in the determination of control loop bandwidth for adaptive optics systems.

In both cases, measuring the winds at specific locations within the atmosphere is important and can be accomplished by determining the wind profile along an optical path which passes through the points of interest.

1.2 Turbulence and Wind Characterization

Differential heating of the Earth causes atmospheric turbulence. This heating generates pockets of air, called eddies, with varying temperatures and pressures, giving rise to varying indexes of refraction. The index of refraction is denoted by n, and is a function of both time and position within the atmosphere. Thus, the fluctuation of n is a temporal and spatial random process (25). Generally, the temporal fluctuations are assumed to be due to atmospheric winds, an assumption known as Taylor's hypothesis (19). Taylor's hypothesis essentially states that the pockets of air do not decay as they are blown across an optical system's line of sight.

The strength of the turbulence is characterized by the spatial power spectral density (psd) of the fluctuations of the index of refraction. The psd is denoted by $\Phi_n(\vec{K})$, where $\vec{K}$ is the spatial wavenumber vector. The magnitude of $\Phi_n(\vec{K})$ is proportional to the atmospheric structure constant, C_n^2. In many optical propagation geometries, the structure constant is a function of position along the optical path. This is particularly true for vertical propagation through the atmosphere. Due to its relationship with the psd, C_n^2 is used as a measure of the strength of the turbulence along the optical path.

As alluded to above, the temporal fluctuations of n are assumed to be due to atmospheric winds. Wind has direction as well as magnitude, and therefore is denoted by the vector $\vec{V}$. If the time it takes for an eddy of known size to blow across the optical path can be measured, then the wind velocity can be determined. Note, however, that only the component of the wind perpendicular to the optical path can be measured in this manner. As will be discussed later, the temporal fluctuations of n can be used to derive information about the transverse wind velocity as a function of position along the optical path.

1.3 *Measurement of C_n^2 and $\vec{V}$*

No instrument can measure C_n^2 directly. Likewise, although anenometers can measure $\vec{V}$, such devices cannot be placed at all the points necessary to obtain a good profile of $\vec{V}$ along an optical path. The usual remote sensing approach is to measure some effect of the atmosphere on a reference beam of light and relate the measured effect to C_n^2 or $\vec{V}$. Numerous techniques have been used to measure C_n^2 and $\vec{V}$ (1, 3, 10, 21). Such techniques have become more practical with recent advances in the generation of artificial guide stars for use as reference sources (4). Most measurement techniques have exploited the spatial or temporal cross-correlation properties of the intensity of the optical field. The research presented here takes a different approach, one based upon the cross-correlation properties of the optical field's phase.

1.4 *Approach*

The basic measurement geometry to be examined is shown in Figure 1.1. Two wave front sensors separated by $\Delta\vec{x}$ are present in the aperture plane of an optical system. The wave front sensors are illuminated by two point sources, p_1 and p_2, which are separated by $\Delta\vec{p}$. The geometry is arranged to give rise to crossed optical paths. The wave front distortions on the two reference beams caused by the turbulence at the intersection point will be highly correlated, while distortions caused by turbulence elsewhere along the paths will not be correlated. This fact is used to determine C_n^2. The intersection altitude can be varied by changing the source or sensor separations, and in this way a vertical profile of the turbulence strength can be obtained.

Additionally, time-lagged correlations of the wave front distortions will be well correlated when the lag equals the time necessary for an eddy to traverse the distance separating the two beams. Thus, the time-lagged correlations of the wave front distortions on the reference beams can be used to determine $\vec{V}$.

Rejack examined the measurement geometry depicted in Figure 1.1 for use in measuring C_n^2 (17). He demonstrated that C_n^2 is related to the correlation of the two wave

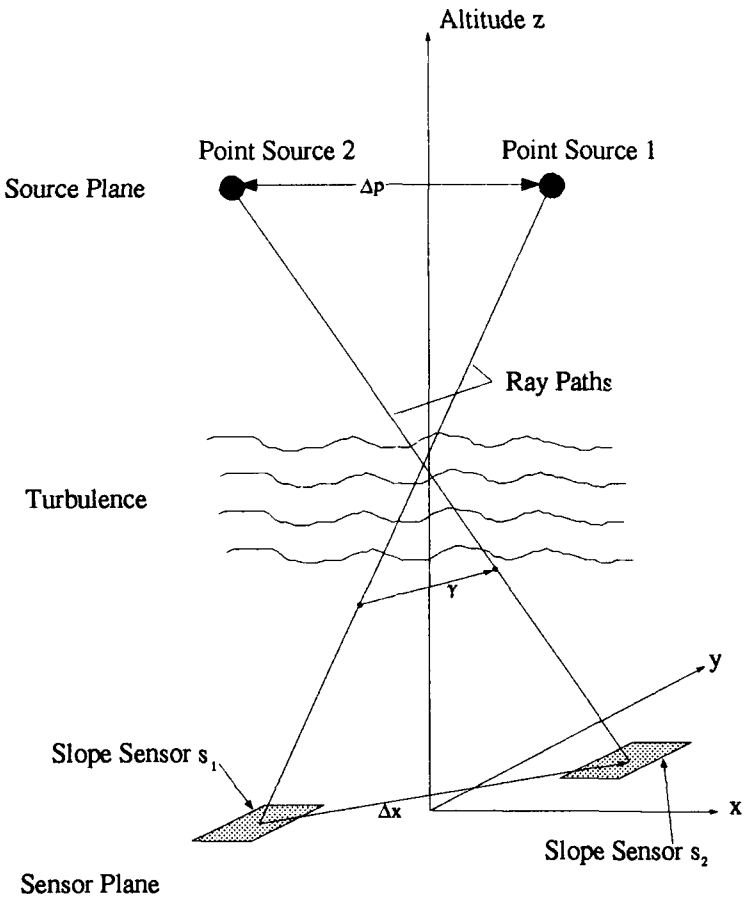

Figure 1.1. Basic Measurement Geometry (17)

front sensor measurements by

$$\begin{aligned} \langle C_s \rangle &= \langle s_1(t) s_2(t) \rangle \\ &= \int \mathrm{d}z' \; C_n^2(z') w_C(z') \end{aligned} \tag{1.1}$$

where $\langle \cdot \rangle$ represents the ensemble average operator, $s_n(t)$ is the output of wave front sensor n at time t, z' is the position along the z axis, and $w_C(z')$ is called the path weighting function. Rejack then improved the system's resolution performance by linearly combining measurements from two sets of wave front sensors.

This thesis investigates the crossed beam measurement geometry of Figure 1.1, but

examines a new method for combining the measurements from the two sets of wave front sensors. There are three basic objectives of this research. The first objective is to derive the new method's C_n^2 path weighting function $w_C(z)$ and evaluate its characteristics. The second objective is to extend the new technique to the remote sensing of transverse atmospheric winds. It is shown that the derivative of the time-lagged correlation of the measurements can be related to $\vec{V}(z)$ by (21)

$$\begin{aligned}\frac{\partial}{\partial\tau}\langle C_s(\tau)\rangle|_{\tau=0} &= \frac{\partial}{\partial\tau}\langle s_1(t)s_2(t+\tau)\rangle|_{\tau=0} \\ &= \int \mathrm{d}z' C_n^2(z')\vec{V}(z')\cdot\vec{w}_V(z') \qquad (1.2)\end{aligned}$$

where $\frac{\partial}{\partial\tau}\langle C_s\rangle$ is the partial derivative with respect to τ of the time lagged correlation of the sensor measurements, s_n is the band pass filtered output of wave front slope sensor n, τ is the amount of time lag, $\vec{V}(z')$ is the wind velocity at the altitude z', and $\vec{w}_V(z')$ is called the wind path weighting function. The wind path weighting function is derived and its characteristics examined. Finally, the third objective is to develop signal-to-noise ratio expressions which will help determine how many measurements are needed to make an accurate estimate of the quantity of interest. Following the fulfillment of these three objectives, an example is presented to demonstrate the C_n^2 and wind path weighting function shapes obtained when a practical measurement geometry is used. Finally, some practical implementation issues and their impact on system performance are discussed.

1.5 Overview

Chapter II contains a review of atmospheric turbulence and wind sensing techniques. Chapter III contains the methodology used in conducting this research, including limiting assumptions. Chapter IV consists of a signal-to-noise ratio analysis of the measurement technique proposed in this thesis. Chapter V presents an example measurement geometry and discusses some implementation issues which affect system performance. Finally, chapter VI provides conclusions and some suggestions for further research.

II. Background

2.1 Theory and Definitions

2.1.1 Turbulence Atmospheric turbulence is the result of differential heating of the Earth. This differential heating causes the formation of various sized pockets of air, called eddies. The atmosphere consists of a random distribution of these eddies, each with a different temperature and pressure. The index of refraction, n, is defined as the ratio of the speed of light within a medium to the speed of light within a vacuum (7). The speed of light within the atmosphere, and therefore the index of refraction, is a function of temperature, humidity, and pressure. Thus, as different portions of an optical wave front pass through different eddies, the wave front sections travel at different speeds. This speed differential distorts the propagating wave front.

2.1.2 Power Spectral Density of n The fluctuation of the index of refraction within the atmosphere is characterized by a wide sense stationary random process and therefore has an associated power spectral density (psd), denoted as $\Phi_n(\vec{K})$, where $\vec{K}$ is the wavenumber vector and is a measure of the number of eddies of size $L = \frac{2\pi}{|\vec{K}|}$ (6). For isotropic turbulence, that is, turbulence for which the autocorrelation of the fluctuation of n has spherical symmetry, $\vec{K}$ is replaced by $K = |\vec{K}|$.

In a classic work, Kolmogorov divided $\Phi_n(\vec{K})$ into three separate regions based upon eddy size (9). The first region contains eddies of size greater than L_0, where L_0 is called the outer scale size. The shape of $\Phi_n(\vec{K})$ in this region is not predictable by his theory. The second region, known as the inertial subrange, contains eddies between the sizes L_0 and ℓ_0, where ℓ_0 is called the inner scale size. The form of $\Phi_n(\vec{K})$ within the inertial subrange can be predicted by the theory of turbulent flow, and is given as

$$\Phi_n(K) = 0.033 C_n^2 K^{\frac{-11}{3}} \tag{2.1}$$

where C_n^2 is the structure constant. The third and final region contains eddies smaller than ℓ_o. The psd in this region decays rapidly towards zero. When modeling atmospheric

turbulence effects on optical systems, the inertial subrange is generally the only region of concern.

2.1.3 Index of Refraction Structure Function The structure function of n is commonly used to characterize the second order moment of n. The structure function is defined as (6)

$$D_n(\vec{r_1}, \vec{r_2}) = \langle [n(\vec{r_1}) - n(\vec{r_2})]^2 \rangle \tag{2.2}$$

where $\vec{r}_1$ and $\vec{r}_2$ are position vectors and $\langle \cdot \rangle$ is the expected value operator. If the turbulence is homogeneous, meaning it is spatially wide sense stationary, as well as isotropic, and if it has a psd given by the Kolmogorov expression of equation 2.1, then the structure function becomes (6)

$$D_n(r) = C_n^2 r^{\frac{2}{3}} \tag{2.3}$$

where $r = |\vec{r_1} - \vec{r_2}|$.

2.2 Turbulence and Wind Profile Models

Now that the atmospheric structure constant, C_n^2, has been related to turbulence strength through use of the structure function, some information about C_n^2 is needed. The atmospheric structure constant cannot be measured directly. However, experimental data has been employed to derive and validate some models for the vertical profile of C_n^2. One of the models most often used is called the Hufnagel-Valley turbulence model and has the form (16)

$$C_n^2(z') = 5.94 \times 10^{-53} \left(\frac{w}{27}\right)^2 z'^{10} \exp\left(\frac{-z'}{1000}\right) + 2.7 \times 10^{-16} \exp\left(\frac{-z'}{1500}\right) + A \exp\left(\frac{-z'}{100}\right) \tag{2.4}$$

where z' is altitude in meters, w is the average wind speed in m/sec, and A is a free parameter adjusted to yield the desired profile shape. The units of C_n^2 are $\mathrm{m}^{\frac{-2}{3}}$. Equation 2.4 is plotted in Figure 2.1 for $w = 27$ and $A = 10^{-14}$ if $z' > 11000$, 0 if $z' < 11000$.

Unlike C_n^2, the wind velocity can be measured directly, and models of the wind velocity profile have been created based upon empirical data. The wind velocity profile

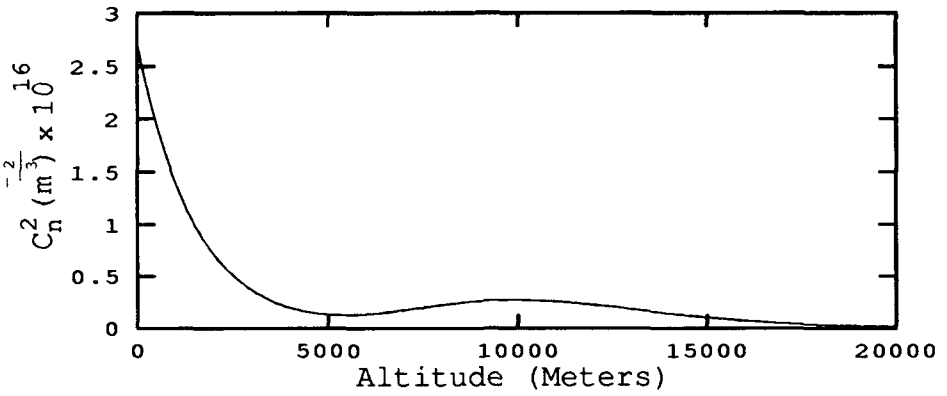

Figure 2.1. Hufnagel-Valley C_n^2 Profile (16)

most often used in turbulence problems is the Bufton model given by

$$V(z') = v_g + 30 \exp\left[-\left(\frac{z' - 9400}{4800}\right)^2\right] \tag{2.5}$$

where z' is altitude in meters, and v_g is ground wind speed in m/sec. Equation 2.5 is plotted in Figure 2.2 for $v_g = 5$ m/sec.

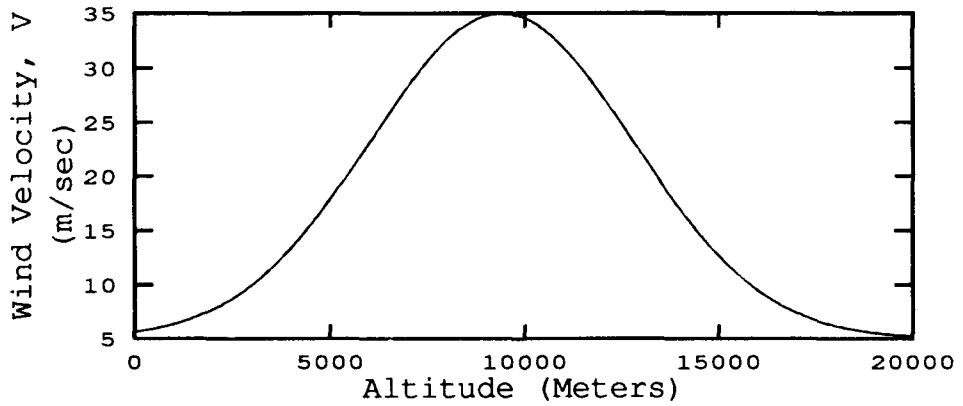

Figure 2.2. Bufton Wind Profile (16)

2.3 *Evaluation of C_n^2 and $\vec{V}$*

The technique most often used to remotely sense C_n^2 and $\vec{V}$ is to extract these values from the correlations of optical scintillations. The scintillation data is obtained by measuring the irradiance intensity produced by a source located within or above the atmosphere. Fried, in 1969, was one of the first to examine the relationship between the spatial covariance of intensity and C_n^2 (3). By including temporal effects, Fried was also able to relate the temporal covariance of the optical scintillations to $\vec{V}$. Because his work is the basis for many similar measurement techniques, Fried's approach is summarized in the next section.

2.3.1 Correlations of Irradiance Measurements Fried proposed measuring the intensities incident on two telescopes using the geometry shown in Figure 2.3. The telescopes have highly restricted fields of view and receive a monochromatic signal from a stellar source. The intensities measured at time t are denoted $i_1(t)$ and $i_2(t)$. The logarithmic

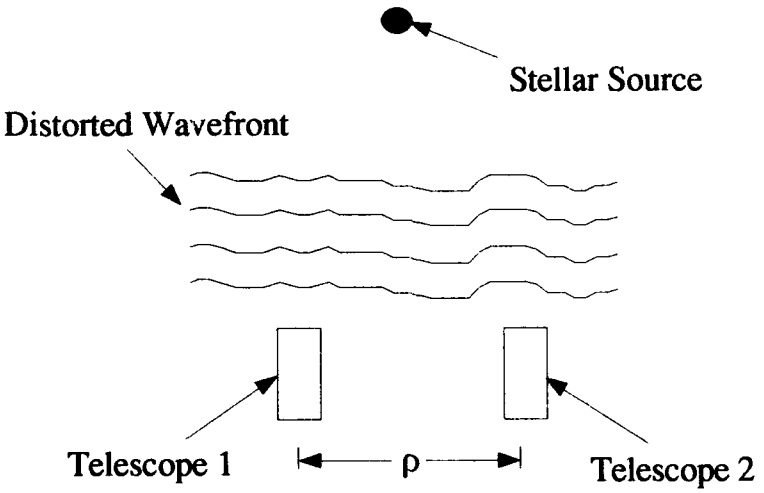

Figure 2.3. Fried's Measurement Geometry (3)

amplitude, $l_m(t)$, is calculated using

$$l_m(t) = \frac{1}{2} \ln \left[\frac{i_m(t)}{\langle i_m \rangle} \right] \tag{2.6}$$

where $\langle i_m \rangle$ is the average value of $i_m(t)$. The spatial-temporal logarithmic amplitude covariance is then given by

$$C_l(\rho, \tau) = \langle [l_1(t) - \langle l_1 \rangle][l_2(t+\tau) - \langle l_2 \rangle] \rangle \tag{2.7}$$

where $l_1(t)$ and $l_2(t)$ are the log-amplitudes as given in equation 2.6, and ρ is the separation of the two telescopes.

Fried suppresses the time dependence by setting $\tau = 0$ and applies Tatarski's result that (18)

$$C_l(\rho) = 0.652k^2 \int_0^L \mathrm{d}z\, C_n^2(z) \int_0^\infty \mathrm{d}\sigma\, \sigma^{\frac{-8}{3}} J_0(\sigma\rho) \left(1 - \cos\frac{\sigma^2 z}{k}\right) \tag{2.8}$$

where $k = \frac{2\pi}{\lambda}$, z is the distance from the telescope to a point along the propagation path, L is the distance from the receiver to the source (in this case infinity), and J_0 is the zero-order Bessel function.

Through a series of integrations, Fried reduces equation 2.8 to

$$C_l(\rho) = k^{\frac{7}{6}} \int_0^\infty \mathrm{d}z\, z^{\frac{5}{6}} C_n^2(z) \mathcal{F}\left(\frac{k\rho^2}{4z}\right) \tag{2.9}$$

where $\mathcal{F}\left(\frac{k\rho^2}{4z}\right)$ groups all of the terms that depend upon $\left(\frac{k\rho^2}{4z}\right)$. Fried tabulates $\mathcal{F}\left(\frac{k\rho^2}{4z}\right)$ for a few values. Thus, Fried has been successful in relating C_n^2 to the measured irradiance correlations through a linear integral equation.

Fried next includes the time dependence of the intensity fluctuations to relate the temporal covariance of the log-amplitudes to atmospheric wind velocities. Thus, equation 2.8 becomes

$$C_l(\vec{\rho}, \tau) = 0.652k^2 \int_0^\infty \mathrm{d}z\, C_n^2(z) \int_0^\infty \mathrm{d}\sigma\, \sigma^{\frac{-8}{3}} J_0(\sigma|\vec{\rho} - \vec{V}(z)\tau|) \left(1 - \cos\frac{\sigma^2 z}{k}\right) \tag{2.10}$$

where $\vec{V}(z)$ is the wind velocity at altitude z.

Accordingly, equation 2.9 becomes

$$C_l(\vec{\rho}, \tau) = k^{\frac{7}{6}} \int_0^\infty \mathrm{d}z\, z^{\frac{5}{6}} C_n^2(z) \mathcal{F}\left(\frac{k|\vec{\rho} - \vec{V(z)}\tau|^2}{4z}\right) \tag{2.11}$$

As can be seen, knowledge of both $C_l(\vec{\rho},\tau)$ and $C_n^2(z)$ is necessary to solve for $\vec{V}(z)$. Even then, determining $\vec{V}(z)$ requires solving a nonlinear integral equation, a difficult if not impossible task. However, Fried states that numerical techniques will yield an approximate solution, although the procedure requires an initial estimate of $\vec{V}(z)$. An interesting and important point is that no data beyond that already obtained to determine $C_n^2(z)$ is necessary to determine $\vec{V}(z)$. However, additional processing is required.

2.3.2 Crossed Beam Technique In 1974, Wang *et al.* (21) used a crossed beam technique to profile both $C_n^2(z)$ and $\vec{V}(z)$. In 1991, Beland and Krause-Polstorff examined the same crossed beam technique, but used range gated lidar pulses to generate optical sources within the atmosphere, allowing vertical profiling of C_n^2 (1). Wang's analysis is based upon the phase screen approach of Lee and Harp (11). The measurement geometry studied by Wang *et al.* is shown in Figure 2.4.

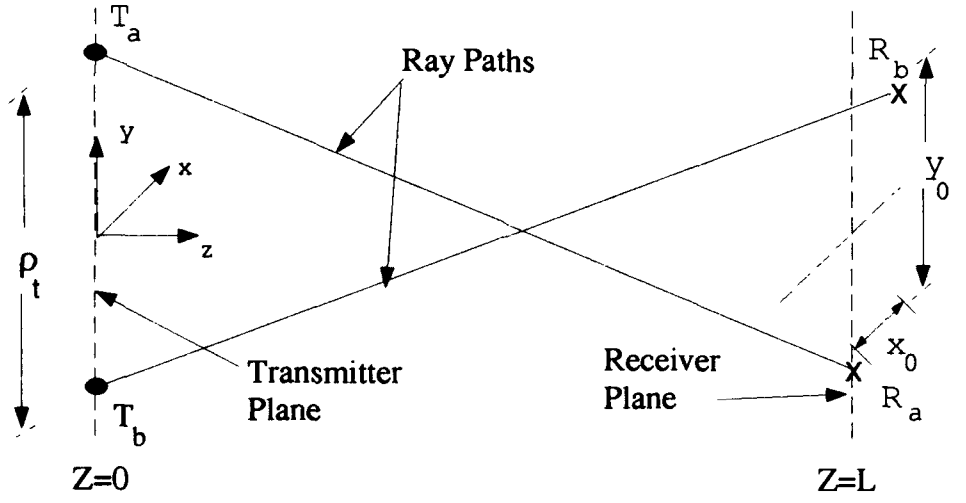

Figure 2.4. Wang *et al.* Measurement Geometry (21)

The measurement geometry was formed by two laser sources, T_a and T_b, separated by ρ_t, and two receivers, R_a and R_b, separated by x_0, y_0. The transmitters and receivers were arranged in such a way that the optical paths from T_a to R_a and from T_b to R_b intersected. The z axis was perpendicular to the planes containing the transmitters and receivers.

Given this measurement geometry, Wang *et al.* found that the amplitude covariance function is given by

$$C_{ab} = \int \mathrm{d}z' C_n^2(z') W_{ab}(z') \tag{2.12}$$

where C_{ab} is the covariance of the intensities measured by R_a and R_b, and W_{ab} is called the C_n^2 path weighting function and is given by

$$W_{ab}(z') = 0.132\pi^2 k^2 \int_0^\infty \mathrm{d}K K^{\frac{-8}{3}} \sin^2\left[\frac{K^2 s(L-z')}{2kL}\right] J_0\left[K\left|\frac{(x_0-y_0)z'}{L} + \vec{\rho}_t\left(1-\frac{z'}{L}\right)\right|\right] \tag{2.13}$$

where L is the distance from the transmitter plane to the receiver plane, and z' is the distance from the transmitter plane to some point along the z axis.

Wang and his colleagues found a similar expression relating the amplitude covariance function to the transverse wind velocity. They accomplished this by inserting the time dependence into the intensity covariance, and then defining a new function, M_{ab}, to be

$$\begin{aligned} M_{ab} &= \left.\frac{\partial C_{ab}(\vec{\rho}_t, \tau)}{\partial \tau}\right|_{\tau=0} \\ &= \int_0^L \mathrm{d}z'\, C_n^2(z') \vec{V}(z') \cdot \vec{W}'_{ab}(z') \end{aligned} \tag{2.14}$$

where $\vec{W}'_{ab}(z')$ is called the wind path weighting function and is expressed as

$$\vec{W}'_{ab}(z') = 0.132\pi^2 k^2 \int_0^\infty \mathrm{d}K K^{\frac{-5}{3}} \sin^2\left[\frac{K^2 z'(L-z')}{2kL}\right] J_1(Kr)\hat{r} \tag{2.15}$$

The function J_1 is the first order Bessel function, and $\hat{r}$ is a unit vector along $\vec{r}$ where $\vec{r}$ is expressed as

$$\vec{r} = (\vec{x}_0 - \vec{y}_0)\frac{z'}{L} + \vec{\rho}_t\left(1-\frac{z'}{L}\right) \tag{2.16}$$

An important aspect of this technique is that it does not measure the wind component parallel to the z axis. This is because an eddy moving parallel to the z axis would intercept both beams at the same time, thus having no effect on the slope of the amplitude covariance at zero time lag.

2.3.3 Correlations of Phase Measurements Rather than measuring intensity correlations, Welsh (22) has proposed using the spatial correlation properties of the optical field's phase to profile $C_n^2(z)$. Welsh examines a crossed beam measurement geometry using artificial guide stars as the atmospheric sources and wave front slope sensors as the receivers. This geometry is shown in Figure 2.5. Welsh shows that the correlation of the

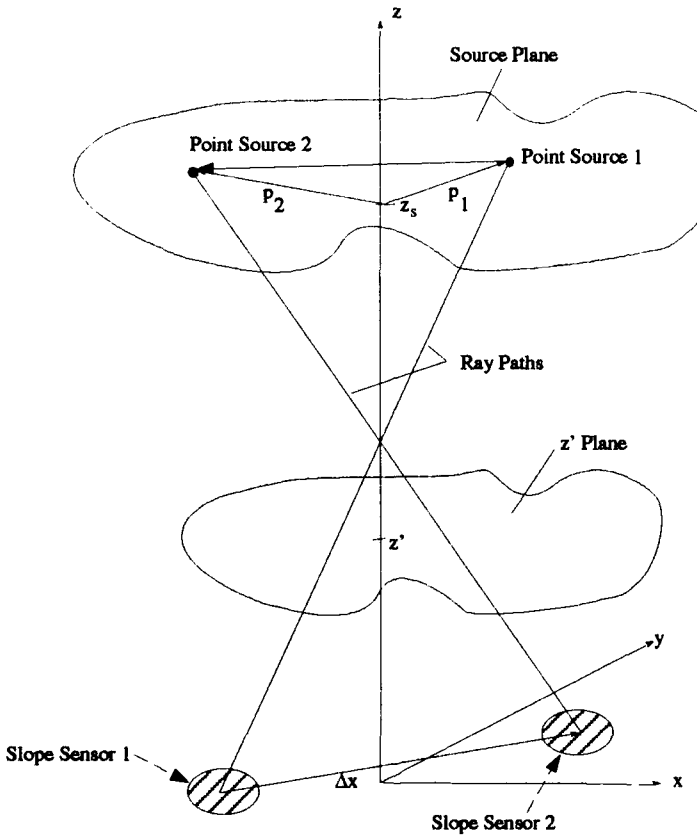

Figure 2.5. Measurement Geometry Examined by Welsh (22)

slope sensor outputs is given by

$$\langle C_\phi \rangle = \int_0^{z_s} \mathrm{d}z' \, C_n^2(z') w_C(z') \tag{2.17}$$

where the weighting function $w_C(z')$ depends upon the source altitude, z_s, source separation, $\vec{p}_1 - \vec{p}_2$, receiver separation $\Delta\vec{x}$, PSD of the refractive index, and the sensor aperture weighting functions. He also includes a term to account for any linear post processing that may be performed on the wave front sensor data.

Welsh, after assuming a Kolmogorov spectrum for Φ_n, evaluated the path weighting function numerically for two cases. First, the weighting function is evaluated for the case correlating the direct phase measurements of the wave front sensors. In the second case, the wave front sensor phase measurements are band pass filtered before being correlated. Welsh found that the band pass filtering provided a more sharply peaked weighting function, which translates into better altitude resolution. Such a result is not surprising. The low frequency phase effects remain well correlated further from the intersection point because these effects are caused by large eddies. Band pass filtering removes these low frequencies and thus helps the phase correlation function to decay more quickly, improving altitude resolution.

Rejack (17) further expanded upon Welsh's technique. Whereas Welsh assumed the wave front sensors actually measured the wave front phase, Rejack considered a more realistic wave front sensor in which the overall wave front slope is measured. Rejack began by deriving an expression for the path weighting function $w_C(z)$ that depended only upon the measurement geometry. In accomplishing this, he assumed a Kolmogorov spectrum. Rejack plotted $w_C(z)$ and showed that, like Welsh's no post processing case, $w_C(z)$ possessed a slow decay rate yielding poor altitude resolution.

Rather than post process the wave front sensors' data, Rejack investigated a technique for combining the weighting functions resulting from the correlations of slope measurements from two different size apertures. Specifically, he subtracted the phase correlation function for a pair of apertures of size L_2 from that for a pair of apertures of size L_1, where $L_1 < L_2$. Rejack plotted the resultant modified weighting function for three different ratios of L_1 to L_2. He found that the new weighting function did decay more rapidly than that due to a single pair of apertures.

2.4 Conclusion

Remote sensing of atmospheric parameters using optical beams is a widely studied field. The crossed beam technique has been used to obtain correlations of optical fields and thus derive information about the distributions of C_n^2 and $\vec{V}$. While many of these methods have relied upon correlations of intensity scintillations, recent works have also examined the use of phase correlations in the crossed beam technique for sensing C_n^2. It is proposed that the time lagged phase correlation properties of the crossed beam technique may be used to obtain a vertical profile of $\vec{V}(z')$. It is also proposed to combine the phase measurements of co-located wave front sensor pairs in a manner which improves the resolution of the measurement technique beyond that previously achieved. The following chapter contains the development of these proposals.

III. Methodology

3.1 Introduction

As discussed in previous chapters, most techniques for sensing C_n^2 and $\vec{V}$ have relied upon measurements of optical scintillations. Some work has also explored the use of measurements of wave front phase to sense C_n^2. This chapter presents a method for combining wave front phase measurements from co-located wave front phase slope sensors to improve the altitude resolution achievable by the crossed beam measurement geometry. Additionally, this chapter shows that wave front phase measurements may also be used to obtain vertical profiles of $\vec{V}$.

Figure 3.1 illustrates the measurement geometry considered in this chapter. Two point sources, denoted as p_1 and p_2 and separated by $\Delta\vec{p}$, are present at altitude z_s. These point sources illuminate four wave front sensors which are present in the aperture plane of an optical system. The sensors are denoted s_1, $s_{1'}$, s_2, and $s_{2'}$. Slope sensors s_n and $s_{n'}$ are centered on the same point in the aperture plane. The vector distance from the center of one sensor pair to the center of the other sensor pair is $\Delta\vec{x}$. The field of view of each wave front sensor is restricted so that sensors s_1 and $s_{1'}$ receive light from p_1 only, and sensors s_2 and $s_{2'}$ receive light from p_2 only. As can be seen from Figure 3.1, this geometry gives rise to crossed optical beams. The altitude of the crossing point is controlled by the source and sensor separations.

In the measurement technique examined here, the output of wave front sensor $s_{n'}$ is subtracted from the output of s_n. This is done for both $n = 1$ and $n = 2$. The subtraction essentially band pass filters the slope measurement of s_n, which Welsh (22) has shown to be a necessary step in obtaining a sharply peaked weighting function. The filtered measurements are then correlated. This correlation is designated $\langle C_s \rangle$ and is defined by

$$\langle C_s \rangle = \langle (s_1 - s_{1'})(s_2 - s_{2'}) \rangle \tag{3.1}$$

The goal of the first derivation presented in this chapter is to relate $\langle C_s \rangle$ to C_n^2. For this first derivation, the beams physically intersect and all measurements are taken simultaneously.

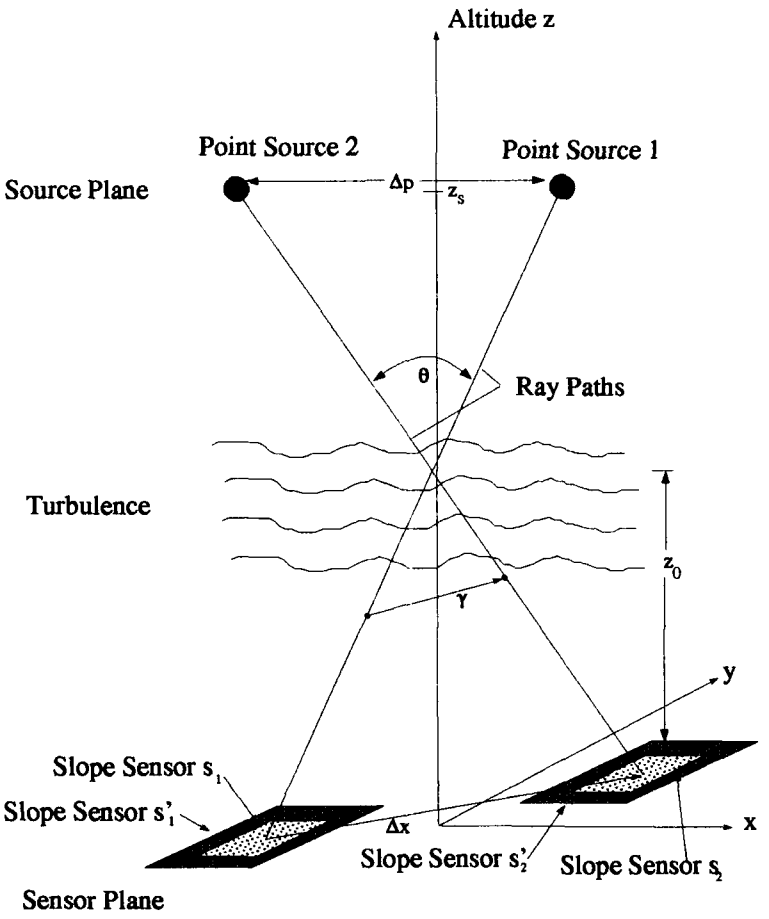

Figure 3.1. Measurement Geometry (17)

The first derivation results in an equation of the form

$$\langle C_s \rangle = \int \mathrm{d}z' \, C_n^2(z') w_C(z') \tag{3.2}$$

where z' is a position along the z axis and $w_C(z')$ is called the C_n^2 path weighting function. Ideally, $w_C(z')$ would have the shape of a Dirac delta function so that the sifting property could be employed to relate the measured correlation directly to C_n^2.

In the second derivation presented, the measurements are not made simultaneously. Instead, the measurements on sensors s_2 and $s_{2'}$ are taken τ seconds after the measurements on sensors s_1 and $s_{1'}$. Additionally, the optical beams are oriented so that there is always

a separation between the two, even at the cross over altitude. Thus, there is a small separation of the beams at the crossing altitude and the beams do not physically intersect.

Given these two conditions, the second derivation shows that the derivative of the time lagged correlation of the wave front slope measurements is related to $\vec{V}$ by (21)

$$\frac{\partial}{\partial\tau}\langle C_s(\tau)\rangle|_{\tau=0} = \frac{\partial}{\partial\tau}\langle[s_1(t) - s_{1'}(t)][s_2(t-\tau) - s_{2'}(t-\tau)]\rangle\Big|_{\tau=0}$$
$$= \int \mathrm{d}z' C_n^2(z')\vec{V}(z') \cdot \vec{w_V}(z') \qquad (3.3)$$

where $\frac{\partial}{\partial\tau}\langle C_s(\tau)\rangle$ is the partial derivative with respect to τ of the time lagged correlations of the sensor measurements, τ is the amount of time lag, $\vec{V}(z')$ is the wind velocity at the altitude z', and $\vec{w_V}(z')$ is called the wind path weighting function.

3.2 Justification of Approach

As mentioned above, the outputs of co-located slope sensors are subtracted before any correlations take place. This subtraction has the effect of band pass filtering the slope measurement of the smaller sensor. Welsh (22) has demonstrated that this approach provides a more sharply peaked path weighting function than that found when no filtering is performed.

To understand how this band pass filtering is accomplished, it is necessary to know something about the frequency response of wave front slope sensors. An idealized wave front slope sensor frequency response is shown in Figure 3.2. The frequency response has an upper cutoff frequency inversely proportional to the size of the slope sensor (22). Thus, the smaller the wave front slope sensor, the higher the cutoff frequency. From this, it is easy to see how subtracting the measurements of a larger slope sensor from those of a smaller co-located slope sensor will result in a band pass filtering of the signal from the smaller sensor. The low frequencies common to the measurements of both sensors will be eliminated, while those frequencies existing between the cutoff frequency of the larger sensor and the cutoff frequency of the smaller sensor will be unaffected. Figure 3.2 presents a graphical depiction of this technique.

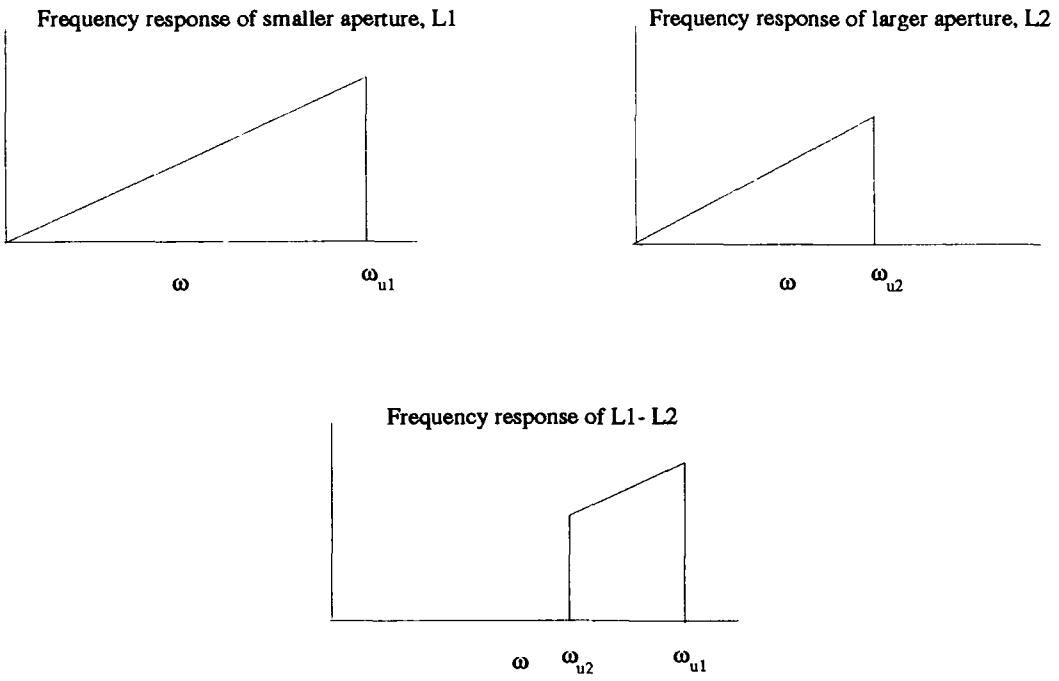

Figure 3.2. Band Pass Filter Creation

In Rejack's analysis (17), he correlated measurements from the sensors s_1 and s_2, and then correlated measurements from the sensors $s_{1'}$ and $s_{2'}$. He then investigated the difference of the two correlations

$$\langle C_s \rangle = \langle s_1 s_2 \rangle - \langle s_{1'} s_{2'} \rangle \tag{3.4}$$

This approach, however, is not equivalent to the band pass filtering method suggested by Welsh. In fact, Welsh (22) showed that such an approach is inferior to the approach adopted in this work where

$$\langle C_s \rangle = \langle (s_1 - s_{1'})(s_2 - s_{2'}) \rangle \tag{3.5}$$

As has been discussed previously, obtaining a vertical profile of the wind velocity requires time lagged correlations of the phase slope measurements. The time lagged correlation is similar to equation 3.5, but with the addition of a time lag for measurements s_2

and $s_{2'}$

$$\langle C_s(\tau)\rangle = \langle [s_1(t) - s_{1'}(t)][s_2(t-\tau) - s_{2'}(t-\tau)]\rangle \tag{3.6}$$

where τ is the time delay between measurements.

3.3 Derivation of C_n^2 Path Weighting Function, $w_C(z')$

3.3.1 Overview The first objective of this research is to find an expression for the C_n^2 path weighting function which results when the slope sensor outputs are combined as shown in equation 3.5. Once the form of this new weighting function is determined, the performance of the measurement technique can be examined. Accordingly, the goal of this derivation is to relate the correlation shown in equation 3.5 to C_n^2 through

$$\langle C_s\rangle = \int \mathrm{d}z'\, C_n^2(z') w_C(z') \tag{3.7}$$

where z' is a position along the z axis and $w_C(z')$ is called the C_n^2 path weighting function. In accomplishing this goal, the first step is to write an expression for the correlation defined in equation 3.5. This requires use of a model for the output of the wave front slope sensors. Then Kolmogorov statistics are assumed for the atmospheric turbulence. This allows the path weighting function to be reduced to an expression which depends only upon the measurement geometry. Thus, it is then possible to examine the characteristics of $w_C(z')$.

3.3.2 Slope Signal Correlation First consider the single realization correlation defined as

$$C_s = (s_1 - s_{1'})(s_2 - s_{2'}) \tag{3.8}$$

where s_n is the output of slope sensor n. Slope sensors s_1 and $s_{1'}$ are co-located and are separated from s_2 and $s_{2'}$ by $\Delta\vec{x}$. The subscripted numbers correspond to the illuminating light source, either p_1 or p_2. Normally, wave front slope sensors consist of multiple sub-apertures. However, it will be assumed throughout this development that the wave front slope sensors are each composed of just one aperture.

Let $\phi_n(\vec{x})$ designate the phase of the incident optical field from source p_n. The output of wave front slope sensor n is a noisy measurement of the average slope of $\phi_n(\vec{x})$ across

the sensor's aperture and is denoted s_n. The expression for s_n is

$$s_n = \int \mathrm{d}^2\vec{x}\, W_n(\vec{x})\,[\nabla\phi_n(\vec{x})\cdot\hat{d}] + \alpha_n \tag{3.9}$$

where $\nabla\phi_n(\vec{x})$ is the spatial gradient of the phase, $W_n(\vec{x})$ is the sensor's aperture weighting function, $\hat{d}$ is a unit vector in the wave front sensor's direction of sensitivity, and α_n is the slope measurement error. The measurement error is caused by photon noise in the detector. The photon noise is sometimes referred to as shot noise.

Wallner integrated equation 3.9 by parts to yield (20)

$$s_n = -\int \mathrm{d}^2\vec{x}\, W_n^s(\vec{x})\phi_n(\vec{x}) + \alpha_n \tag{3.10}$$

where $W_n^s(\vec{x})$ is the gradient of $W_n(\vec{x})$ in the wave front sensor's direction of sensitivity.

Referring to Figure 3.1, it will be assumed that the inner sensors, described by W_1 and W_2, are identical except for being placed at different positions. The same assumption is applied to $W_{1'}$ and $W_{2'}$. Using these assumptions, the notation can be simplified by letting $W_1(\vec{x}) = W_2(\vec{x}) = W_{L_1}(\vec{x})$, and $W_{1'}(\vec{x}) = W_{2'}(\vec{x}) = W_{L_2}(\vec{x})$ from here on. The subscripts L_1 and L_2 refer to the dimensions of the apertures.

With the aid of the slope sensor output model given by equation 3.10, equation 3.5 may be written as

$$\begin{aligned} C_s = &\left\{\left[-\int \mathrm{d}^2\vec{x}\, W_{L_1}^s(\vec{x})\phi_1(\vec{x}) + \alpha_1\right] - \left[-\int \mathrm{d}^2\vec{x}'\, W_{L_2}^s(\vec{x}')\phi_1(\vec{x}') + \alpha_{1'}\right]\right\} \\ &\times\left\{\left[-\int \mathrm{d}^2\vec{x}''\, W_{L_1}^s(\vec{x}''-\Delta\vec{x})\phi_2(\vec{x}'') + \alpha_2\right] - \left[-\int \mathrm{d}^2\vec{x}'''\, W_{L2}^s(\vec{x}'''-\Delta\vec{x})\phi_2(\vec{x}''') + \alpha_{2'}\right]\right\} \end{aligned} \tag{3.11}$$

Note that the subscripts 1 and 2 on the wave front phase ϕ refer to the source of the wave front. Performing the multiplication indicated in equation 3.11 results in

$$
\begin{aligned}
C_s = & \\
& \int \mathrm{d}^2\vec{x} \int \mathrm{d}^2\vec{x}'' \, W^s_{L_1}(\vec{x}) W^s_{L_1}(\vec{x}'' - \Delta\vec{x}) \left[\phi_1(\vec{x})\phi_2(\vec{x}'')\right] \\
& - \int \mathrm{d}^2\vec{x} \, W^s_{L_1}(\vec{x})\phi_1(\vec{x})\alpha_2 \\
& - \int \mathrm{d}^2\vec{x}'' \, W^s_{L_1}(\vec{x}'' - \Delta\vec{x})\phi_2(\vec{x}'')\alpha_1 \\
& + \alpha_1\alpha_2 \\
& + \int \mathrm{d}^2\vec{x}' \int \mathrm{d}^2\vec{x}''' \, W^s_{L_2}(\vec{x}') W^s_{L_2}(\vec{x}''' - \Delta\vec{x}) \left[\phi_1(\vec{x}')\phi_2(\vec{x}''')\right] \\
& - \int \mathrm{d}^2\vec{x}' \, W^s_{L_2}(\vec{x}')\phi_1(\vec{x}')\alpha_{2'} \\
& - \int \mathrm{d}^2\vec{x}''' \, W^s_{L_2}(\vec{x}''' - \Delta\vec{x})\phi_2(\vec{x}''')\alpha_{1'} \\
& + \alpha_{1'}\alpha_{2'} \\
& - \int \mathrm{d}^2\vec{x}' \int \mathrm{d}^2\vec{x}'' \, W^s_{L_2}(\vec{x}') W^s_{L_1}(\vec{x}'' - \Delta\vec{x}) \left[\phi_1(\vec{x}')\phi_2(\vec{x}'')\right] \\
& + \int \mathrm{d}^2\vec{x}' \, W^s_{L_2}(\vec{x})\phi_1(\vec{x})\alpha_2 \\
& + \int \mathrm{d}^2\vec{x}'' \, W^s_{L_1}(\vec{x}'' - \Delta\vec{x})\phi_2(\vec{x}'')\alpha_{1'} \\
& - \alpha_{1'}\alpha_2 \\
& - \int \mathrm{d}^2\vec{x} \int \mathrm{d}^2\vec{x}''' \, W^s_{L_1}(\vec{x}) W^s_{L_2}(\vec{x}''' - \Delta\vec{x}) \left[\phi_1(\vec{x})\phi_2(\vec{x}''')\right] \\
& + \int \mathrm{d}^2\vec{x} \, W^s_{L_1}(\vec{x})\phi_1(\vec{x})\alpha_{2'} \\
& + \int \mathrm{d}^2\vec{x}''' \, W^s_{L_2}(\vec{x}''' - \Delta\vec{x})\phi_2(\vec{x}''')\alpha_1 \\
& - \alpha_1\alpha_{2'}
\end{aligned}
\tag{3.12}
$$

Equation 3.12 contains the random quantities ϕ_n and α_n, therefore further progress requires a statistical approach. Assuming that α_n is a zero mean random process independent of ϕ_n, the ensemble average of equation 3.12 gives the desired correlation $\langle C_s \rangle$

$$
\begin{aligned}
\langle C_s \rangle = & \int \mathrm{d}^2\vec{x} \int \mathrm{d}^2\vec{x}'' \, W^s_{L_1}(\vec{x}) W^s_{L_1}(\vec{x}'' - \Delta\vec{x}) \langle \phi_1(\vec{x})\phi_2(\vec{x}'') \rangle \\
& - 0 \\
& - 0 \\
& + \langle \alpha_1\alpha_2 \rangle
\end{aligned}
$$

$$
\begin{aligned}
&+\int \mathrm{d}^2\vec{x}' \int \mathrm{d}^2\vec{x}''' \, W^s_{L_2}(\vec{x}') W^s_{L_2}(\vec{x}''' - \Delta\vec{x}) \langle \phi_1(\vec{x}') \phi_2(\vec{x}''') \rangle \\
&-0 \\
&-0 \\
&+\langle \alpha_{1'} \alpha_{2'} \rangle \\
&-\int \mathrm{d}^2\vec{x}' \int \mathrm{d}^2\vec{x}'' \, W^s_{L_2}(\vec{x}') W^s_{L_1}(\vec{x}'' - \Delta\vec{x}) \langle \phi_1(\vec{x}') \phi_2(\vec{x}'') \rangle \\
&+0 \\
&+0 \\
&-\langle \alpha_{1'} \alpha_2 \rangle \\
&-\int \mathrm{d}^2\vec{x} \int \mathrm{d}^2\vec{x}''' \, W^s_{L_1}(\vec{x}) W^s_{L_2}(\vec{x}''' - \Delta\vec{x}) \langle \phi_1(\vec{x}) \phi_2(\vec{x}''') \rangle \\
&+0 \\
&+0 \\
&-\langle \alpha_1 \alpha_{2'} \rangle
\end{aligned}
\tag{3.13}
$$

Wallner has shown that the correlation of the noise process α is given by (20)

$$
\langle \alpha_n \alpha_m \rangle = \sigma^2 \delta(n - m) \tag{3.14}
$$

where n and m refer to the sensors' apertures, σ^2 is the variance of the slope measurement due to photon noise, and $\delta(x)$ is the Dirac delta function. Basically, equation 3.14 states that the correlation of the noise processes from two subapertures is zero unless the subapertures coincide. Notice that none of the noise process correlations in equation 3.13 are due to subapertures that coincide. Therefore, equation 3.13 reduces to

$$
\begin{aligned}
\langle C_s \rangle = &\int \mathrm{d}^2\vec{x} \int \mathrm{d}^2\vec{x}'' \, W^s_{L_1}(\vec{x}) W^s_{L_1}(\vec{x}'' - \Delta\vec{x}) \langle \phi_1(\vec{x}) \phi_2(\vec{x}'') \rangle \\
&+\int \mathrm{d}^2\vec{x}' \int \mathrm{d}^2\vec{x}''' \, W^s_{L_2}(\vec{x}') W^s_{L_2}(\vec{x}''' - \Delta\vec{x}) \langle \phi_1(\vec{x}') \phi_2(\vec{x}''') \rangle \\
&-\int \mathrm{d}^2\vec{x}' \int \mathrm{d}^2\vec{x}'' \, W^s_{L_2}(\vec{x}') W^s_{L_1}(\vec{x}'' - \Delta\vec{x}) \langle \phi_1(\vec{x}') \phi_2(\vec{x}'') \rangle \\
&-\int \mathrm{d}^2\vec{x} \int \mathrm{d}^2\vec{x}''' \, W^s_{L_1}(\vec{x}) W^s_{L_2}(\vec{x}''' - \Delta\vec{x}) \langle \phi_1(\vec{x}) \phi_2(\vec{x}''') \rangle
\end{aligned}
\tag{3.15}
$$

Consider the third and fourth terms of equation 3.15. Their forms are nearly identical, with

the only difference being the fact that apertures W_{L_1} and W_{L_2} have switched positions. It is shown in section 3.3.3 that the correlation of the phases, $\langle \phi_1(\vec{x})\phi_2(\vec{x}') \rangle$, is spatially wide sense stationary, with the value of the correlation depending upon only the magnitude of the aperture separation. Using this fact, the last two terms have the same value and may be combined so $\langle C_s \rangle$ becomes

$$\begin{aligned}\langle C_s \rangle = &\int \mathrm{d}^2\vec{x} \int \mathrm{d}^2\vec{x}'' \, W^s_{L_1}(\vec{x}) W^s_{L_1}(\vec{x}'' - \Delta\vec{x}) \langle \phi_1(\vec{x})\phi_2(\vec{x}'') \rangle \\ &+ \int \mathrm{d}^2\vec{x}' \int \mathrm{d}^2\vec{x}''' \, W^s_{L_2}(\vec{x}') W^s_{L_2}(\vec{x}''' - \Delta\vec{x}) \langle \phi_1(\vec{x}')\phi_2(\vec{x}''') \rangle \\ &-2 \int \mathrm{d}^2\vec{x}' \int \mathrm{d}^2\vec{x}'' \, W^s_{L_2}(\vec{x}') W^s_{L_1}(\vec{x}'' - \Delta\vec{x}) \langle \phi_1(\vec{x}')\phi_2(\vec{x}'') \rangle \end{aligned} \tag{3.16}$$

3.3.3 Evaluation of First Term in $\langle C_s \rangle$ As equation 3.16 shows, the first term of $\langle C_s \rangle$ is given by

$$\text{Term 1} = \int \mathrm{d}^2\vec{x} \int \mathrm{d}^2\vec{x}'' \, W^s_{L_1}(\vec{x}) W^s_{L_1}(\vec{x}'' - \Delta\vec{x}) \langle \phi_1(\vec{x})\phi_2(\vec{x}'') \rangle \tag{3.17}$$

where $\langle \phi_1(\vec{x})\phi_2(\vec{x}'') \rangle$ is the correlation of the two wave front phases. The correlation of the phases may be expressed in terms of the phase structure function as

$$\langle \phi_1(\vec{x})\phi_2(\vec{x}'') \rangle = -\frac{1}{2} D_{12}(\vec{x}, \vec{x}'') + \frac{1}{2}\langle \phi_1^2(\vec{x}) \rangle + \frac{1}{2}\langle \phi_2^2(\vec{x}'') \rangle \tag{3.18}$$

where $D_{12}(\vec{x}, \vec{x}'')$ is the phase structure function defined by

$$D_{12}(\vec{x}, \vec{x}'') = \langle [\phi_1(\vec{x}) - \phi_2(\vec{x}'')]^2 \rangle \tag{3.19}$$

Taking note of the fact that $W^s_n(\vec{x})$ is an odd function and that ϕ_1 and ϕ_2 are wide sense stationary random processes, the integrations which result when equation 3.18 is substituted into equation 3.17 will yield zeroes for all terms in equation 3.18 except the term containing $D_{12}(\vec{x}, \vec{x}'')$. So, the first term may now be expressed as

$$\text{Term 1} = -\frac{1}{2} \int \mathrm{d}^2\vec{x} \int \mathrm{d}^2\vec{x}'' \, W^s_{L_1}(\vec{x}) W^s_{L_1}(\vec{x}'' - \Delta\vec{x}) D_{12}(\vec{x}, \vec{x}'') \tag{3.20}$$

Further progress requires an expression for $D_{12}(\vec{x}, \vec{x}'')$. For spatially stationary, isotropic turbulence, Lutomirski and Buser have shown the structure function for the geometry in Figure 3.1 is (12)

$$D_{12}(\vec{x} - \vec{x}'') = 8\pi^2 k^2 \int \mathrm{d}z' \int \mathrm{d}K_\perp \, \Phi_n(K_\perp, 0, z') \times \left\{ 1 - J_0 \left(K_\perp \left| (\Delta\vec{p}) \left(\frac{z'}{z_s} \right) + (\vec{x} - \vec{x}'') \left(1 - \frac{z'}{z_s} \right) \right| \right) \right\} \tag{3.21}$$

where

$\Phi_n(K_\perp, K_z, z')$ is the psd of the fluctuations of the index of refraction, n,

$K_\perp$ is the wavenumber component perpendicular to the z axis,

K_z is the wavenumber component parallel to the z axis,

$\Delta\vec{p}$ is the vector separation of the sources,

J_0 is the zero order Bessel function,

z' is the distance from the aperture plane to some point along the z axis,

z_s is the altitude of the point sources,

and $\vec{x}$ and $\vec{x}''$ are points in the aperture plane of the optical system.

Notice the psd Φ_n is a function of the wavenumber components perpendicular ($K_\perp$) and parallel (K_z) to the z axis. By making the assumption that Φ_n is separable in the perpendicular and parallel wavenumber components, and z', Welsh expresses the psd as (22)

$$\Phi_n(K_\perp, K_z, z') = \Phi_n'(K_\perp, K_z) C_n^2(z') \tag{3.22}$$

Using the structure function given by Lutomirski and Buser and making Welsh's assumption of psd separability allows the first term of equation 3.16 to be written as

$$\text{Term 1} = \int \mathrm{d}^2\vec{x} \int \mathrm{d}^2\vec{x}'' \, W_{L_1}^s(\vec{x}) W_{L_1}^s(\vec{x}'' - \Delta\vec{x}) \times (-4\pi^2 k^2) \int_0^{z_s} \mathrm{d}z' \int_0^\infty \mathrm{d}K_\perp \, K_\perp \Phi_n'(K_\perp, 0) \, C_n^2(z') \times \left\{ 1 - J_0 \left(K_\perp \left| (\Delta\vec{p}) \left(\frac{z'}{z_s} \right) + (\vec{x} - \vec{x}'') \left(1 - \frac{z'}{z_s} \right) \right| \right) \right\} \tag{3.23}$$

Now that C_n^2 has been introduced, this first term may be written as

$$\text{Term } 1 = \int_0^{z_s} \mathrm{d}z'\, C_n^2(z')\, w_1(z') \tag{3.24}$$

where $w_1(z')$ is a path weighting function defined by

$$w_1(z') = -4\pi^2 k^2 \int \mathrm{d}^2\vec{x} \int \mathrm{d}^2\vec{x}''\, W_{L_1}^s(\vec{x}) W_{L_1}^s(\vec{x}'' - \Delta\vec{x}) \times \int_0^\infty \mathrm{d}K_\perp\, K_\perp \Phi_n'(K_\perp, 0) \left\{ 1 - J_0\left(K_\perp \left| (\Delta\vec{p}) \left(\frac{z'}{z_s}\right) + (\vec{x} - \vec{x}'') \left(1 - \frac{z'}{z_s}\right) \right| \right) \right\} \tag{3.25}$$

The goal now is to find an expression for $w_1(z')$ that depends upon the measurement geometry alone (i.e. z_s, $\Delta\vec{x}$, $\Delta\vec{p}$). The first step is to make use of the Kolmogorov spectrum discussed in Chapter 2 to assume a form for Φ_n' given by (9)

$$\Phi_n'(K_\perp, K_z) = 0.033 K^{-\frac{11}{3}} \tag{3.26}$$

where $K = |K_\perp + K_z|$. Substituting equation 3.26 into equation 3.25 yields

$$w_1(z') = -4\pi^2 k^2 \int \mathrm{d}^2\vec{x} \int \mathrm{d}^2\vec{x}''\, W_{L_1}^s(\vec{x}) W_{L_1}^s(\vec{x}'' - \Delta\vec{x}) \times \int_0^\infty \mathrm{d}K_\perp\, 0.033 K_\perp^{-\frac{8}{3}} \left\{ 1 - J_0\left(K_\perp \left| (\Delta\vec{p}) \left(\frac{z'}{z_s}\right) + (\vec{x} - \vec{x}'') \left(1 - \frac{z'}{z_s}\right) \right| \right) \right\} \tag{3.27}$$

Now consider the change of variables

$$K' = K_\perp \left| (\Delta\vec{p}) \left(\frac{z'}{z_s}\right) + (\vec{x} - \vec{x}'') \left(1 - \frac{z'}{z_s}\right) \right| \tag{3.28}$$

and

$$\mathrm{d}K' = \left| (\Delta\vec{p}) \left(\frac{z'}{z_s}\right) + (\vec{x} - \vec{x}'') \left(1 - \frac{z'}{z_s}\right) \right| \mathrm{d}K_\perp \tag{3.29}$$

Employing the integral identity (15)

$$\int_0^\infty \mathrm{d}x[1 - J_0(x)]x^{-p} = \pi \left\{ 2^p \left[\Gamma\left(\frac{p+1}{2}\right) \right]^2 \sin\frac{\pi(p-1)}{2} \right\}^{-1} \tag{3.30}$$

for $1 < p < 3$, reduces the path weighting function to

$$w_1(z') = -1.46k^2 \int \mathrm{d}^2\vec{x} \int \mathrm{d}^2\vec{x}'' \, W^s_{L_1}(\vec{x}) W^s_{L_1}(\vec{x}'' - \Delta\vec{x}) \times \left| (\Delta\vec{p}) \left(\frac{z'}{z_s}\right) + (\vec{x} - \vec{x}'') \left(1 - \frac{z'}{z_s}\right) \right|^{\frac{5}{3}} \tag{3.31}$$

At this point, the path weighting function depends upon the measurement geometry and the slope sensor aperture weighting functions. Square apertures are commonly used in wave front sensors, and the transmittance of such apertures can be modeled as

$$W_L(\vec{x}) = \frac{1}{L^2} \mathrm{rect}\left(\frac{x}{L}\right) \mathrm{rect}\left(\frac{y}{L}\right) \tag{3.32}$$

where rect is the rectangle function, L is the dimension of the aperture along one side, and the factor $\frac{1}{L^2}$ is necessary to achieve normalization of the aperture weighting function. Assuming that the slope sensor apertures under consideration possess a transmittance function of the form given in equation 3.32 and, without loss of generality, that they measure the wave front phase slope in the x direction only, then the gradient of the slope sensor aperture weighting functions may be written as

$$W^s_{L_1}(\vec{x}) = \frac{1}{L_1^2} \left[\delta\left(x + \frac{L_1}{2}\right) - \delta\left(x - \frac{L_1}{2}\right) \right] \mathrm{rect}\left(\frac{y}{L_1}\right) \tag{3.33}$$

where δ is the Dirac delta function.

Before the slope sensor gradient functions just presented can be useful in equation 3.31, the absolute value quantity in equation 3.31 must be written in terms of the x- and y-directed components of $\Delta\vec{p}$, $\vec{x}$, and $\vec{x}''$. The absolute value term can be seen to be

$$\left|(\Delta\vec{p})\left(\frac{z'}{z_s}\right)+(\vec{x}-\vec{x}'')\left(1-\frac{z'}{z_s}\right)\right|^{\frac{5}{3}}=$$
$$\left\{\left[\Delta p_x\left(\frac{z'}{z_s}\right)+(x-x'')\left(1-\frac{z'}{z_s}\right)\right]^2+\left[\Delta p_y\left(\frac{z'}{z_s}\right)+(y-y'')\left(1-\frac{z'}{z_s}\right)\right]^2\right\}^{\frac{5}{6}} \tag{3.34}$$

where Δp_x and Δp_y are the x- and y-directed components of $\Delta\vec{p}$, x and x'' are the x-directed components of $\vec{x}$ and $\vec{x}''$, and y and y'' are the y-directed components of $\vec{x}$ and $\vec{x}''$. It is convenient to represent equation 3.34 with the function $f(x-x'',y-y'')$

$$f(x-x'',y-y'')=$$
$$\left\{\left[\Delta p_x\left(\frac{z'}{z_s}\right)+(x-x'')\left(1-\frac{z'}{z_s}\right)\right]^2+\left[\Delta p_y\left(\frac{z'}{z_s}\right)+(y-y'')\left(1-\frac{z'}{z_s}\right)\right]^2\right\}^{\frac{5}{6}} \tag{3.35}$$

Substituting equations 3.35 and 3.33 into equation 3.31 yields

$$\begin{aligned}w_1(z')=-1.46k^2L_1^{-4}\int \mathrm{d}^2\vec{x}\int \mathrm{d}^2\vec{x}''f(x-x'',y-y'')\\ \times\left\{\left[\delta\left(x+\frac{L_1}{2}\right)-\delta\left(x-\frac{L_1}{2}\right)\right]\mathrm{rect}\left(\frac{y}{L_1}\right)\right\}\\ \times\left\{\left[\delta\left(x''-\Delta x+\frac{L_1}{2}\right)-\delta\left(x''-\Delta x-\frac{L_1}{2}\right)\right]\mathrm{rect}\left(\frac{y''-\Delta y}{L_1}\right)\right\}\end{aligned} \tag{3.36}$$

Taking advantage of the sifting property of the Dirac delta function, the integrations over x and x'' yield

$$\begin{aligned}w_1(z')=-1.46k^2L_1^{-4}\int \mathrm{d}y\,\mathrm{rect}\left(\frac{y}{L_1}\right)\int \mathrm{d}y''\,\mathrm{rect}\left(\frac{y''-\Delta y}{L_1}\right)\\ \times\{f(-\Delta x,y-y'')-f(-\Delta x-L_1,y-y'')-f(-\Delta x+L_1,y-y'')+f(-\Delta x,y-y'')\}\end{aligned} \tag{3.37}$$

At this point, it is convenient to define the function $g(y-y'')$ as the bracketed term of equation 3.37

$$g(y-y'') = f(-\Delta x, y-y'') - f(-\Delta x - L_1, y-y'')$$
$$-f(-\Delta x + L_1, y-y'') + f(-\Delta x, y-y'') \tag{3.38}$$

Use of equation 3.38 allows the path weighting function to be written as

$$w_1(z') = -1.46k^2 L_1^{-4} \int \mathrm{d}y \,\mathrm{rect}\left(\frac{y}{L_1}\right) \int \mathrm{d}y'' \,\mathrm{rect}\left(\frac{y''-\Delta y}{L_1}\right) g(y-y'') \tag{3.39}$$

Making the change of variables $u = y - y''$ and $v = \frac{y+y''}{2}$ allows equation 3.39 to be written as

$$w_1(z') = -1.46k^2 L_1^{-4} \int \mathrm{d}u \,\mathrm{rect}\left(\frac{v+\frac{u}{2}}{L_1}\right) \int \mathrm{d}v \,\mathrm{rect}\left(\frac{v-\frac{u}{2}-\Delta y}{L_1}\right) g(u) \tag{3.40}$$

One more change of variables, letting $v' = v + \frac{u}{2}$, results in

$$w_1(z') = -1.46k^2 L_1^{-4} \int \mathrm{d}u \, g(u) \int \mathrm{d}v' \,\mathrm{rect}\left(\frac{v'}{L_1}\right) \mathrm{rect}\left(\frac{v'-u-\Delta y}{L_1}\right) \tag{3.41}$$

Notice that the integral over v' is simply the autocorrelation of a rect function. Thus evaluating the integral over v' yields

$$w_1(z') = -1.46k^2 L_1^{-3} \int \mathrm{d}u \, g(u) \,\mathrm{tri}\left(\frac{u-\Delta y}{L_1}\right) \tag{3.42}$$

where tri is the triangle function defined by

$$\mathrm{tri}(x) = \begin{cases} 1-|x| & -1 < x < 1 \\ 0 & \text{elsewhere} \end{cases} \tag{3.43}$$

Evaluating $g(u)$ through use of equations 3.38 and 3.35 and placing the result in equation 3.42 yields the expanded expression

$$w_1(z') = -1.46k^2 L_1^{-3} \int \mathrm{d}u \,\mathrm{tri}\left(\frac{u-\Delta y}{L_1}\right)$$
$$\times \left\{ 2\left\{ \left[\Delta p_x \left(\frac{z'}{z_s}\right) - \left(1-\frac{z'}{z_s}\right)\Delta x\right]^2 + \left[\Delta p_y \left(\frac{z'}{z_s}\right) + u\left(1-\frac{z'}{z_s}\right)\right]^2 \right\}^{\frac{5}{6}}$$

$$- \left\{ \left[\Delta p_x \left(\frac{z'}{z_s} \right) - \left(1 - \frac{z'}{z_s} \right) (\Delta x + L_1) \right]^2 + \left[\Delta p_y \left(\frac{z'}{z_s} \right) + u \left(1 - \frac{z'}{z_s} \right) \right]^2 \right\}^{\frac{5}{6}}$$
$$- \left\{ \left[\Delta p_x \left(\frac{z'}{z_s} \right) - \left(1 - \frac{z'}{z_s} \right) (\Delta x - L_1) \right]^2 + \left[\Delta p_y \left(\frac{z'}{z_s} \right) + u \left(1 - \frac{z'}{z_s} \right) \right]^2 \right\}^{\frac{5}{6}} \Bigg\} \tag{3.44}$$

Referring to Figure 3.1, it makes intuitive sense that the most sharply peaked weighting function occurs when the two optical beams physically intersect. Without loss of generality, $\Delta\vec{p}$ and $\Delta\vec{x}$ are assumed to be oriented along the x axis so that $\Delta p_y = \Delta y = 0$. Using this assumption results in

$$\begin{aligned} w_1(z') = -1.46k^2 L_1^{-3} \int \mathrm{d}u \, \mathrm{tri}\left(\frac{u}{L_1}\right) \\ \times \Bigg\{ 2 \left\{ \left[\Delta p_x \left(\frac{z'}{z_s} \right) - \Delta x + \left(\frac{z'}{z_s} \right) \Delta x \right]^2 + \left[u \left(1 - \frac{z'}{z_s} \right) \right]^2 \right\}^{\frac{5}{6}} \\ - \left\{ \left[\Delta p_x \left(\frac{z'}{z_s} \right) - \Delta x - L_1 + \frac{z'}{z_s} (\Delta x + L_1) \right]^2 + \left[u \left(1 - \frac{z'}{z_s} \right) \right]^2 \right\}^{\frac{5}{6}} \\ - \left\{ \left[\Delta p_x \left(\frac{z'}{z_s} \right) - \Delta x + L_1 + \frac{z'}{z_s} (\Delta x - L_1) \right]^2 + \left[u \left(1 - \frac{z'}{z_s} \right) \right]^2 \right\}^{\frac{5}{6}} \Bigg\} \end{aligned} \tag{3.45}$$

where some algebraic expansions have also been performed. The expression $\Delta p_x \left(\frac{z'}{z_s} \right) - \Delta x$ is the distance between the two ray paths as a function of altitude (see Figure 3.1). Let $\gamma = \Delta p_x \left(\frac{z'}{z_s} \right) - \Delta x$ and rewrite equation 3.45 as

$$\begin{aligned} w_1(z') = -1.46k^2 L_1^{-3} \int \mathrm{d}u \, \mathrm{tri}\left(\frac{u}{L_1}\right) \\ \times \Bigg\{ 2 \left\{ \left[\gamma + \left(\frac{z'}{z_s} \right) \Delta x \right]^2 + \left[u \left(1 - \frac{z'}{z_s} \right) \right]^2 \right\}^{\frac{5}{6}} \\ - \left\{ \left[\gamma - L_1 + \frac{z'}{z_s} (\Delta x + L_1) \right]^2 + \left[u \left(1 - \frac{z'}{z_s} \right) \right]^2 \right\}^{\frac{5}{6}} \\ - \left\{ \left[\gamma + L_1 + \frac{z'}{z_s} (\Delta x - L_1) \right]^2 + \left[u \left(1 - \frac{z'}{z_s} \right) \right]^2 \right\}^{\frac{5}{6}} \Bigg\} \end{aligned} \tag{3.46}$$

Finally, letting $u' = \frac{u}{L_1}$ yields a dimensionless variable of integration. The resulting ex-

pression is

$$w_1(z') = -1.46k^2 L_1^{-\frac{1}{3}} \int_{-1}^{1} \mathrm{d}u' \, \mathrm{tri}(u') \times \left\{ 2 \left\{ \left[\frac{\gamma}{L_1} + \left(\frac{z'}{z_s} \right) \frac{\Delta x}{L_1} \right]^2 + \left[u' \left(1 - \frac{z'}{z_s} \right) \right]^2 \right\}^{\frac{5}{6}} - \left\{ \left[\frac{\gamma}{L_1} - 1 + \frac{z'}{z_s} \left(\frac{\Delta x}{L_1} + 1 \right) \right]^2 + \left[u' \left(1 - \frac{z'}{z_s} \right) \right]^2 \right\}^{\frac{5}{6}} - \left\{ \left[\frac{\gamma}{L_1} + 1 + \frac{z'}{z_s} \left(\frac{\Delta x}{L_1} - 1 \right) \right]^2 + \left[u' \left(1 - \frac{z'}{z_s} \right) \right]^2 \right\}^{\frac{5}{6}} \right\} \tag{3.47}$$

The weighting function in equation 3.47 above, coupled with equation 3.24, completes the evaluation of the first term of $\langle C_s \rangle$. The second term in equation 3.16 will be examined next.

3.3.4 Evaluation of Second Term in $\langle C_s \rangle$ The second term of equation 3.15 is given by

$$\text{Term 2} = \int \mathrm{d}^2 \vec{x}' \int \mathrm{d}^2 \vec{x}''' \, W_{L_2}^s(\vec{x}') W_{L_2}^s(\vec{x}''' - \Delta\vec{x}) \langle \phi_1(\vec{x}') \phi_2(\vec{x}''') \rangle \tag{3.48}$$

Notice that this term is identical in form to the first term with one exception: L_1 has been replaced by L_2 in the aperture weighting function. Performing the same analysis for this term as that performed for Term 1 will yield a result identical to that obtained for Term 1, but with L_1 replaced by L_2. Thus, the second term can be written

$$\text{Term 2} = \int_0^{z_s} \mathrm{d}z' \, C_n^2(z') \, w_2(z') \tag{3.49}$$

where $w_2(z')$ is given by

$$w_2(z') = -1.46k^2 L_2^{-\frac{1}{3}} \int_{-1}^{1} \mathrm{d}u' \, \mathrm{tri}(u') \times \left\{ 2 \left\{ \left[\frac{\gamma}{L_2} + \left(\frac{z'}{z_s} \right) \frac{\Delta x}{L_2} \right]^2 + \left[u' \left(1 - \frac{z'}{z_s} \right) \right]^2 \right\}^{\frac{5}{6}} - \left\{ \left[\frac{\gamma}{L_2} - 1 + \frac{z'}{z_s} \left(\frac{\Delta x}{L_2} + 1 \right) \right]^2 + \left[u' \left(1 - \frac{z'}{z_s} \right) \right]^2 \right\}^{\frac{5}{6}}$$

$$-\left\{\left[\frac{\gamma}{L_2}+1+\frac{z'}{z_s}\left(\frac{\Delta x}{L_2}-1\right)\right]^2+\left[u'\left(1-\frac{z'}{z_s}\right)\right]^2\right\}^{\frac{5}{6}}\Bigg\} \tag{3.50}$$

Now that expressions for the first two terms in equation 3.16 have been obtained, it is time to evaluate the third term.

3.3.5 Evaluation of Third Term in $\langle C_s \rangle$ The third term in equation 3.16 is

$$\text{Term 3} = -2\int \mathrm{d}^2\vec{x}' \int \mathrm{d}^2\vec{x}''\, W^s_{L_2}(\vec{x}')W^s_{L_1}(\vec{x}''-\Delta\vec{x})\langle\phi_1(\vec{x}')\phi_2(\vec{x}'')\rangle \tag{3.51}$$

This term is essentially the cross correlation of the phase slope measurement on an aperture of dimension L_1 with the phase slope measurement on an aperture of dimension L_2, where the two apertures are separated by $\Delta\vec{x}$. The derivation of an expression for the third term follows the same development as that for the first term until models are assumed for the gradients of the slope sensor weighting functions. Thus, the starting point of this derivation is

$$\text{Term 3} = \int_0^{z_s} \mathrm{d}z'\, C_n^2(z')\, w_3(z') \tag{3.52}$$

where $w_3(z')$ is given by

$$w_3(z') = -2.92k^2 \int \mathrm{d}^2\vec{x}' \int \mathrm{d}^2\vec{x}''\, W^s_{L_2}(\vec{x}')W^s_{L_1}(\vec{x}''-\Delta\vec{x}) \times \left|(\Delta\vec{p})\left(\frac{z'}{z_s}\right)+(\vec{x}'-\vec{x}'')\left(1-\frac{z'}{z_s}\right)\right|^{\frac{5}{3}} \tag{3.53}$$

Once again, the slope sensors are assumed to measure the wave front slope in the x-direction only, so

$$W^s_{L_n}(\vec{x}') = \frac{1}{L_n^2}\left[\delta\left(x'+\frac{L_n}{2}\right)-\delta\left(x'-\frac{L_n}{2}\right)\right]\mathrm{rect}\left(\frac{y'}{L_n}\right) \tag{3.54}$$

where $n = 1$ or 2. The absolute value quantity present in equation 3.53 is again designated with the function f defined in equation 3.35. Substituting equations 3.35 and 3.54 into equation 3.53 and performing the integrations over x' and x'' yields

$$w_3(z') = -2.92k^2 L_1^{-2} L_2^{-2} \int \mathrm{d}y' \,\mathrm{rect}\left(\frac{y'}{L_2}\right) \int \mathrm{d}y'' \,\mathrm{rect}\left(\frac{y''-\Delta y}{L_1}\right)$$
$$\times \left\{ f\left(-\Delta x - \frac{L_2}{2} + \frac{L_1}{2}, y - y''\right) - f\left(-\Delta x - \frac{L_2}{2} - \frac{L_1}{2}, y - y''\right) \right.$$
$$\left. -f\left(-\Delta x + \frac{L_2}{2} + \frac{L_1}{2}, y - y''\right) + f\left(-\Delta x + \frac{L_2}{2} - \frac{L_1}{2}, y - y''\right) \right\} \qquad (3.55)$$

As was done during the derivation of Term 1, let the bracketed term be designated

$$g_3(y' - y'') =$$
$$f\left(-\Delta x - \frac{L_2}{2} + \frac{L_1}{2}, y - y''\right) - f\left(-\Delta x - \frac{L_2}{2} - \frac{L_1}{2}, y - y''\right)$$
$$-f\left(-\Delta x + \frac{L_2}{2} + \frac{L_1}{2}, y - y''\right) + f\left(-\Delta x + \frac{L_2}{2} - \frac{L_1}{2}, y - y''\right) \qquad (3.56)$$

Use of equation 3.56 allows equation 3.55 to be written as

$$w_3(z') = -2.92k^2 L_1^{-2} L_2^{-2} \int \mathrm{d}y' \,\mathrm{rect}\left(\frac{y'}{L_2}\right) \int \mathrm{d}y'' \,\mathrm{rect}\left(\frac{y''-\Delta y}{L_1}\right) g_3(y' - y'') \qquad (3.57)$$

Making the same substitutions of variables as accomplished in subsection 3.3.3 results in

$$w_3(z') = -2.92k^2 L_1^{-2} L_2^{-2} \int \mathrm{d}u \, g_3(u) \int \mathrm{d}v' \,\mathrm{rect}\left(\frac{v'}{L_2}\right) \,\mathrm{rect}\left(\frac{v'-u-\Delta y}{L_1}\right) \qquad (3.58)$$

The integral over v' in equation 3.58 is simply the correlation of two different sized rect functions. Performing the correlation yields

$$\int \mathrm{d}v' \,\mathrm{rect}\left(\tfrac{v'}{L_2}\right) \,\mathrm{rect}\left(\tfrac{v'-u-\Delta y}{L_1}\right) =$$
$$\begin{cases} u + \frac{L_2+L_1}{2} + \Delta y & \text{for} \quad -\left(\frac{L_1+L_2}{2} + \Delta y\right) \le u < \frac{L_1-L_2}{2} - \Delta y \\ L_1 & \text{for} \quad \frac{L_1-L_2}{2} - \Delta y \le u < \frac{L_2-L_1}{2} - \Delta y \\ \frac{L_1+L_2}{2} - u - \Delta y & \text{for} \quad \frac{L_2-L_1}{2} - \Delta y \le u \le \frac{L_1+L_2}{2} - \Delta y \\ 0 & \text{otherwise} \end{cases} \qquad (3.59)$$

Once again assuming $\Delta y = \Delta p_y = 0$, use of equation 3.59 in equation 3.58 results in

$$w_3(z') =$$
$$-2.92k^2L_1^{-2}L_2^{-2}\left\{\int_{-\left(\frac{L_1+L_2}{2}\right)}^{\frac{L_1-L_2}{2}} du\left(u+\frac{L_2+L_1}{2}\right)g_3(u)+L_1\int_{\frac{L_1-L_2}{2}}^{\frac{L_2-L_1}{2}} du\, g_3(u)\right.$$
$$\left.+\int_{\frac{L_2-L_1}{2}}^{\frac{L_1+L_2}{2}}\left(\frac{L_1+L_2}{2}-u\right)g_3(u)\right\} \qquad (3.60)$$

where $g_3(u)$ has evolved to the following expression

$$g_3(u) = \left\{\left[\Delta p_x\frac{z'}{z_s}+\left(-\Delta x+\frac{L_2-L_1}{2}\right)\left(1-\frac{z'}{z_s}\right)\right]^2+\left[u\left(1-\frac{z'}{z_s}\right)\right]^2\right\}^{\frac{5}{6}}$$
$$-\left\{\left[\Delta p_x\frac{z'}{z_s}+\left(-\Delta x-\frac{L_1+L_2}{2}\right)\left(1-\frac{z'}{z_s}\right)\right]^2+\left[u\left(1-\frac{z'}{z_s}\right)\right]^2\right\}^{\frac{5}{6}}$$
$$-\left\{\left[\Delta p_x\frac{z'}{z_s}+\left(-\Delta x+\frac{L_1+L_2}{2}\right)\left(1-\frac{z'}{z_s}\right)\right]^2+\left[u\left(1-\frac{z'}{z_s}\right)\right]^2\right\}^{\frac{5}{6}}$$
$$+\left\{\left[\Delta p_x\frac{z'}{z_s}+\left(-\Delta x+\frac{L_1-L_2}{2}\right)\left(1-\frac{z'}{z_s}\right)\right]^2+\left[u\left(1-\frac{z'}{z_s}\right)\right]^2\right\}^{\frac{5}{6}} \qquad (3.61)$$

Letting $\gamma = \Delta p_x\left(\frac{z'}{z_s}\right)-\Delta x$ and performing some algebraic expansions, $g_3(u)$ can be written as

$$g_3(u) = \left\{\left[\gamma+\frac{L_2-L_1}{2}+\frac{z'}{z_s}\left(\Delta x-\frac{L_2-L_1}{2}\right)\right]^2+\left[u\left(1-\frac{z'}{z_s}\right)\right]^2\right\}^{\frac{5}{6}}$$
$$-\left\{\left[\gamma-\frac{L_1+L_2}{2}+\frac{z'}{z_s}\left(\Delta x+\frac{L_1+L_2}{2}\right)\right]^2+\left[u\left(1-\frac{z'}{z_s}\right)\right]^2\right\}^{\frac{5}{6}}$$
$$-\left\{\left[\gamma+\frac{L_1+L_2}{2}+\frac{z'}{z_s}\left(\Delta x-\frac{L_1+L_2}{2}\right)\right]^2+\left[u\left(1-\frac{z'}{z_s}\right)\right]^2\right\}^{\frac{5}{6}}$$
$$+\left\{\left[\gamma+\frac{L_1-L_2}{2}+\frac{z'}{z_s}\left(\Delta x-\frac{L_1-L_2}{2}\right)\right]^2+\left[u\left(1-\frac{z'}{z_s}\right)\right]^2\right\}^{\frac{5}{6}} \qquad (3.62)$$

The first step in making the integrals over u dimensionless is to let R be the ratio of $\frac{L_1}{L_2}$. The result is

$$w_3(z') =$$
$$2.92k^2R^{-2}L_2^{-4}\left\{\int_{-\left(\frac{L_2(R+1)}{2}\right)}^{\frac{L_2(R-1)}{2}} du\left(u+\frac{L_2(1+R)}{2}\right)g_3(u)+RL_2\int_{\frac{L_2(R-1)}{2}}^{\frac{L_2(1-R)}{2}} du\, g_3(u)\right.$$

$$+\int_{\frac{L_2(1-R)}{2}}^{\frac{L_2(R+1)}{2}}\left(\frac{L_2(R+1)}{2}-u\right)g_3(u)\Bigg\} \tag{3.63}$$

where

$$\begin{aligned}
g_3(u) = &\left\{\left[\gamma+\frac{L_2(1-R)}{2}+\frac{z'}{z_s}\left(\Delta x-\frac{L_2(1-R)}{2}\right)\right]^2+\left[u\left(1-\frac{z'}{z_s}\right)\right]^2\right\}^{\frac{5}{6}} \\
&-\left\{\left[\gamma-\frac{L_2(R+1)}{2}+\frac{z'}{z_s}\left(\Delta x+\frac{L_2(R+1)}{2}\right)\right]^2+\left[u\left(1-\frac{z'}{z_s}\right)\right]^2\right\}^{\frac{5}{6}} \\
&-\left\{\left[\gamma+\frac{L_2(R+1)}{2}+\frac{z'}{z_s}\left(\Delta x-\frac{L_2(R+1)}{2}\right)\right]^2+\left[u\left(1-\frac{z'}{z_s}\right)\right]^2\right\}^{\frac{5}{6}} \\
&+\left\{\left[\gamma+\frac{L_2(R-1)}{2}+\frac{z'}{z_s}\left(\Delta x-\frac{L_2(R-1)}{2}\right)\right]^2+\left[u\left(1-\frac{z'}{z_s}\right)\right]^2\right\}^{\frac{5}{6}}
\end{aligned} \tag{3.64}$$

Making the change of variables $u' = \frac{u}{L_2}$ reduces $w_3(z')$ to

$$\begin{aligned}
&w_3(z') = \\
&2.92k^2R^{-2}L_2^{-\frac{1}{3}}\left\{\int_{-\left(\frac{(R+1)}{2}\right)}^{\frac{(R-1)}{2}}\mathrm{d}u'\left(u'+\frac{(1+R)}{2}\right)g_3(u')+R\int_{\frac{(R-1)}{2}}^{\frac{(1-R)}{2}}\mathrm{d}u'\,g_3(u')\right. \\
&\qquad\left.+\int_{\frac{(1-R)}{2}}^{\frac{(R+1)}{2}}\left(\frac{(R+1)}{2}-u'\right)g_3(u')\right\}
\end{aligned} \tag{3.65}$$

where

$$\begin{aligned}
g_3(u') = &\left\{\left[\frac{\gamma}{L_2}+\frac{(1-R)}{2}+\frac{z'}{z_s}\left(\frac{\Delta x}{L_2}-\frac{(1-R)}{2}\right)\right]^2+\left[u'\left(1-\frac{z'}{z_s}\right)\right]^2\right\}^{\frac{5}{6}} \\
&-\left\{\left[\frac{\gamma}{L_2}-\frac{(R+1)}{2}+\frac{z'}{z_s}\left(\frac{\Delta x}{L_2}+\frac{(R+1)}{2}\right)\right]^2+\left[u'\left(1-\frac{z'}{z_s}\right)\right]^2\right\}^{\frac{5}{6}} \\
&-\left\{\left[\frac{\gamma}{L_2}+\frac{(R+1)}{2}+\frac{z'}{z_s}\left(\frac{\Delta x}{L_2}-\frac{(R+1)}{2}\right)\right]^2+\left[u'\left(1-\frac{z'}{z_s}\right)\right]^2\right\}^{\frac{5}{6}} \\
&+\left\{\left[\frac{\gamma}{L_2}+\frac{(R-1)}{2}+\frac{z'}{z_s}\left(\frac{\Delta x}{L_2}-\frac{(R-1)}{2}\right)\right]^2+\left[u'\left(1-\frac{z'}{z_s}\right)\right]^2\right\}^{\frac{5}{6}}
\end{aligned} \tag{3.66}$$

This completes the evaluation of the third term in equation 3.16. The third term is given by

$$\text{Term 3} = \int \mathrm{d}z'\,C_n^2(z')\,w_3(z') \tag{3.67}$$

where $w_3(z')$ is given in equation 3.65 above. The three terms in equation 3.16 are combined in the next section.

3.3.6 Combination of Terms Equation 3.16 has been broken into three terms and each term evaluated separately. The three terms may now be combined to yield

$$\langle C_s \rangle = \int \mathrm{d}z'\, C_n^2(z')\, w_C(z') \tag{3.68}$$

where $w_C(z') = w_1(z') + w_2(z') - w_3(z')$. Using the results derived previously, and letting $R = \frac{L_1}{L_2}$, $w_C(z')$ may be written as

$$\begin{aligned}
w_C(z') = {} & -1.46k^2 L_2^{-\frac{1}{3}} R^{-\frac{1}{3}} \int_{-1}^{1} \mathrm{d}u'\, \mathrm{tri}(u') \\
& \times \left\{ 2\left\{ \left[\frac{\gamma}{RL_2} + \left(\frac{z'}{z_s}\right) \frac{\Delta x}{RL_2} \right]^2 + \left[u'\left(1 - \frac{z'}{z_s}\right) \right]^2 \right\}^{\frac{5}{6}} \right. \\
& - \left\{ \left[\frac{\gamma}{RL_2} - 1 + \frac{z'}{z_s}\left(\frac{\Delta x}{RL_2} + 1\right) \right]^2 + \left[u'\left(1 - \frac{z'}{z_s}\right) \right]^2 \right\}^{\frac{5}{6}} \\
& \left. - \left\{ \left[\frac{\gamma}{RL_2} + 1 + \frac{z'}{z_s}\left(\frac{\Delta x}{RL_2} - 1\right) \right]^2 + \left[u'\left(1 - \frac{z'}{z_s}\right) \right]^2 \right\}^{\frac{5}{6}} \right\} \\
& -1.46k^2 L_2^{-\frac{1}{3}} \int_{-1}^{1} \mathrm{d}u'\, \mathrm{tri}(u') \\
& \times \left\{ 2\left\{ \left[\frac{\gamma}{L_2} + \left(\frac{z'}{z_s}\right) \frac{\Delta x}{L_2} \right]^2 + \left[u'\left(1 - \frac{z'}{z_s}\right) \right]^2 \right\}^{\frac{5}{6}} \right. \\
& - \left\{ \left[\frac{\gamma}{L_2} - 1 + \frac{z'}{z_s}\left(\frac{\Delta x}{L_2} + 1\right) \right]^2 + \left[u'\left(1 - \frac{z'}{z_s}\right) \right]^2 \right\}^{\frac{5}{6}} \\
& \left. - \left\{ \left[\frac{\gamma}{L_2} + 1 + \frac{z'}{z_s}\left(\frac{\Delta x}{L_2} - 1\right) \right]^2 + \left[u'\left(1 - \frac{z'}{z_s}\right) \right]^2 \right\}^{\frac{5}{6}} \right\} \\
& +2.92k^2 R^{-2} L_2^{-\frac{1}{3}} \left\{ \int_{-\left(\frac{(R+1)}{2}\right)}^{\frac{(R-1)}{2}} \mathrm{d}u' \left(u' + \frac{(1+R)}{2} \right) g_3(u') + R \int_{\frac{(R-1)}{2}}^{\frac{(1-R)}{2}} \mathrm{d}u'\, g_3(u') \right. \\
& \qquad \left. + \int_{\frac{(1-R)}{2}}^{\frac{(R+1)}{2}} \left(\frac{(R+1)}{2} - u' \right) g_3(u') \right\}
\end{aligned} \tag{3.69}$$

where

$$g_3(u') = \left\{\left[\frac{\gamma}{L_2} + \frac{(1-R)}{2} + \frac{z'}{z_s}\left(\frac{\Delta x}{L_2} - \frac{(1-R)}{2}\right)\right]^2 + \left[u'\left(1 - \frac{z'}{z_s}\right)\right]^2\right\}^{\frac{5}{6}}$$
$$- \left\{\left[\frac{\gamma}{L_2} - \frac{(R+1)}{2} + \frac{z'}{z_s}\left(\frac{\Delta x}{L_2} + \frac{(R+1)}{2}\right)\right]^2 + \left[u'\left(1 - \frac{z'}{z_s}\right)\right]^2\right\}^{\frac{5}{6}}$$
$$- \left\{\left[\frac{\gamma}{L_2} + \frac{(R+1)}{2} + \frac{z'}{z_s}\left(\frac{\Delta x}{L_2} - \frac{(R+1)}{2}\right)\right]^2 + \left[u'\left(1 - \frac{z'}{z_s}\right)\right]^2\right\}^{\frac{5}{6}}$$
$$+ \left\{\left[\frac{\gamma}{L_2} + \frac{(R-1)}{2} + \frac{z'}{z_s}\left(\frac{\Delta x}{L_2} - \frac{(R-1)}{2}\right)\right]^2 + \left[u'\left(1 - \frac{z'}{z_s}\right)\right]^2\right\}^{\frac{5}{6}} \qquad (3.70)$$

Equation 3.69 is the most general form of $w_C(z')$. However, the path weighting function can be simplified further if the assumption is made that $1 - \frac{z'}{z_s} \approx 1$. This assumption is often valid when the point sources are artificial guide stars created in the mesospheric sodium layer. In this case z_s is on the order of 90 km, and z' is often no greater than 20 km because $C_n^2 \approx 0$ for $z' > 20$km. The simplified form of the path weighting function is

$$w_C(z') = -1.46k^2 L_2^{-\frac{1}{3}} R^{-\frac{1}{3}} \int_{-1}^{1} \mathrm{d}u' \, \mathrm{tri}(u')$$
$$\times \left\{2\left[\left(\frac{\gamma}{RL_2}\right)^2 + u'^2\right]^{\frac{5}{6}} - \left[\left(\frac{\gamma}{RL_2} - 1\right)^2 + u'^2\right]^{\frac{5}{6}} - \left[\left(\frac{\gamma}{RL_2} + 1\right)^2 + u'^2\right]^{\frac{5}{6}}\right\}$$
$$-1.46k^2 L_2^{-\frac{1}{3}} \int_{-1}^{1} \mathrm{d}u' \, \mathrm{tri}(u')$$
$$\times \left\{2\left[\left(\frac{\gamma}{L_2}\right)^2 + u'^2\right]^{\frac{5}{6}} - \left[\left(\frac{\gamma}{L_2} - 1+\right)^2 + u'^2\right]^{\frac{5}{6}} - \left[\left(\frac{\gamma}{L_2} + 1\right)^2 + u'^2\right]^{\frac{5}{6}}\right\}$$
$$+2.92k^2 R^{-2} L_2^{-\frac{1}{3}} \left[\int_{-\left(\frac{(R+1)}{2}\right)}^{\frac{(R-1)}{2}} \mathrm{d}u' \left(u' + \frac{(1+R)}{2}\right) g_3'(u') + R\int_{\frac{(R-1)}{2}}^{\frac{(1-R)}{2}} \mathrm{d}u' \, g_3'(u')\right.$$
$$\left. + \int_{\frac{(1-R)}{2}}^{\frac{(R+1)}{2}} \left(\frac{(R+1)}{2} - u'\right) g_3'(u')\right] \qquad (3.71)$$

where

$$g_3'(u') = \left\{\left[\frac{\gamma}{L_2} + \frac{(1-R)}{2}\right]^2 + [u']^2\right\}^{\frac{5}{6}} - \left\{\left[\frac{\gamma}{L_2} - \frac{(R+1)}{2}\right]^2 + [u']^2\right\}^{\frac{5}{6}}$$
$$- \left\{\left[\frac{\gamma}{L_2} + \frac{(R+1)}{2}\right]^2 + [u']^2\right\}^{\frac{5}{6}} + \left\{\left[\frac{\gamma}{L_2} + \frac{(R-1)}{2}\right]^2 + [u']^2\right\}^{\frac{5}{6}} \qquad (3.72)$$

The simplified path weighting function given by equation 3.71 is examined in the next section. Recall that the z' dependence of $w_C(z')$ is contained in γ, where $\gamma = \Delta p_x \frac{z'}{z_s} - \Delta x$ and may be interpreted as the distance between the optical beams as a function of altitude (see Figure 3.1). In the results which follow, $w_C(z')$ is plotted versus γ rather than z'.

3.4 Form of C_n^2 Path Weighting Function

The form of the C_n^2 path weighting function for the new measurement technique is one of the primary objectives of this research. As already shown in equation 3.68, there is an integral relationship between the measured wave front phase correlations and C_n^2. If the path weighting function $w_C(z')$ approximates a Dirac delta function, then the measured quantity $\langle C_s \rangle$ can be directly related to C_n^2. A normalized plot of the simplified path weighting function given by equation 3.71 is shown in Figure 3.3 for three reasonable values of the ratio $R = \frac{L_1}{L_2}$.

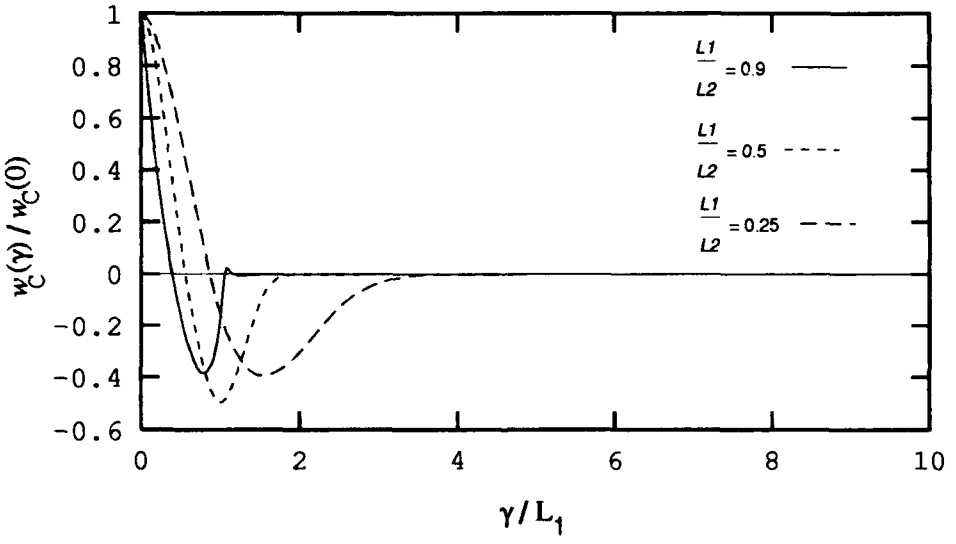

Figure 3.3. Normalized C_n^2 Path Weighting Function

The weighting function displays the desired characteristic of being sharply peaked at the altitude where the optical beams intersect ($\gamma = 0$) and decaying rapidly to zero away from the intersection altitude. The plot is shown one sided because the path weighting

function is symmetrical about the intersection altitude. Notice that the γ values on the x axis of Figure 3.3 are normalized by L_1. As an example, if $L_1 = 10$ cm and $R = 0.9$, then the path weighting function is zero by the time $\gamma = 20$ cm. The figure also demonstrates the role of $R = \frac{L_1}{L_2}$ in shaping the path weighting function. As $R \rightarrow 1$, the path weighting function becomes more sharply peaked. This makes sense because as R approaches one, higher frequencies are being removed from the sensor measurements. In other words, the pass band of the filtering operation accomplished by the subtraction of the measurements is becoming more narrow. This corresponds to reducing the eddy sizes which contribute to the correlation. Such eddies simultaneously intersect both beams only when γ, which is the separation of the two beams, is small. Therefore, as the eddy sizes contributing to the correlation decrease, the correlation decay rate increases.

3.5 Resolution of C_n^2 Path Weighting Function, $w_C(z')$

As Figure 3.3 shows, the path weighting function is not a Dirac delta function, but does have its peak value where the beams intersect and decays to zero away from the intersection point. The width of w_C with respect to z may be considered a measure of the vertical resolution. The narrower $w_C(z)$ is, the better its vertical resolution will be, and thus a more accurate estimate of $C_n^2(z)$ will be obtained.

A method similar to that presented by Rejack (17) is used to measure the vertical resolution. Recall from Figure 3.1 that the transverse distance between the two optical beams is given by

$$\gamma = \Delta p_x \frac{z'}{z_s} - \Delta x \tag{3.73}$$

where Δp_x is the source separation, z_s is the source altitude, and Δx is the sensor separation. The altitude z_0 where the optical beams cross is found by setting $\gamma = 0$ and solving for z_0

$$z_0 = \frac{\Delta x \, z_s}{\Delta p_x} \tag{3.74}$$

Now let the measure of the width of $w_C(z')$ be the point $\gamma = \gamma'$ where γ' is the one

sided root mean square (rms) width of $w_C\left(\frac{\gamma}{L_1}\right)$ defined by

$$\gamma' = L_1 \frac{\int_0^\infty \left(\frac{\gamma}{L_1}\right)^2 w_C\left(\frac{\gamma}{L_1}\right) \mathrm{d}\frac{\gamma}{L_1}}{\int_0^\infty w_C\left(\frac{\gamma}{L_1}\right) \mathrm{d}\frac{\gamma}{L_1}} \tag{3.75}$$

Denote the altitude corresponding to γ' as $z_{\gamma'}$, where

$$z_{\gamma'} = \frac{(\gamma' + \Delta x) z_s}{\Delta p_x} \tag{3.76}$$

Due to the even symmetry of the path weighting function about the intersection altitude, the width of w_C with respect to z is

$$\Delta z = 2(z_0 - z_{\gamma'}) = \frac{2\gamma' z_s}{\Delta p_x} \tag{3.77}$$

Let θ denote the angle between the optical beams. Referring to Figure 3.1, basic geometry yields

$$\frac{\theta}{2} = \arctan\left(\frac{\Delta p_x}{2(z_s - z_0)}\right) \tag{3.78}$$

The assumption that $z_s \gg z_0$ allows θ to be equated to the angular separation of the sources given by

$$\frac{\theta}{2} = \arctan\left(\frac{\Delta p_x}{2z_s}\right) \tag{3.79}$$

Solving for Δp_x yields

$$\Delta p_x = 2z_s \tan\left(\frac{\theta}{2}\right) \tag{3.80}$$

Substituting equation 3.80 into equation 3.77 results in

$$\Delta z = \frac{\gamma'}{\tan\left(\frac{\theta}{2}\right)} \tag{3.81}$$

All the expressions necessary to calculate the vertical resolution of $w_C(z')$ are now present. An example calculation can be performed based upon the results in Figure 3.3. For $R = 0.9$ and $L_1 = 10$ cm, the rms width of $w_C(z_0)$ is $\gamma' = 0.136$ m. Using this value in equation 3.81 yields the vertical resolution as a function of θ plotted in Figure 3.4.

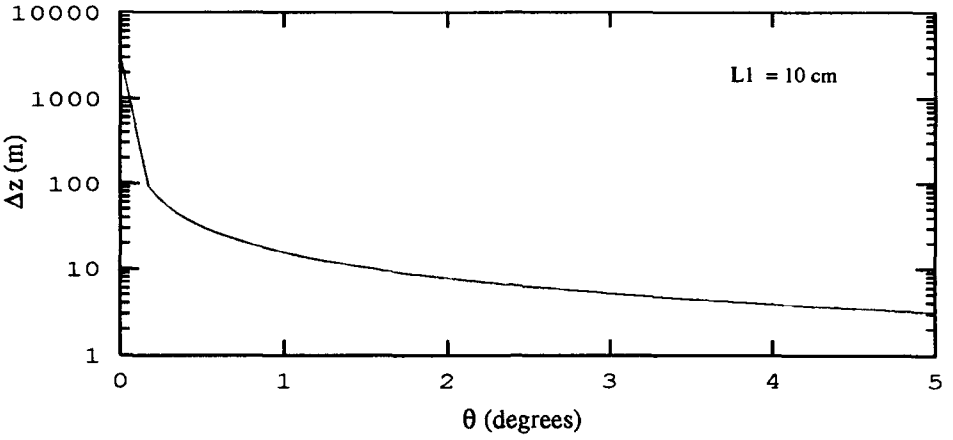

Figure 3.4. Vertical Resolution of w_C

The figure demonstrates the relationship of the vertical resolution to the separation of the point sources. As the point source separation increases, so does the vertical resolution. The reason for this behavior is that a larger source separation increases the angle at which the beams intersect. As a result, less vertical movement away from the intersection altitude is needed to reach a point where the separation of the beams is greater than the size of the eddies which are contributing to the measurement correlations.

3.6 Derivation of $\vec{V}$ Path Weighting Function

3.6.1 Overview The second objective of this research is to extend the new measurement technique to the remote sensing of transverse atmospheric winds. Accordingly, the goal of this derivation is to relate the derivative of $\langle C_s(\tau)\rangle$ with respect to τ to the vertical wind profile $\vec{V}$ through

$$\langle C_s'(0)\rangle = \left.\frac{\partial\langle[s_1(t) - s_{1'}(t)][s_2(t+\tau) - s_{2'}(t+\tau)]\rangle}{\partial\tau}\right|_{\tau=0} = \int \mathrm{d}z'\, C_n^2(z')\vec{V}(z')\cdot\vec{w}_V(z') \tag{3.82}$$

where $\langle C_s'(\tau)\rangle$ is the partial derivative with respect to τ of $\langle C_s(\tau)\rangle$, z' is a position along the optical path, and $\vec{w}_V(z')$ is the wind path weighting function. This derivation closely parallels the C_n^2 path weighting function derivation just completed and will often refer to it. Eventually, the path weighting function is reduced to an expression that depends

only upon the measurement geometry. The reasons for taking the partial derivative with respect to τ and evaluating it at $\tau = 0$ will be discussed at the appropriate points within the derivation. The first step in this derivation is to find an expression for $C_s(\tau)$.

3.6.2 Slope Signal Time-lagged Correlation As shown above, the single realization time-lagged correlation is defined as

$$C_s(\tau) = [s_1(t) - s_{1'}(t)][s_2(t+\tau) - s_{2'}(t+\tau)] \tag{3.83}$$

where $s_n(t)$ is the output of slope sensor n at time t and τ is the time delay between measurements. Using the wave front slope sensor output model given by equation 3.10, equation 3.83 can be written as

$$\begin{aligned} C_s(\tau) = & \\ & \left\{\left[-\int \mathrm{d}^2\vec{x}\, W^s_{L_1}(\vec{x})\phi_1(\vec{x},t) + \alpha_1(t)\right] - \left[-\int \mathrm{d}^2\vec{x}'\, W^s_{L_2}(\vec{x}')\phi_1(\vec{x}',t) + \alpha_{1'}(t)\right]\right\} \\ & \times \left\{\left[-\int \mathrm{d}^2\vec{x}''\, W^s_{L_1}(\vec{x}'' - \Delta\vec{x})\phi_2(\vec{x}'', t+\tau) + \alpha_2(t+\tau)\right]\right. \\ & \left. - \left[-\int \mathrm{d}^2\vec{x}'''\, W^s_{L2}(\vec{x}''' - \Delta\vec{x})\phi_2(\vec{x}''', t+\tau) + \alpha_{2'}(t+\tau)\right]\right\} \end{aligned} \tag{3.84}$$

where $\alpha_n(t)$ is the slope measurement noise from sensor n at time t and $\phi_n(\vec{x},t)$ is the wave front phase arriving from source n at time t. Performing the multiplication results in

$$\begin{aligned} C_s(\tau) = & \int \mathrm{d}^2\vec{x} \int \mathrm{d}^2\vec{x}''\, W^s_{L_1}(\vec{x}) W^s_{L_1}(\vec{x}'' - \Delta\vec{x})\,[\phi_1(\vec{x},t)\phi_2(\vec{x}'', t+\tau)] \\ & - \int \mathrm{d}^2\vec{x}\, W^s_{L_1}(\vec{x})\phi_1(\vec{x},t)\alpha_2(t+\tau) \\ & - \int \mathrm{d}^2\vec{x}''\, W^s_{L_1}(\vec{x}'' - \Delta\vec{x})\phi_2(\vec{x}'', t+\tau)\alpha_1(t) \\ & + \alpha_1(t)\alpha_2(t+\tau) \\ & + \int \mathrm{d}^2\vec{x}' \int \mathrm{d}^2\vec{x}'''\, W^s_{L_2}(\vec{x}') W^s_{L_2}(\vec{x}''' - \Delta\vec{x})\,[\phi_1(\vec{x}',t)\phi_2(\vec{x}''', t+\tau)] \\ & - \int \mathrm{d}^2\vec{x}'\, W^s_{L_2}(\vec{x}')\phi_1(\vec{x}',t)\alpha_{2'}(t+\tau) \\ & - \int \mathrm{d}^2\vec{x}'''\, W^s_{L_2}(\vec{x}''' - \Delta\vec{x})\phi_2(\vec{x}''', t+\tau)\alpha_{1'}(t) \\ & + \alpha_{1'}(t)\alpha_{2'}(t+\tau) \end{aligned}$$

$$
\begin{aligned}
&- \int \mathrm{d}^2\vec{x}' \int \mathrm{d}^2\vec{x}'' \, W^s_{L_2}(\vec{x}') W^s_{L_1}(\vec{x}'' - \Delta\vec{x}) \left[\phi_1(\vec{x}', t)\phi_2(\vec{x}'', t+\tau)\right] \\
&+ \int \mathrm{d}^2\vec{x}' \, W^s_{L_2}(\vec{x})\phi_1(\vec{x}, t)\alpha_2(t+\tau) \\
&+ \int \mathrm{d}^2\vec{x}'' \, W^s_{L_1}(\vec{x}'' - \Delta\vec{x})\phi_2(\vec{x}'', t+\tau)\alpha_{1'}(t) \\
&-\alpha_{1'}(t)\alpha_2(t+\tau) \\
&- \int \mathrm{d}^2\vec{x} \int \mathrm{d}^2\vec{x}''' \, W^s_{L_1}(\vec{x}) W^s_{L_2}(\vec{x}''' - \Delta\vec{x}) \left[\phi_1(\vec{x}, t)\phi_2(\vec{x}''', t+\tau)\right] \\
&+ \int \mathrm{d}^2\vec{x} \, W^s_{L_1}(\vec{x})\phi_1(\vec{x}, t)\alpha_{2'}(t+\tau) \\
&+ \int \mathrm{d}^2\vec{x}''' \, W^s_{L_2}(\vec{x}''' - \Delta\vec{x})\phi_2(\vec{x}''', t+\tau)\alpha_1(t) \\
&-\alpha_1(t)\alpha_{2'}(t+\tau)
\end{aligned}
\tag{3.85}
$$

Once again, further progress requires a statistical approach. Assuming that α_n is a zero mean random process independent of ϕ_n, and using the fact that the noise processes from separate apertures are uncorrelated (see equation 3.14), the ensemble average of equation 3.85 is

$$
\begin{aligned}
\langle C_s(\tau)\rangle = &\int \mathrm{d}^2\vec{x} \int \mathrm{d}^2\vec{x}'' \, W^s_{L_1}(\vec{x}) W^s_{L_1}(\vec{x}'' - \Delta\vec{x}) \langle\phi_1(\vec{x}, t)\phi_2(\vec{x}'', t+\tau)\rangle \\
&+ \int \mathrm{d}^2\vec{x}' \int \mathrm{d}^2\vec{x}''' \, W^s_{L_2}(\vec{x}') W^s_{L_2}(\vec{x}''' - \Delta\vec{x}) \langle\phi_1(\vec{x}', t)\phi_2(\vec{x}''', t+\tau)\rangle \\
&- \int \mathrm{d}^2\vec{x}' \int \mathrm{d}^2\vec{x}'' \, W^s_{L_2}(\vec{x}') W^s_{L_1}(\vec{x}'' - \Delta\vec{x}) \langle\phi_1(\vec{x}', t)\phi_2(\vec{x}'', t+\tau)\rangle \\
&- \int \mathrm{d}^2\vec{x} \int \mathrm{d}^2\vec{x}''' \, W^s_{L_1}(\vec{x}) W^s_{L_2}(\vec{x}''' - \Delta\vec{x}) \langle\phi_1(\vec{x}, t)\phi_2(\vec{x}''', t+\tau)\rangle
\end{aligned}
\tag{3.86}
$$

The third and fourth terms of equation 3.86 can be combined for the same reasons that the third and fourth terms of equation 3.15 were combined. Thus, the ensemble average is given by

$$
\begin{aligned}
\langle C_s(\tau)\rangle = &\int \mathrm{d}^2\vec{x} \int \mathrm{d}^2\vec{x}'' \, W^s_{L_1}(\vec{x}) W^s_{L_1}(\vec{x}'' - \Delta\vec{x}) \langle\phi_1(\vec{x}, t)\phi_2(\vec{x}'', t+\tau)\rangle \\
&+ \int \mathrm{d}^2\vec{x}' \int \mathrm{d}^2\vec{x}''' \, W^s_{L_2}(\vec{x}') W^s_{L_2}(\vec{x}''' - \Delta\vec{x}) \langle\phi_1(\vec{x}', t)\phi_2(\vec{x}''', t+\tau)\rangle \\
&-2 \int \mathrm{d}^2\vec{x}' \int \mathrm{d}^2\vec{x}'' \, W^s_{L_2}(\vec{x}') W^s_{L_1}(\vec{x}'' - \Delta\vec{x}) \langle\phi_1(\vec{x}', t)\phi_2(\vec{x}'', t+\tau)\rangle
\end{aligned}
\tag{3.87}
$$

Equation 3.87 consists of three terms. Each of these terms is evaluated separately

and the results combined.

3.6.3 Evaluation of First Term in $\langle C_s(\tau)\rangle$ The first term of equation 3.87 is given by

$$\text{Term 1} = \int \mathrm{d}^2\vec{x} \int \mathrm{d}^2\vec{x}'' \, W^s_{L_1}(\vec{x}) W^s_{L_1}(\vec{x}'' - \Delta\vec{x}) \langle \phi_1(\vec{x}, t)\phi_2(\vec{x}'', t+\tau)\rangle \tag{3.88}$$

where $\langle \phi_1(\vec{x}, t)\phi_2(\vec{x}'', t+\tau)\rangle$ is the cross correlation of the wave front phases. Once again, the cross correlation of the wave front phases corresponds to the structure function as

$$\langle \phi_1(\vec{x}, t)\phi_2(\vec{x}'', t+\tau)\rangle = -\frac{1}{2} D_{12}(\vec{x}, \vec{x}'', \tau) + \frac{1}{2}\langle \phi_1^2(\vec{x}, t)\rangle + \frac{1}{2}\langle \phi_2^2(\vec{x}'', t+\tau)\rangle \tag{3.89}$$

where the structure function is now defined as

$$D_{12}(\vec{x}, \vec{x}'', \tau) = \langle [\phi_1(\vec{x}, t) - \phi_2(\vec{x}'', t+\tau)]^2 \rangle \tag{3.90}$$

Due to the odd symmetry of $W^s_n(\vec{x})$ and the fact that ϕ_1 and ϕ_2 are wide sense stationary processes, only the term containing $D_{12}(\vec{x}, \vec{x}'', \tau)$ will yield a non-zero result when equation 3.89 is placed in equation 3.88. An expression for $D_{12}(\vec{x}, \vec{x}'')$ is given in equation 3.21. However, equation 3.89 requires that the time lag be accounted for in the structure function. This is accomplished in the same manner used by Lee and Harp, which is to replace $(\vec{x} - \vec{x}'')\left(1 - \frac{z'}{z_s}\right)$ in equation 3.21 with $(\vec{x} - \vec{x}'')\left(1 - \frac{z'}{z_s}\right) - \vec{V}(z')\tau$. This substitution accounts for the distance traveled by the turbulent eddies between measurements. Figure 3.5 illustrates the situation. Recall that the measurement of ϕ_2 is made τ seconds after the measurement of ϕ_1. The eddy present at a point z' along the ray path from p_2 at time t was a distance $-\vec{V}(z')\tau$ away at time $t - \tau$. Thus, the time-lagged measurements are equivalent to making simultaneous measurements for the geometry depicted with dotted lines in Figure 3.5. Making such a statement requires use of Taylor's frozen flow hypothesis, which assumes that the eddies do not decay as they are blown across the optical line of sight (19). So, making the substitution into the structure function given by Lutomirski and Buser yields

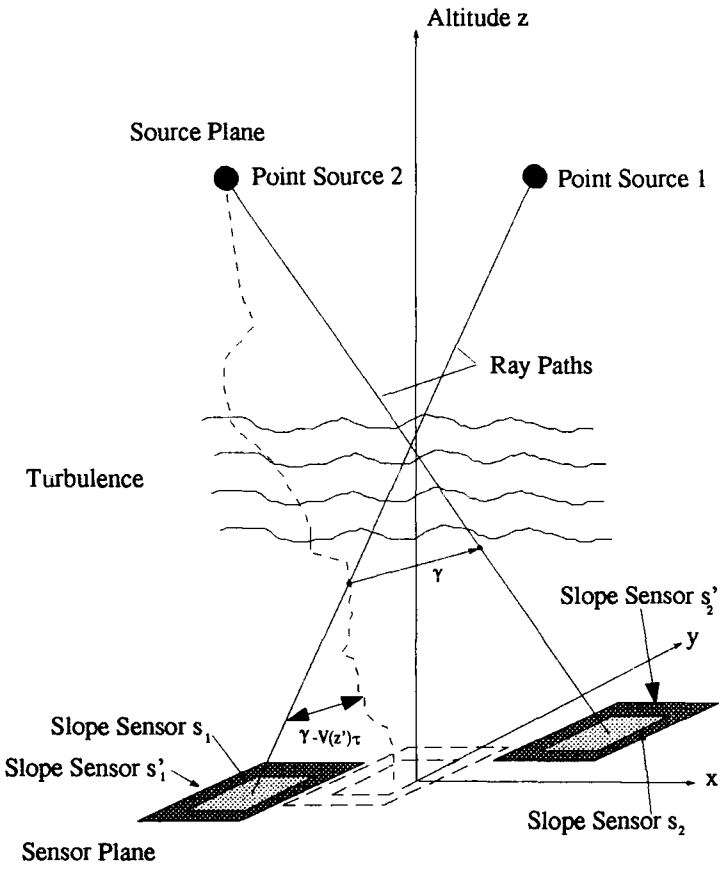

Figure 3.5. Effect of $\vec{V}$ on Measurement Geometry

$$D_{12}(\vec{x}-\vec{x}'',\tau) = 8\pi^2 k^2 \int \mathrm{d}z' \int \mathrm{d}K_\perp \, \Phi_n(K_\perp, 0, z') \times \left\{1 - J_0\left(K_\perp \left|(\Delta\vec{p})\left(\frac{z'}{z_s}\right) + (\vec{x}-\vec{x}'')\left(1-\frac{z'}{z_s}\right) - \vec{V}(z')\tau\right|\right)\right\} \qquad (3.91)$$

where, as before,

$\Phi_n(K_\perp, K_z, z')$ is the psd of the fluctuations of the index of refraction,

$\Delta\vec{p}$ is the vector separation of the sources,

J_0 is the zero order Bessel function,

z' is the distance from the aperture plane to some point along the z axis,

z_s is the altitude of the point sources,

and $\vec{x}$ and $\vec{x}''$ are points in the aperture plane of the optical system.

Substituting equation 3.91 into equation 3.88 and using equations 3.22 and 3.26 to describe the psd of the fluctuations of the index of refraction, the first term in equation 3.87 is

$$\begin{aligned}\text{Term 1} = & \\ & -4\pi^2 k^2 \int_0^{z_s} \mathrm{d}z'\, C_n^2(z') \int \mathrm{d}^2\vec{x} \int \mathrm{d}^2\vec{x}''\, W_{L_1}^s(\vec{x}) W_{L_1}^s(\vec{x}'' - \Delta\vec{x}) \\ & \times \int_0^{\infty} \mathrm{d}K_\perp\, 0.033 K_\perp^{-\frac{8}{3}} \\ & \times \left\{ 1 - J_0\left(K_\perp \left| (\Delta\vec{p}) \left(\frac{z'}{z_s}\right) + (\vec{x} - \vec{x}'') \left(1 - \frac{z'}{z_s}\right) - \vec{V}(z')\tau \right| \right) \right\} \end{aligned} \tag{3.92}$$

Performing the integration over $K_\perp$ in a similar fashion to the integration shown in equations 3.28 through 3.30 yields

$$\begin{aligned}\text{Term 1} = -1.46k^2 \int_0^{z_s} \mathrm{d}z'\, C_n^2(z') \int \mathrm{d}^2\vec{x} \int \mathrm{d}^2\vec{x}''\, W_{L_1}^s(\vec{x}) W_{L_1}^s(\vec{x}'' - \Delta\vec{x}) \\ \times \left| (\Delta\vec{p}) \left(\frac{z'}{z_s}\right) + (\vec{x} - \vec{x}'') \left(1 - \frac{z'}{z_s}\right) - \vec{V}(z')\tau \right|^{\frac{5}{3}} \end{aligned} \tag{3.93}$$

which may also be written as

$$\begin{aligned}\text{Term 1} = -1.46k^2 \int_0^{z_s} \mathrm{d}z'\, C_n^2(z') \int \mathrm{d}^2\vec{x} \int \mathrm{d}^2\vec{x}''\, W_{L_1}^s(\vec{x}) W_{L_1}^s(\vec{x}'' - \Delta\vec{x}) \\ \times \left\{ \left[\Delta p_x \frac{z'}{z_s} + (x - x'') \left(1 - \frac{z'}{z_s}\right) - V_x(z')\tau \right]^2 + \left[\Delta p_y \frac{z'}{z_s} + (y - y'') \left(1 - \frac{z'}{z_s}\right) - V_y(z')\tau \right]^2 \right\}^{\frac{5}{6}} \end{aligned} \tag{3.94}$$

where V_x and V_y are the x- and y-directed components of $\vec{V}$, Δp_x and Δp_y are the x- and y-directed components of $\Delta\vec{p}$, x and y are the x and y directed components of $\vec{x}$, and x'' and y'' are the x and y directed components of $\vec{x}''$. To facilitate a later step where the above equation is differentiated with respect to τ, some algebraic manipulation of the squared terms results in

$$\text{Term 1} = -1.46k^2 \int_0^{z_s} \mathrm{d}z'\, C_n^2(z') \int \mathrm{d}^2\vec{x} \int \mathrm{d}^2\vec{x}''\, W_{L_1}^s(\vec{x}) W_{L_1}^s(\vec{x}'' - \Delta\vec{x})$$
$$\times \left\{ \left[\Delta p_x \frac{z'}{z_s} + (x - x'') \left(1 - \frac{z'}{z_s}\right) \right]^2 + V_x^2(z')\tau^2 - 2V_x(z')\tau \left[\Delta p_x \frac{z'}{z_s} + (x - x'') \left(1 - \frac{z'}{z_s}\right) \right] \right.$$
$$\left. + \left[\Delta p_y \frac{z'}{z_s} + (y - y'') \left(1 - \frac{z'}{z_s}\right) \right]^2 + V_y^2(z')\tau^2 - 2V_y(z')\tau \left[\Delta p_y \frac{z'}{z_s} + (y - y'') \left(1 - \frac{z'}{z_s}\right) \right] \right\}^{\frac{5}{6}} \tag{3.95}$$

For now, Term 1 will be left in the form given by equation 3.95. Differentiation of this expression with respect to τ is easily accomplished, so further simplification is not necessary.

3.6.4 Evaluation of Second and Third Terms in $\langle C_s(\tau) \rangle$ Notice that the second and third terms in equation 3.87 have the same form as Term 1 with two exceptions: they contain different dummy variables of integration, and they contain different aperture weighting functions. The different dummy variables of integration are of no consequence. Additionally, no information about the aperture weighting functions in Term 1 was necessary to obtain equation 3.95. Thus, the second and third terms can both be expressed in a form identical to equation 3.95, but with $W_{L_1}^s$ replaced with the appropriate aperture weighting function gradient. The second term in equation 3.87 is

$$\text{Term 2} = -1.46k^2 \int_0^{z_s} \mathrm{d}z'\, C_n^2(z') \int \mathrm{d}^2\vec{x}' \int \mathrm{d}^2\vec{x}'''\, W_{L_2}^s(\vec{x}') W_{L_2}^s(\vec{x}''' - \Delta\vec{x})$$
$$\times \left\{ \left[\Delta p_x \frac{z'}{z_s} + (x' - x''') \left(1 - \frac{z'}{z_s}\right) \right]^2 + V_x^2(z')\tau^2 - 2V_x(z')\tau \left[\Delta p_x \frac{z'}{z_s} + (x' - x''') \left(1 - \frac{z'}{z_s}\right) \right] \right.$$
$$\left. + \left[\Delta p_y \frac{z'}{z_s} + (y' - y''') \left(1 - \frac{z'}{z_s}\right) \right]^2 + V_y^2(z')\tau^2 - 2V_y(z')\tau \left[\Delta p_y \frac{z'}{z_s} + (y' - y''') \left(1 - \frac{z'}{z_s}\right) \right] \right\}^{\frac{5}{6}} \tag{3.96}$$

and the third term is

$$\text{Term 3} = 2.92k^2 \int_0^{z_s} \mathrm{d}z'\, C_n^2(z') \int \mathrm{d}^2\vec{x}' \int \mathrm{d}^2\vec{x}''\, W_{L_2}^s(\vec{x}') W_{L_1}^s(\vec{x}'' - \Delta\vec{x})$$
$$\times \left\{ \left[\Delta p_x \frac{z'}{z_s} + (x' - x'') \left(1 - \frac{z'}{z_s}\right) \right]^2 + V_x^2(z')\tau^2 - 2V_x(z')\tau \left[\Delta p_x \frac{z'}{z_s} + (x' - x'') \left(1 - \frac{z'}{z_s}\right) \right] \right.$$

$$+\left[\Delta p_y \frac{z'}{z_s} + (y' - y'')\left(1 - \frac{z'}{z_s}\right)\right]^2 + V_y^2(z')\tau^2 - 2V_y(z')\tau\left[\Delta p_y \frac{z'}{z_s} + (y' - y'')\left(1 - \frac{z'}{z_s}\right)\right]\Bigg\}^{\frac{5}{6}} \tag{3.97}$$

These three terms will be combined and the result differentiated with respect to τ in the next section.

3.6.5 Differentiation of $\langle C_s(\tau)\rangle$ With Respect to τ The previous section has provided equations for the three terms that compose $\langle C_s(\tau)\rangle$. The next step in arriving at an expression with the form given by equation 3.82 is to combine the three terms and differentiate the sum with respect to τ. Setting $\tau = 0$ in the result of the differentiation yields an expression of the desired form. Before taking these steps, however, some justification of these steps is necessary.

One of the first techniques for sensing $\vec{V}$ using crossed optical beams was to measure the difference in the time of arrival of a turbulent eddy at one beam and its time of arrival at a second beam. This time delay τ can be measured by making time-lagged correlations of the optical beams' wave front phases. The correlation is calculated for several values of τ, and the value of τ which yields the peak correlation value is used to compute $\vec{V}$. However, Lawrence *et al* have pointed out that this method gives results which are systematically high, particularly for low wind velocities (10). At low wind velocities, eddy decay causes the turbulence crossing the second beam to bear little resemblance to that crossing the first beam. Therefore, the correlation peak occurs sooner than it should, and an alternate approach is needed.

This problem can be avoided by measuring the slope of the correlation function at $\tau = 0$. In practice, the slope can be measured by subtracting the correlation value at time t from the correlation value at time $t + \tau$ and dividing the result by τ. The time difference τ can be sufficiently small that there is little eddy decay between measurements. Evaluating the slope at $\tau = 0$ results in an expression with the form of equation 3.82. Analytically, differentiating the time-lagged correlation function with respect to τ yields an expression for the slope, and setting $\tau = 0$ evaluates the slope at zero time lag.

Proceeding with the derivation, terms 1, 2, and 3 are combined to yield

$$
\begin{aligned}
&\langle C_s(\Delta\vec{x},\tau)\rangle = \\
&\quad -1.46k^2\int_0^{z_s} \mathrm{d}z'\, C_n^2(z') \int \mathrm{d}^2\vec{x} \int \mathrm{d}^2\vec{x}''\, W_{L_1}^s(\vec{x}) W_{L_1}^s(\vec{x}'' - \Delta\vec{x}) \\
&\quad \times \left\{ \left[\Delta p_x \frac{z'}{z_s} + (x - x'') \left(1 - \frac{z'}{z_s}\right) \right]^2 + V_x^2(z')\tau^2 - 2V_x(z')\tau \left[\Delta p_x \frac{z'}{z_s} + (x - x'') \left(1 - \frac{z'}{z_s}\right) \right] \right. \\
&\quad \left. + \left[\Delta p_y \frac{z'}{z_s} + (y - y'') \left(1 - \frac{z'}{z_s}\right) \right]^2 + V_y^2(z')\tau^2 - 2V_y(z')\tau \left[\Delta p_y \frac{z'}{z_s} + (y - y'') \left(1 - \frac{z'}{z_s}\right) \right] \right\}^{\frac{5}{6}} \\
&\quad -1.46k^2\int_0^{z_s} \mathrm{d}z'\, C_n^2(z') \int \mathrm{d}^2\vec{x}' \int \mathrm{d}^2\vec{x}'''\, W_{L_2}^s(\vec{x}') W_{L_2}^s(\vec{x}''' - \Delta\vec{x}) \\
&\quad \times \left\{ \left[\Delta p_x \frac{z'}{z_s} + (x' - x''') \left(1 - \frac{z'}{z_s}\right) \right]^2 + V_x^2(z')\tau^2 - 2V_x(z')\tau \left[\Delta p_x \frac{z'}{z_s} + (x' - x''') \left(1 - \frac{z'}{z_s}\right) \right] \right. \\
&\quad \left. + \left[\Delta p_y \frac{z'}{z_s} + (y' - y''') \left(1 - \frac{z'}{z_s}\right) \right]^2 + V_y^2(z')\tau^2 - 2V_y(z')\tau \left[\Delta p_y \frac{z'}{z_s} + (y' - y''') \left(1 - \frac{z'}{z_s}\right) \right] \right\}^{\frac{5}{6}} \\
&\quad +2.92k^2\int_0^{z_s} \mathrm{d}z'\, C_n^2(z') \int \mathrm{d}^2\vec{x}' \int \mathrm{d}^2\vec{x}''\, W_{L_2}^s(\vec{x}') W_{L_1}^s(\vec{x}'' - \Delta\vec{x}) \\
&\quad \times \left\{ \left[\Delta p_x \frac{z'}{z_s} + (x' - x'') \left(1 - \frac{z'}{z_s}\right) \right]^2 + V_x^2(z')\tau^2 - 2V_x(z')\tau \left[\Delta p_x \frac{z'}{z_s} + (x' - x'') \left(1 - \frac{z'}{z_s}\right) \right] \right. \\
&\quad \left. + \left[\Delta p_y \frac{z'}{z_s} + (y' - y'') \left(1 - \frac{z'}{z_s}\right) \right]^2 + V_y^2(z')\tau^2 - 2V_y(z')\tau \left[\Delta p_y \frac{z'}{z_s} + (y' - y'') \left(1 - \frac{z'}{z_s}\right) \right] \right\}^{\frac{5}{6}}
\end{aligned}
\tag{3.98}
$$

The partial derivative with respect to τ of equation 3.98 is

$$
\begin{aligned}
&\frac{\partial\langle C_s(\Delta\vec{x},\tau)\rangle}{\partial\tau} = \\
&\quad -1.46k^2\int_0^{z_s} \mathrm{d}z'\, C_n^2(z') \int \mathrm{d}^2\vec{x} \int \mathrm{d}^2\vec{x}''\, W_{L_1}^s(\vec{x}) W_{L_1}^s(\vec{x}'' - \Delta\vec{x}) \\
&\quad \times \frac{5}{6} \left\{ \left[\Delta p_x \frac{z'}{z_s} + (x - x'') \left(1 - \frac{z'}{z_s}\right) \right]^2 + V_x^2(z')\tau^2 - 2V_x(z')\tau \left[\Delta p_x \frac{z'}{z_s} + (x - x'') \left(1 - \frac{z'}{z_s}\right) \right] \right. \\
&\quad \left. + \left[\Delta p_y \frac{z'}{z_s} + (y - y'') \left(1 - \frac{z'}{z_s}\right) \right]^2 + V_y^2(z')\tau^2 - 2V_y(z')\tau \left[\Delta p_y \frac{z'}{z_s} + (y - y'') \left(1 - \frac{z'}{z_s}\right) \right] \right\}^{-\frac{1}{6}} \\
&\quad \times \left\{ 2V_x^2(z')\tau - 2V_x(z') \left[\Delta p_x \frac{z'}{z_s} + (x - x'') \left(1 - \frac{z'}{z_s}\right) \right] \right. \\
&\quad \left. +2V_y^2(z')\tau - 2V_y(z') \left[\Delta p_y \frac{z'}{z_s} + (y - y'') \left(1 - \frac{z'}{z_s}\right) \right] \right\}
\end{aligned}
$$

$$
\begin{aligned}
&-1.46k^2\int_0^{z_s} \mathrm{d}z'\, C_n^2(z') \int \mathrm{d}^2\vec{x}' \int \mathrm{d}^2\vec{x}''' \, W_{L_2}^s(\vec{x}') W_{L_2}^s(\vec{x}''' - \Delta\vec{x}) \\
&\times \frac{5}{6}\left\{\left[\Delta p_x \frac{z'}{z_s} + (x' - x''')\left(1 - \frac{z'}{z_s}\right)\right]^2 + V_x^2(z')\tau^2 - 2V_x(z')\tau\left[\Delta p_x \frac{z'}{z_s} + (x' - x''')\left(1 - \frac{z'}{z_s}\right)\right]\right. \\
&\left. + \left[\Delta p_y \frac{z'}{z_s} + (y' - y''')\left(1 - \frac{z'}{z_s}\right)\right]^2 + V_y^2(z')\tau^2 - 2V_y(z')\tau\left[\Delta p_y \frac{z'}{z_s} + (y' - y''')\left(1 - \frac{z'}{z_s}\right)\right]\right\}^{-\frac{1}{6}} \\
&\times \left\{2V_x^2(z')\tau - 2V_x(z')\left[\Delta p_x \frac{z'}{z_s} + (x' - x''')\left(1 - \frac{z'}{z_s}\right)\right]\right. \\
&\quad \left. + 2V_y^2(z')\tau - 2V_y(z')\left[\Delta p_y \frac{z'}{z_s} + (y' - y''')\left(1 - \frac{z'}{z_s}\right)\right]\right\} \\
&+2.92k^2\int_0^{z_s} \mathrm{d}z'\, C_n^2(z') \int \mathrm{d}^2\vec{x}' \int \mathrm{d}^2\vec{x}'' \, W_{L_2}^s(\vec{x}') W_{L_1}^s(\vec{x}'' - \Delta\vec{x}) \\
&\times \frac{5}{6}\left\{\left[\Delta p_x \frac{z'}{z_s} + (x' - x'')\left(1 - \frac{z'}{z_s}\right)\right]^2 + V_x^2(z')\tau^2 - 2V_x(z')\tau\left[\Delta p_x \frac{z'}{z_s} + (x' - x'')\left(1 - \frac{z'}{z_s}\right)\right]\right. \\
&\left. + \left[\Delta p_y \frac{z'}{z_s} + (y' - y'')\left(1 - \frac{z'}{z_s}\right)\right]^2 + V_y^2(z')\tau^2 - 2V_y(z')\tau\left[\Delta p_y \frac{z'}{z_s} + (y' - y'')\left(1 - \frac{z'}{z_s}\right)\right]\right\}^{-\frac{1}{6}} \\
&\times \left\{2V_x^2(z')\tau - 2V_x(z')\left[\Delta p_x \frac{z'}{z_s} + (x' - x'')\left(1 - \frac{z'}{z_s}\right)\right]\right. \\
&\quad \left. + 2V_y^2(z')\tau - 2V_y(z')\left[\Delta p_y \frac{z'}{z_s} + (y' - y'')\left(1 - \frac{z'}{z_s}\right)\right]\right\} \qquad (3.99)
\end{aligned}
$$

Setting $\tau = 0$ gives

$$
\begin{aligned}
&\frac{\partial C_s(\Delta\vec{x}, \tau)}{\partial \tau}\Big|_{\tau=0} = \\
&\quad -1.46k^2\int_0^{z_s} \mathrm{d}z'\, C_n^2(z') \int \mathrm{d}^2\vec{x} \int \mathrm{d}^2\vec{x}'' \, W_{L_1}^s(\vec{x}) W_{L_1}^s(\vec{x}'' - \Delta\vec{x}) \\
&\quad \times \frac{5}{6}\left\{\left[\Delta p_x \frac{z'}{z_s} + (x - x'')\left(1 - \frac{z'}{z_s}\right)\right]^2 + \left[\Delta p_y \frac{z'}{z_s} + (y - y'')\left(1 - \frac{z'}{z_s}\right)\right]^2\right\}^{-\frac{1}{6}} \\
&\quad \times -2\left\{V_x(z')\left[\Delta p_x \frac{z'}{z_s} + (x - x'')\left(1 - \frac{z'}{z_s}\right)\right] + V_y(z')\left[\Delta p_y \frac{z'}{z_s} + (y - y'')\left(1 - \frac{z'}{z_s}\right)\right]\right\} \\
&\quad -1.46k^2\int_0^{z_s} \mathrm{d}z'\, C_n^2(z') \int \mathrm{d}^2\vec{x}' \int \mathrm{d}^2\vec{x}''' \, W_{L_2}^s(\vec{x}') W_{L_2}^s(\vec{x}''' - \Delta\vec{x}) \\
&\quad \times \frac{5}{6}\left\{\left[\Delta p_x \frac{z'}{z_s} + (x' - x''')\left(1 - \frac{z'}{z_s}\right)\right]^2 + \left[\Delta p_y \frac{z'}{z_s} + (y' - y''')\left(1 - \frac{z'}{z_s}\right)\right]^2\right\}^{-\frac{1}{6}} \\
&\quad \times -2\left\{V_x(z')\left[\Delta p_x \frac{z'}{z_s} + (x' - x''')\left(1 - \frac{z'}{z_s}\right)\right] + V_y(z')\left[\Delta p_y \frac{z'}{z_s} + (y' - y''')\left(1 - \frac{z'}{z_s}\right)\right]\right\} \\
&\quad +2.92k^2\int_0^{z_s} \mathrm{d}z'\, C_n^2(z') \int \mathrm{d}^2\vec{x}' \int \mathrm{d}^2\vec{x}'' \, W_{L_2}^s(\vec{x}') W_{L_1}^s(\vec{x}'' - \Delta\vec{x})
\end{aligned}
$$

$$\times\frac{5}{6}\left\{\left[\Delta p_x\frac{z'}{z_s}+(x'-x'')\left(1-\frac{z'}{z_s}\right)\right]^2+\left[\Delta p_y\frac{z'}{z_s}+(y'-y'')\left(1-\frac{z'}{z_s}\right)\right]^2\right\}^{-\frac{1}{6}}$$
$$\times-2\left\{V_x(z')\left[\Delta p_x\frac{z'}{z_s}+(x'-x'')\left(1-\frac{z'}{z_s}\right)\right]+V_y(z')\left[\Delta p_y\frac{z'}{z_s}+(y'-y'')\left(1-\frac{z'}{z_s}\right)\right]\right\} \tag{3.100}$$

Notice that

$$V_x(z')\left[\Delta p_x\frac{z'}{z_s}+(x'-x'')\left(1-\frac{z'}{z_s}\right)\right]+V_y(z')\left[\Delta p_y\frac{z'}{z_s}+(y'-y'')\left(1-\frac{z'}{z_s}\right)\right]=$$
$$\vec{V}(z')\cdot\left[\Delta\vec{p}\frac{z'}{z_s}+(\vec{x}-\vec{x}')\left(1-\frac{z'}{z_s}\right)\right] \tag{3.101}$$

So, equation 3.100 may be rewritten as

$$\frac{\partial C_s(\Delta\vec{x},\tau)}{\partial\tau}|_{\tau=0}=$$
$$2.43k^2\int_0^{z_s}\mathrm{d}z'\,C_n^2(z')\int\mathrm{d}^2\vec{x}\int\mathrm{d}^2\vec{x}''\,W_{L_1}^s(\vec{x})W_{L_1}^s(\vec{x}''-\Delta\vec{x})$$
$$\times\left\{\left[\Delta p_x\frac{z'}{z_s}+(x-x'')\left(1-\frac{z'}{z_s}\right)\right]^2+\left[\Delta p_y\frac{z'}{z_s}+(y-y'')\left(1-\frac{z'}{z_s}\right)\right]^2\right\}^{-\frac{1}{6}}$$
$$\times\vec{V}(z')\cdot\left[\Delta\vec{p}\frac{z'}{z_s}+(\vec{x}-\vec{x}'')\left(1-\frac{z'}{z_s}\right)\right]$$
$$+2.43k^2\int_0^{z_s}\mathrm{d}z'\,C_n^2(z')\int\mathrm{d}^2\vec{x}'\int\mathrm{d}^2\vec{x}'''\,W_{L_2}^s(\vec{x}')W_{L_2}^s(\vec{x}'''-\Delta\vec{x})$$
$$\times\left\{\left[\Delta p_x\frac{z'}{z_s}+(x'-x''')\left(1-\frac{z'}{z_s}\right)\right]^2+\left[\Delta p_y\frac{z'}{z_s}+(y'-y''')\left(1-\frac{z'}{z_s}\right)\right]^2\right\}^{-\frac{1}{6}}$$
$$\times\vec{V}(z')\cdot\left[\Delta\vec{p}\frac{z'}{z_s}+(\vec{x}'-\vec{x}''')\left(1-\frac{z'}{z_s}\right)\right]$$
$$-4.86k^2\int_0^{z_s}\mathrm{d}z'\,C_n^2(z')\int\mathrm{d}^2\vec{x}'\int\mathrm{d}^2\vec{x}''\,W_{L_2}^s(\vec{x}')W_{L_1}^s(\vec{x}''-\Delta\vec{x})$$
$$\times\frac{5}{6}\left\{\left[\Delta p_x\frac{z'}{z_s}+(x'-x'')\left(1-\frac{z'}{z_s}\right)\right]^2+\left[\Delta p_y\frac{z'}{z_s}+(y'-y'')\left(1-\frac{z'}{z_s}\right)\right]^2\right\}^{-\frac{1}{6}}$$
$$\times\vec{V}(z')\cdot\left[\Delta p\frac{z'}{z_s}+(\vec{x}'-\vec{x}'')\left(1-\frac{z'}{z_s}\right)\right] \tag{3.102}$$

To match the form of equation 3.82, rewrite equation 3.102 as

$$\frac{\partial C_s(\Delta\vec{x},\tau)}{\partial\tau}|_{\tau=0}=\int_0^{z_s}\mathrm{d}z'\,C_n^2(z')\,\vec{V}(z')\cdot\vec{w}_V(z') \tag{3.103}$$

where $\vec{w}_V(z')$ is the wind path weighting function given by

$$\begin{aligned}
\vec{w}_V(z') = \Bigg\{ & 2.43k^2 \int_0^{z_s} \mathrm{d}z'\, C_n^2(z') \int \mathrm{d}^2\vec{x} \int \mathrm{d}^2\vec{x}''\, W_{L_1}^s(\vec{x}) W_{L_1}^s(\vec{x}'' - \Delta\vec{x}) \\
& \times \left\{ \left[\Delta p_x \frac{z'}{z_s} + (x - x'') \left(1 - \frac{z'}{z_s}\right) \right]^2 + \left[\Delta p_y \frac{z'}{z_s} + (y - y'') \left(1 - \frac{z'}{z_s}\right) \right]^2 \right\}^{\frac{1}{3}} \\
& + 2.43k^2 \int_0^{z_s} \mathrm{d}z'\, C_n^2(z') \int \mathrm{d}^2\vec{x}' \int \mathrm{d}^2\vec{x}'''\, W_{L_2}^s(\vec{x}') W_{L_2}^s(\vec{x}''' - \Delta\vec{x}) \\
& \times \left\{ \left[\Delta p_x \frac{z'}{z_s} + (x' - x''') \left(1 - \frac{z'}{z_s}\right) \right]^2 + \left[\Delta p_y \frac{z'}{z_s} + (y' - y''') \left(1 - \frac{z'}{z_s}\right) \right]^2 \right\}^{\frac{1}{3}} \\
& - 4.86k^2 \int_0^{z_s} \mathrm{d}z'\, C_n^2(z') \int \mathrm{d}^2\vec{x}' \int \mathrm{d}^2\vec{x}''\, W_{L_2}^s(\vec{x}') W_{L_1}^s(\vec{x}'' - \Delta\vec{x}) \\
& \times \frac{5}{6} \left\{ \left[\Delta p_x \frac{z'}{z_s} + (x' - x'') \left(1 - \frac{z'}{z_s}\right) \right]^2 + \left[\Delta p_y \frac{z'}{z_s} + (y' - y'') \left(1 - \frac{z'}{z_s}\right) \right]^2 \right\}^{\frac{1}{3}} \Bigg\} \hat{r}
\end{aligned} \tag{3.104}$$

where $\hat{r}$ is a unit vector along $\Delta\vec{p}\frac{z'}{z_s} + (\vec{x} - \vec{x}')\left(1 - \frac{z'}{z_s}\right)$ given by

$$\hat{r} = \frac{\left[\Delta p_x \frac{z'}{z_s} - \Delta x \left(1 - \frac{z'}{z_s}\right) \right] \hat{x} + \left[\Delta p_y \frac{z'}{z_s} - \Delta y \left(1 - \frac{z'}{z_s}\right) \right] \hat{y}}{\left\{ \left[\Delta p_x \frac{z'}{z_s} - \Delta x \left(1 - \frac{z'}{z_s}\right) \right]^2 + \left[\Delta p_y \frac{z'}{z_s} - \Delta y \left(1 - \frac{z'}{z_s}\right) \right]^2 \right\}^{\frac{1}{2}}} \tag{3.105}$$

3.6.6 Reduction of $\vec{V}$ Path Weighting Function, $\vec{w}_V(z')$ The steps taken to simplify equation 3.104 are identical to the steps taken in equations 3.31 through 3.44 of the C_n^2 path weighting function derivation. The result is

$$\begin{aligned}
\vec{w}_V(z') = \Bigg\{ & 2.43k^2 L_1^{-3} \int \mathrm{d}u\, \mathrm{tri}\left(\frac{u - \Delta y}{L_1}\right) \\
& \times \Bigg\{ 2 \left\{ \left[\Delta p_x \left(\frac{z'}{z_s}\right) - \left(1 - \frac{z'}{z_s}\right) \Delta x \right]^2 + \left[\Delta p_y \left(\frac{z'}{z_s}\right) + u \left(1 - \frac{z'}{z_s}\right) \right]^2 \right\}^{\frac{1}{3}} \\
& - \left\{ \left[\Delta p_x \left(\frac{z'}{z_s}\right) - \left(1 - \frac{z'}{z_s}\right) (\Delta x + L_1) \right]^2 + \left[\Delta p_y \left(\frac{z'}{z_s}\right) + u \left(1 - \frac{z'}{z_s}\right) \right]^2 \right\}^{\frac{1}{3}} \\
& - \left\{ \left[\Delta p_x \left(\frac{z'}{z_s}\right) - \left(1 - \frac{z'}{z_s}\right) (\Delta x - L_1) \right]^2 + \left[\Delta p_y \left(\frac{z'}{z_s}\right) + u \left(1 - \frac{z'}{z_s}\right) \right]^2 \right\}^{\frac{1}{3}} \Bigg\} \\
& + 2.43k^2 L_2^{-3} \int \mathrm{d}u\, \mathrm{tri}\left(\frac{u - \Delta y}{L_2}\right)
\end{aligned}$$

$$\times \left\{ 2 \left\{ \left[\Delta p_x \left(\frac{z'}{z_s} \right) - \left(1 - \frac{z'}{z_s} \right) \Delta x \right]^2 + \left[\Delta p_y \left(\frac{z'}{z_s} \right) + u \left(1 - \frac{z'}{z_s} \right) \right]^2 \right\}^{\frac{1}{3}} \right.$$
$$- \left\{ \left[\Delta p_x \left(\frac{z'}{z_s} \right) - \left(1 - \frac{z'}{z_s} \right) (\Delta x + L_2) \right]^2 + \left[\Delta p_y \left(\frac{z'}{z_s} \right) + u \left(1 - \frac{z'}{z_s} \right) \right]^2 \right\}^{\frac{1}{3}}$$
$$\left. - \left\{ \left[\Delta p_x \left(\frac{z'}{z_s} \right) - \left(1 - \frac{z'}{z_s} \right) (\Delta x - L_2) \right]^2 + \left[\Delta p_y \left(\frac{z'}{z_s} \right) + u \left(1 - \frac{z'}{z_s} \right) \right]^2 \right\}^{\frac{1}{3}} \right\}$$
$$-4.86 k^2 L_1^{-2} L_2^{-2} \left[\int_{-\left(\frac{L_1+L_2}{2}\right)+\Delta y}^{\frac{L_1-L_2}{2}+\Delta y} du \left(u + \frac{L_2 + L_1}{2} - \Delta y \right) g w_3(u) \right.$$
$$\left. + L_1 \int_{\frac{L_1-L_2}{2}+\Delta y}^{\frac{L_2-L_1}{2}+\Delta y} du \, g w_3(u) + \int_{\frac{L_2-L_1}{2}+\Delta y}^{\frac{L_1+L_2}{2}+\Delta y} \left(\frac{L_1 + L_2}{2} - u + \Delta y \right) g w_3(u) \right] \right\} \hat{r} \tag{3.106}$$

where

$$g w_3(u) =$$
$$\left\{ \left[\Delta p_x \frac{z'}{z_s} + \left(-\Delta x + \frac{L_2 - L_1}{2} \right) \left(1 - \frac{z'}{z_s} \right) \right]^2 + \left[\Delta p_y \frac{z'}{z_s} + u \left(1 - \frac{z'}{z_s} \right) \right]^2 \right\}^{\frac{1}{3}}$$
$$- \left\{ \left[\Delta p_x \frac{z'}{z_s} + \left(-\Delta x - \frac{L_1 + L_2}{2} \right) \left(1 - \frac{z'}{z_s} \right) \right]^2 + \left[\Delta p_y \frac{z'}{z_s} + u \left(1 - \frac{z'}{z_s} \right) \right]^2 \right\}^{\frac{1}{3}}$$
$$- \left\{ \left[\Delta p_x \frac{z'}{z_s} + \left(-\Delta x + \frac{L_1 + L_2}{2} \right) \left(1 - \frac{z'}{z_s} \right) \right]^2 + \left[\Delta p_y \frac{z'}{z_s} + u \left(1 - \frac{z'}{z_s} \right) \right]^2 \right\}^{\frac{1}{3}}$$
$$+ \left\{ \left[\Delta p_x \frac{z'}{z_s} + \left(-\Delta x + \frac{L_1 - L_2}{2} \right) \left(1 - \frac{z'}{z_s} \right) \right]^2 + \left[\Delta p_y \frac{z'}{z_s} + u \left(1 - \frac{z'}{z_s} \right) \right]^2 \right\}^{\frac{1}{3}} \tag{3.107}$$

Recall that both Δy and Δp_y were set equal to zero for the C_n^2 path weighting function. This resulted in no separation of the optical beams in the y direction. However, such a separation is crucial for measuring wind velocity. The underlying phenomenon being exploited is the transport of eddies from one ray path to the other. If the ray paths intersect, it is impossible to infer anything about the rate of this eddy transport. Let the separation in the x direction equal zero at the crossing altitude, therefore some offset of the ray paths in the y direction is required. As shown in Figure 3.6, this offset is achieved

by letting $\Delta p_y = 0$ and Δy equal some non-zero value.

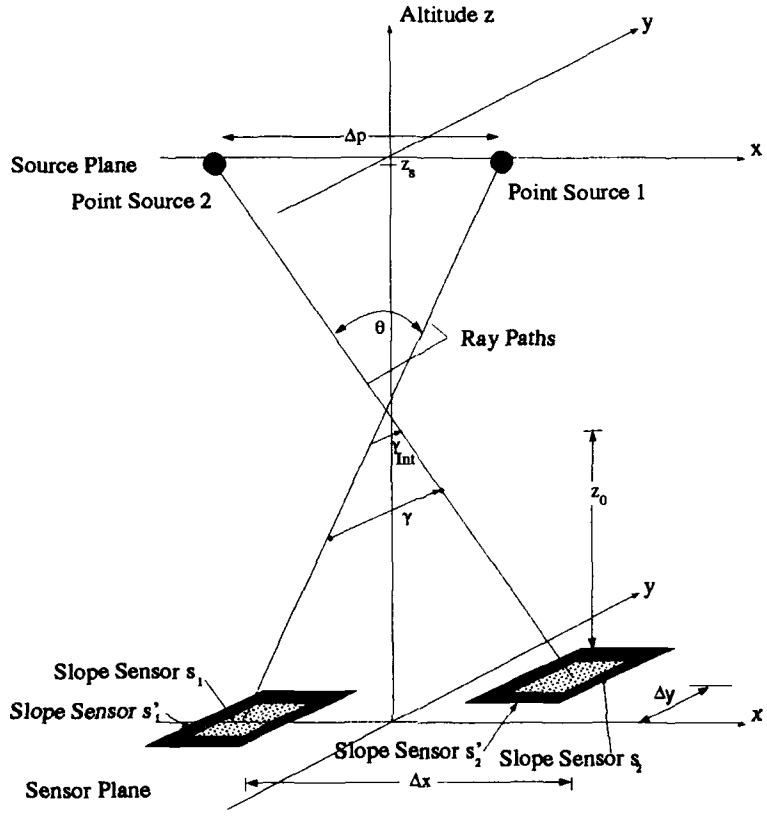

Figure 3.6. Measurement Geometry Showing Offset of Beams in y Direction

Thus, equation 3.106 becomes

$$\begin{aligned}
\vec{w}_V(z') = &\left\{2.43k^2L_1^{-\frac{4}{3}}\int \mathrm{d}u' \,\mathrm{tri}\left(u' - \frac{\Delta y}{L_1}\right)\right. \\
&\times\left\{2\left\{\left[\frac{\gamma}{L_1} + \left(\frac{z'}{z_s}\right)\frac{\Delta x}{L_1}\right]^2 + \left[u'\left(1 - \frac{z'}{z_s}\right)\right]^2\right\}^{\frac{1}{3}}\right. \\
&-\left\{\left[\frac{\gamma}{L_1} - 1 + \frac{z'}{z_s}\left(\frac{\Delta x}{L_1} + 1\right)\right]^2 + \left[u\left(1 - \frac{z'}{z_s}\right)\right]^2\right\}^{\frac{1}{3}} \\
&\left.\left.-\left\{\left[\frac{\gamma}{L_1} + 1 + \frac{z'}{z_s}\left(\frac{\Delta x}{L_1} - 1\right)\right]^2 + \left[u\left(1 - \frac{z'}{z_s}\right)\right]^2\right\}^{\frac{1}{3}}\right\}\right. \\
&+2.43k^2L_2^{-\frac{4}{3}}\int \mathrm{d}u' \,\mathrm{tri}\left(\frac{u' - \Delta y}{L_2}\right)
\end{aligned}$$

$$
\times \left\{ 2 \left\{ \left[\frac{\gamma}{L_2} + \left(\frac{z'}{z_s} \right) \frac{\Delta x}{L_2} \right]^2 + \left[u' \left(1 - \frac{z'}{z_s} \right) \right]^2 \right\}^{\frac{1}{3}} \right.
$$

$$
- \left\{ \left[\frac{\gamma}{L_2} - 1 + \frac{z'}{z_s} \left(\frac{\Delta x}{L_2} + 1 \right) \right]^2 + \left[u' \left(1 - \frac{z'}{z_s} \right) \right]^2 \right\}^{\frac{1}{3}}
$$

$$
\left. - \left\{ \left[\frac{\gamma}{L_2} + 1 + \frac{z'}{z_s} \left(\frac{\Delta x}{L_2} - 1 \right) \right]^2 + \left[u' \left(1 - \frac{z'}{z_s} \right) \right]^2 \right\}^{\frac{1}{3}} \right\}
$$

$$
-4.86 k^2 L_1^{-2} L_2^{-2} \left[\int_{-\left(\frac{L_1+L_2}{2}\right)+\Delta y}^{\frac{L_1-L_2}{2}+\Delta y} \mathrm{d}u \left(u + \frac{L_2 + L_1}{2} - \Delta y \right) g w_3(u) \right.
$$

$$
\left. + L_1 \int_{\frac{L_1-L_2}{2}+\Delta y}^{\frac{L_2-L_1}{2}+\Delta y} \mathrm{d}u \, g w_3(u) + \int_{\frac{L_2-L_1}{2}+\Delta y}^{\frac{L_1+L_2}{2}+\Delta y} \left(\frac{L_1 + L_2}{2} - u + \Delta y \right) g w_3(u) \right] \Bigg\} \hat{r} \tag{3.108}
$$

where

$$
g w_3(u) = \left\{ \left[\Delta p_x \frac{z'}{z_s} + \left(-\Delta x + \frac{L_2 - L_1}{2} \right) \left(1 - \frac{z'}{z_s} \right) \right]^2 + \left[u \left(1 - \frac{z'}{z_s} \right) \right]^2 \right\}^{\frac{1}{3}}
$$

$$
- \left\{ \left[\Delta p_x \frac{z'}{z_s} + \left(-\Delta x - \frac{L_1 + L_2}{2} \right) \left(1 - \frac{z'}{z_s} \right) \right]^2 + \left[u \left(1 - \frac{z'}{z_s} \right) \right]^2 \right\}^{\frac{1}{3}}
$$

$$
- \left\{ \left[\Delta p_x \frac{z'}{z_s} + \left(-\Delta x + \frac{L_1 + L_2}{2} \right) \left(1 - \frac{z'}{z_s} \right) \right]^2 + \left[u \left(1 - \frac{z'}{z_s} \right) \right]^2 \right\}^{\frac{1}{3}}
$$

$$
+ \left\{ \left[\Delta p_x \frac{z'}{z_s} + \left(-\Delta x + \frac{L_1 - L_2}{2} \right) \left(1 - \frac{z'}{z_s} \right) \right]^2 + \left[u \left(1 - \frac{z'}{z_s} \right) \right]^2 \right\}^{\frac{1}{3}} \tag{3.109}
$$

To make the integrals over u dimensionless, make the changes of variables $L_1 = RL_2$ and $u' = \frac{u}{L_2}$. The result is

$$
\dot{w_V}(z') = \left\{ 2.43 k^2 R^{-\frac{4}{3}} L_2^{-\frac{4}{3}} \int \mathrm{d}u' \, \mathrm{tri} \left(u' - \frac{\Delta y}{RL_2} \right) \right.
$$

$$
\times \left\{ 2 \left\{ \left[\frac{\gamma}{RL_2} + \left(\frac{z'}{z_s} \right) \frac{\Delta x}{RL_2} \right]^2 + \left[u' \left(1 - \frac{z'}{z_s} \right) \right]^2 \right\}^{\frac{1}{3}} \right.
$$

$$
- \left\{ \left[\frac{\gamma}{RL_2} - 1 + \frac{z'}{z_s} \left(\frac{\Delta x}{RL_2} + 1 \right) \right]^2 + \left[u \left(1 - \frac{z'}{z_s} \right) \right]^2 \right\}^{\frac{1}{3}}
$$

$$
\left. \left. - \left\{ \left[\frac{\gamma}{RL_2} + 1 + \frac{z'}{z_s} \left(\frac{\Delta x}{RL_2} - 1 \right) \right]^2 + \left[u \left(1 - \frac{z'}{z_s} \right) \right]^2 \right\}^{\frac{1}{3}} \right\}
$$

$$
\begin{aligned}
&+2.43k^2L_2^{-\frac{4}{3}}\int \mathrm{d}u'\,\mathrm{tri}\left(u'-\frac{\Delta y}{L_2}\right)\\
&\times\left\{2\left\{\left[\frac{\gamma}{L_2}+\left(\frac{z'}{z_s}\right)\frac{\Delta x}{L_2}\right]^2+\left[u'\left(1-\frac{z'}{z_s}\right)\right]^2\right\}^{\frac{1}{3}}\right.\\
&\quad-\left\{\left[\frac{\gamma}{L_2}-1+\frac{z'}{z_s}\left(\frac{\Delta x}{L_2}+1\right)\right]^2+\left[u'\left(1-\frac{z'}{z_s}\right)\right]^2\right\}^{\frac{1}{3}}\\
&\quad\left.-\left\{\left[\frac{\gamma}{L_2}+1+\frac{z'}{z_s}\left(\frac{\Delta x}{L_2}-1\right)\right]^2+\left[u'\left(1-\frac{z'}{z_s}\right)\right]^2\right\}^{\frac{1}{3}}\right\}\\
&-4.86k^2R^{-2}L_2^{\frac{-4}{3}}\left[\int_{-\left(\frac{R+1}{2}\right)+\frac{\Delta y}{L_2}}^{\frac{R-1}{2}+\frac{\Delta y}{L_2}}\mathrm{d}u'\left(u'+\frac{1+R}{2}-\frac{\Delta y}{L_2}\right)gw_3(u')\right.\\
&\left.+R\int_{\frac{R-1}{2}+\frac{\Delta y}{L_2}}^{\frac{1-R}{2}+\frac{\Delta y}{L_2}}\mathrm{d}u'\,gw_3(u')+\int_{\frac{1-R}{2}+\frac{\Delta y}{L_2}}^{\frac{R+1}{2}+\frac{\Delta y}{L_2}}\left(\frac{R+1}{2}-u'+\frac{\Delta y}{L_2}\right)gw_3(u')\right]\hat{r}
\end{aligned}
\tag{3.110}
$$

where

$$
\begin{aligned}
gw_3(u') = &\left\{\left[\frac{\gamma}{L_2}+\frac{1-R}{2}+\frac{z'}{z_s}\left(\frac{\Delta x}{L_2}-\frac{1-R}{2}\right)\right]^2+\left[u'\left(1-\frac{z'}{z_s}\right)\right]^2\right\}^{\frac{1}{3}}\\
&-\left\{\left[\frac{\gamma}{L_2}-\frac{R+1}{2}+\frac{z'}{z_s}\left(\frac{\Delta x}{L_2}+\frac{R+1}{2}\right)\right]^2+\left[u'\left(1-\frac{z'}{z_s}\right)\right]^2\right\}^{\frac{1}{3}}\\
&-\left\{\left[\frac{\gamma}{L_2}+\frac{R+1}{2}+\frac{z'}{z_s}\left(\frac{\Delta x}{L_2}-\frac{R+1}{2}\right)\right]^2+\left[u'\left(1-\frac{z'}{z_s}\right)\right]^2\right\}^{\frac{1}{3}}\\
&+\left\{\left[\frac{\gamma}{L_2}+\frac{R-1}{2}+\frac{z'}{z_s}\left(\frac{\Delta x}{L_2}-\frac{R-1}{2}\right)\right]^2+\left[u'\left(1-\frac{z'}{z_s}\right)\right]^2\right\}^{\frac{1}{3}}
\end{aligned}
\tag{3.111}
$$

where $\gamma = \Delta p_x \frac{z'}{z_s} - \Delta x$. Equation 3.110 is the most general form of the wind path weighting function. However, it can be simplified by assuming $1-\frac{z'}{z_s} \approx 1$. The simplified form is

$$
\begin{aligned}
\vec{w}_V(z') = &\left\{2.43k^2R^{-\frac{4}{3}}L_2^{-\frac{4}{3}}\int \mathrm{d}u'\,\mathrm{tri}\left(u'-\frac{\Delta y}{RL_2}\right)\right.\\
&\times\left\{2\left[\left(\frac{\gamma}{RL_2}\right)^2+u'^2\right]^{\frac{1}{3}}-\left[\left(\frac{\gamma}{RL_2}-1\right)^2+u'^2\right]^{\frac{1}{3}}-\left[\left(\frac{\gamma}{RL_2}+1\right)^2+u'^2\right]^{\frac{1}{3}}\right\}\\
&\left.+2.43k^2L_2^{-\frac{4}{3}}\int \mathrm{d}u'\,\mathrm{tri}\left(u'-\frac{\Delta y}{L_2}\right)\right.
\end{aligned}
$$

$$\times \left\{ 2\left[\left(\frac{\gamma}{L_2}\right)^2 + u'^2\right]^{\frac{1}{3}} - \left[\left(\frac{\gamma}{L_2} - 1\right)^2 + u'^2\right]^{\frac{1}{3}} - \left[\left(\frac{\gamma}{L_2} + 1\right)^2 + u'^2\right]^{\frac{1}{3}} \right\}$$

$$-4.86k^2R^{-2}L_2^{\frac{-4}{3}} \left[\int_{-\left(\frac{R+1}{2}\right)+\frac{\Delta y}{L_2}}^{\frac{R-1}{2}+\frac{\Delta y}{L_2}} du' \left(u' + \frac{1+R}{2} - \frac{\Delta y}{L_2}\right) gw_3(u') \right.$$

$$\left. + R \int_{\frac{R-1}{2}+\frac{\Delta y}{L_2}}^{\frac{1-R}{2}+\frac{\Delta y}{L_2}} du'\, gw_3(u') + \int_{\frac{1-R}{2}+\frac{\Delta y}{L_2}}^{\frac{R+1}{2}+\frac{\Delta y}{L_2}} \left(\frac{R+1}{2} - u' + \frac{\Delta y}{L_2}\right) gw_3(u') \right] \right\} \hat{r} \tag{3.112}$$

where

$$gw_3(u') = \left\{ \left[\frac{\gamma}{L_2} + \frac{1-R}{2}\right]^2 + u'^2 \right\}^{\frac{1}{3}} - \left\{ \left[\frac{\gamma}{L_2} - \frac{R+1}{2}\right]^2 + u'^2 \right\}^{\frac{1}{3}}$$

$$- \left\{ \left[\frac{\gamma}{L_2} + \frac{R+1}{2}\right]^2 + u'^2 \right\}^{\frac{1}{3}} + \left\{ \left[\frac{\gamma}{L_2} + \frac{R-1}{2}\right]^2 + u'^2 \right\}^{\frac{1}{3}} \tag{3.113}$$

Again recall that the dependence of $\vec{w}_V(z')$ upon z' is contained in γ.

3.7 Form of the $\vec{V}$ Path Weighting Function

The key result in extending the new measurement technique to the remote sensing of transverse atmospheric winds is the form of the wind path weighting function, $\vec{w}_V$. Normalized plots of the x- and y-directed components of $\vec{w}_V(z')$ are shown in Figures 3.7 and 3.8. In both cases, the value used for the aperture separation in the y direction was $\Delta y = \sqrt{L_2}$. Such a separation could be easily achieved and maintained in most optical systems. Figure 3.9 demonstrates that a larger separation results in a slower decay rate for the path weighting function.

These figures illustrate the important point that this measurement technique measures the wind velocity in the y direction only. As seen in Figure 3.7, the x-directed path weighting function has odd symmetry about the intersection point ($\gamma = 0$). This behavior occurs because eddies above the intersection point shown on Figure 3.6 and moving in the x direction intersect the beam from p_2 first, while eddies below the intersection point intercept the beam from p_1 first.

The y-directed wind path weighting functions shown in Figures 3.8 and 3.9 are sym-

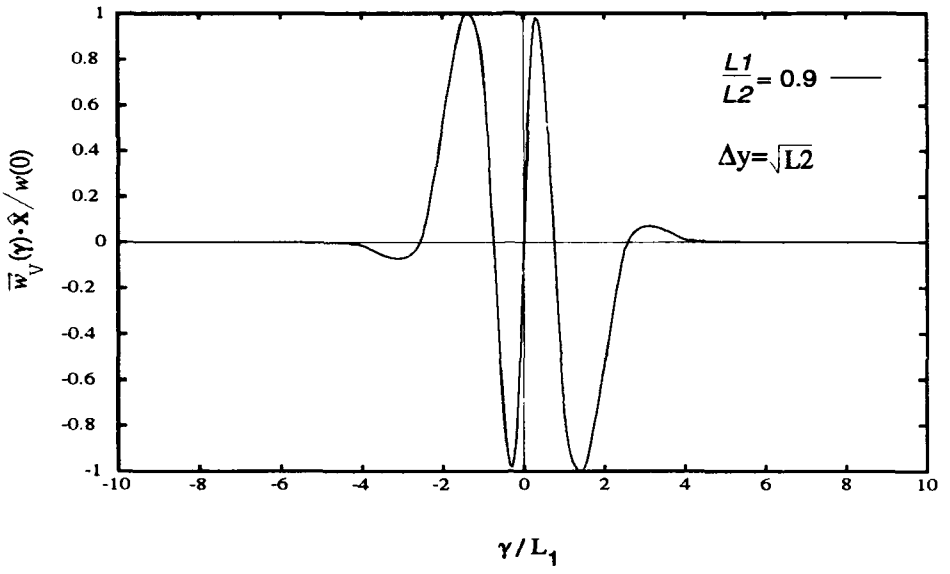

Figure 3.7. x-Directed Component of the Wind Path Weighting Function $\vec{w}_V$

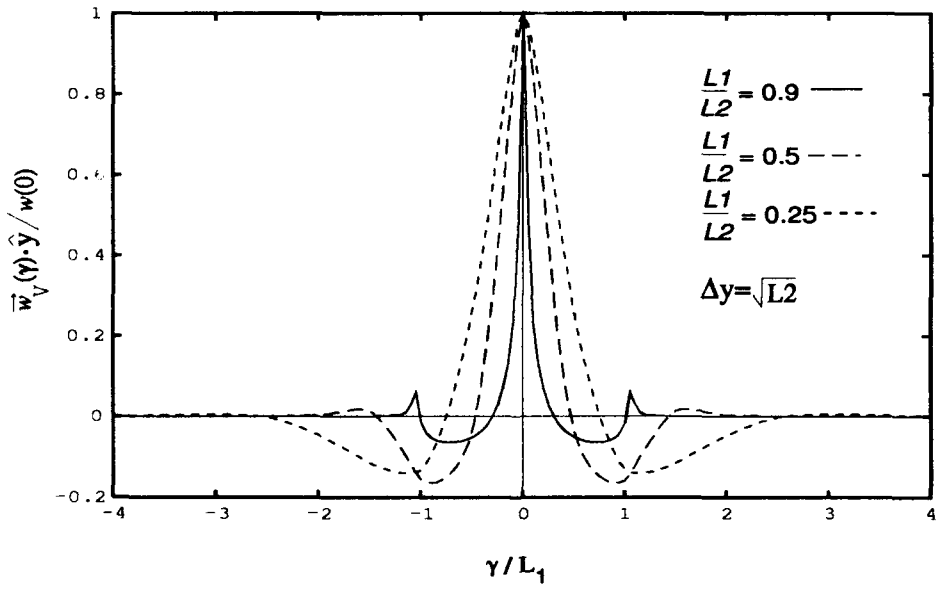

Figure 3.8. y-Directed Component of the Wind Path Weighting Function $\vec{w}_V$

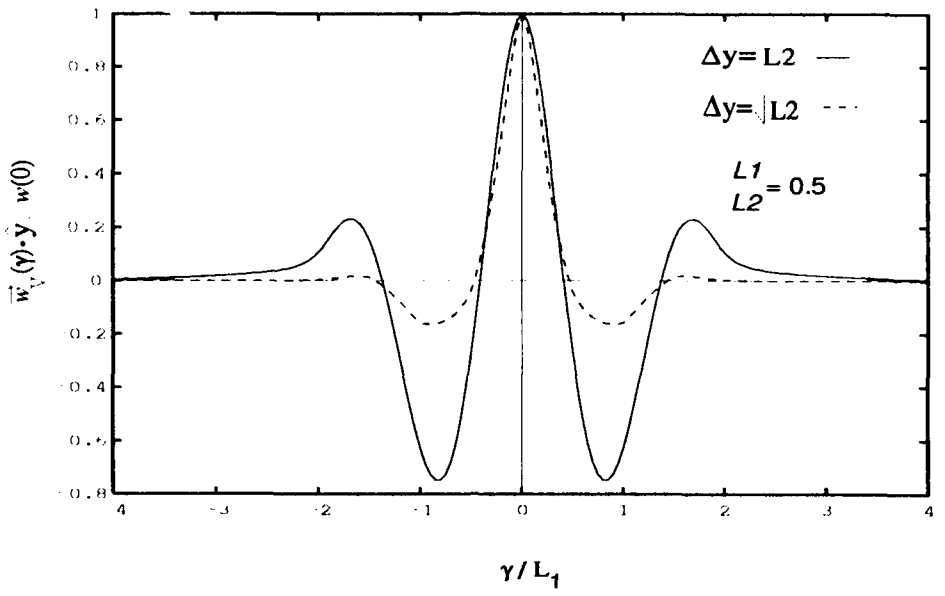

Figure 3.9. y-Directed Component of the Wind Path Weighting Function $\vec{w}_V$ for Two Values of Δy

metrical about $\frac{\gamma}{L_1} = 0$ and exhibit rapid decay away from the intersection point. Both properties are desirable in order to measure the y component of the wind. Notice that, just as for the C_n^2 path weighting function, the horizontal axis of the plot is normalized by L_1. Once again, the ratio $R = \frac{L_1}{L_2}$ plays an important role in determining the shape of the path weighting function. As R approaches one, the wind path weighting function becomes more sharply peaked.

3.8 Resolution of $\vec{V}$ Path Weighting Function

As was done for the C_n^2 path weighting function, the RMS width of the $\vec{V}$ path weighting function was computed and then used to determine the path weighting function's vertical resolution. Figure 3.10 presents the resolution of the wind weighting function as a function of the source separation. The values used in generating the plot were $\Delta y = \sqrt{L_2}$, $R = 0.9$, $L_1 = 10$ cm, and a calculated RMS width of the path weighting function of $\gamma' = 0.045$ meters. Reading from the figure, 10 centimeter vertical resolution is possible using guide stars separated by 45 degrees. It should be noted, however, that these results

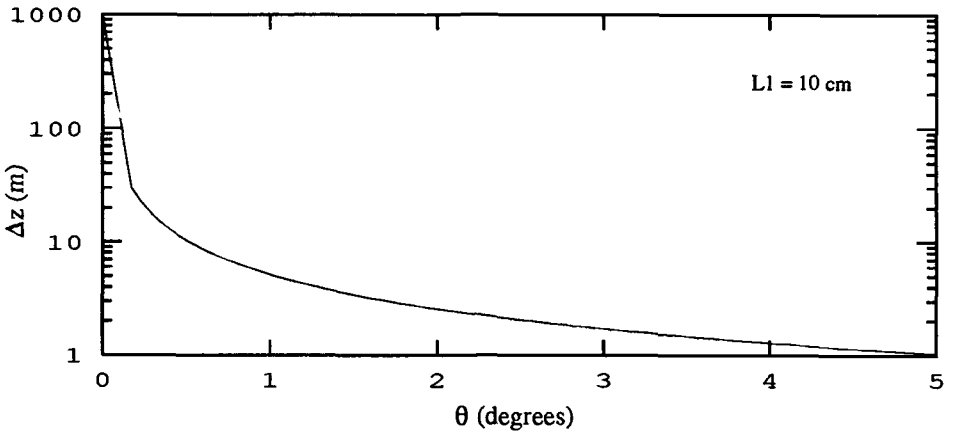

Figure 3.10. Vertical Resolution of $\vec{V}$ Path Weighting Function

are based upon the assumption that the vertical profile of C_n^2 is perfectly known. If C_n^2 can only be measured to within some resolution $\Delta z'$, and its value is changing over $\Delta z'$, then the resolution of the wind path weighting function will be reduced.

3.9 Conclusion

This chapter has presented the derivation of the C_n^2 and $\vec{V}$ path weighting functions for a new crossed beam measurement technique which relies upon correlations of band pass filtered outputs of wave front slope sensors. The shapes of these functions have been presented and their theoretical vertical resolutions calculated. The sampling function nature of the weighting functions indicates that this technique allows vertical profiling of C_n^2 and $\vec{V}$, with vertical resolution dependent upon the angular separation of the reference sources. The next chapter will examine the ability of the proposed measurement technique to accurately estimate C_n^2 and $\vec{V}$.

IV. Signal-to-Noise Ratio Analysis

4.1 Introduction

The signal-to-noise ratio of the measurement correlations gives insight to the usefulness of the measurement techniques presented in Chapter 3. The quantities of interest, C_n^2 and $\vec{V}$, are derived from correlations of wave front phase measurements, $\langle C_s \rangle$. However, C_s is a random process, and the correlation value obtained by a single measurement represents only one of the many possible values of the correlation function. The ratio of the mean of C_s to the standard deviation of C_s is a good indication of the accuracy of the estimate of the correlation from a single measurement (24). This chapter presents the derivation of the signal-to-noise ratio expressions for the estimates of $\langle C_s \rangle$ and $\langle C_s'(0) \rangle$. Additionally, signal-to-noise ratio results are shown for both cases, and the effects of measurement noise on the SNR are examined.

4.2 Derivation of SNR Expression for $\langle C_s \rangle$

4.2.1 Definition of $\langle C_s \rangle$ SNR The SNR of $\langle C_s \rangle$ is defined as

$$\text{SNR} = \frac{|\langle C_s \rangle|}{[\langle C_s^2 \rangle - \langle C_s \rangle^2]^{\frac{1}{2}}} \tag{4.1}$$

where $|\langle C_s \rangle|$ is the magnitude of the mean value of C_s, and $\langle C_s^2 \rangle$ is the mean square value of C_s.

The mean has been derived in Chapter 3 and is given in equation 3.2, where $w_C(z')$ is found in equation 3.69. The remaining task is to find an expression for $\langle C_s^2 \rangle$.

4.2.2 Derivation of $\langle C_s^2 \rangle$ The mean square value of C_s is defined by

$$\langle C_s^2 \rangle = \langle [(s_1 - s_{1'})(s_2 - s_{2'})]^2 \rangle \tag{4.2}$$

where s_n is the output of slope sensor n. The expanded version of equation 4.2 is

$$\langle C_s^2 \rangle =$$
$$\langle (s_1 s_2)^2 \rangle + \langle (s_{1'} s_{2'})^2 \rangle + \langle (s_{1'} s_2)^2 \rangle + \langle (s_1 s_{2'})^2 \rangle$$
$$+4\langle s_{1'} s_{2'} s_1 s_2 \rangle - 2\langle s_1 s_2 s_1 s_{2'} \rangle - 2\langle s_1 s_2 s_{1'} s_2 \rangle$$
$$-2\langle s_1 s_{2'} s_{1'} s_{2'} \rangle - 2\langle s_{1'} s_2 s_{1'} s_{2'} \rangle \tag{4.3}$$

As can be seen, the mean square value of the measurement correlations is composed of many terms. Results for each term will be presented separately and later combined. Many of the assumptions and results found in Chapter 3 will be referred to here. Making use of the slope sensor output model given in equation 3.10 and beginning with the first term in equation 4.3

$$\langle (s_1 s_2)^2 \rangle =$$
$$\int\int\int\int \mathrm{d}^2\vec{x}\mathrm{d}^2\vec{x}'\mathrm{d}^2\vec{x}''\mathrm{d}^2\vec{x}''' W^s_{L_1}(\vec{x}) W^s_{L_1}(\vec{x}' - \Delta\vec{x}) W^s_{L_1}(\vec{x}'') W^s_{L_1}(\vec{x}''' - \Delta\vec{x})$$
$$\times \langle \phi_1(\vec{x}) \phi_2(\vec{x}') \phi_1(\vec{x}'') \phi_2(\vec{x}''') \rangle$$
$$+ \int\int \mathrm{d}^2\vec{x}\mathrm{d}^2\vec{x}'' W^s_{L_1}(\vec{x}) W^s_{L_1}(\vec{x}'') \langle \phi_1(\vec{x}) \phi_1(\vec{x}'') \rangle \langle \alpha_2 \alpha_2 \rangle$$
$$+ \int\int \mathrm{d}^2\vec{x}'\mathrm{d}^2\vec{x}''' W^s_{L_1}(\vec{x}' - \Delta\vec{x}) W^s_{L_1}(\vec{x}''' - \Delta\vec{x}) \langle \phi_2(\vec{x}') \phi_2(\vec{x}''') \rangle \langle \alpha_1 \alpha_1 \rangle$$
$$+ \langle \alpha_1 \alpha_1 \rangle \langle \alpha_2 \alpha_2 \rangle \tag{4.4}$$

where α_n is the measurement noise of sensor n.

Most of the terms in equation 4.3 have a form similar to equation 4.4. In the interest of brevity, the first term will be derived in some detail, but only the final expressions for the other terms will be presented.

The first component of the first term contains the fourth order moment of the wave front phase. Assuming Gaussian statistics for the wave front phase, the fourth order moment may be written as a combination of second order moments as follows (6)

$$\langle \phi_1(\vec{x}) \phi_2(\vec{x}') \phi_1(\vec{x}'') \phi_2(\vec{x}''') \rangle =$$
$$\langle \phi_1(\vec{x}) \phi_2(\vec{x}') \rangle \langle \phi_1(\vec{x}'') \phi_2(\vec{x}''') \rangle + \langle \phi_1(\vec{x}) \phi_1(\vec{x}'') \rangle \langle \phi_2(\vec{x}') \phi_2(\vec{x}''') \rangle$$
$$+ \langle \phi_1(\vec{x}) \phi_2(\vec{x}''') \rangle \langle \phi_2(\vec{x}') \phi_1(\vec{x}'') \rangle \tag{4.5}$$

Use of equation 4.5 in equation 4.4 results in

$$\begin{aligned}
&\langle (s_1 s_2)^2 \rangle = \\
&\quad \int\int\int\int \mathrm{d}^2\vec{x}\mathrm{d}^2\vec{x}'\mathrm{d}^2\vec{x}''\mathrm{d}^2\vec{x}''' W^s_{L_1}(\vec{x}) W^s_{L_1}(\vec{x}' - \Delta\vec{x}) W^s_{L_1}(\vec{x}'') W^s_{L_1}(\vec{x}''' - \Delta\vec{x}) \\
&\quad \times [\langle \phi_1(\vec{x})\phi_2(\vec{x}')\rangle\langle \phi_1(\vec{x}'')\phi_2(\vec{x}''')\rangle + \langle \phi_1(\vec{x})\phi_1(\vec{x}'')\rangle\langle \phi_2(\vec{x}')\phi_2(\vec{x}''')\rangle \\
&\qquad\qquad + \langle \phi_1(\vec{x})\phi_2(\vec{x}''')\rangle\langle \phi_2(\vec{x}')\phi_1(\vec{x}'')\rangle] \\
&\quad + \int\int \mathrm{d}^2\vec{x}\mathrm{d}^2\vec{x}'' W^s_{L_1}(\vec{x}) W^s_{L_1}(\vec{x}'') \langle \phi_1(\vec{x})\phi_1(\vec{x}'')\rangle\langle \alpha_2\alpha_2\rangle \\
&\quad + \int\int \mathrm{d}^2\vec{x}'\mathrm{d}^2\vec{x}''' W^s_{L_1}(\vec{x}' - \Delta\vec{x}) W^s_{L_1}(\vec{x}''' - \Delta\vec{x}) \langle \phi_2(\vec{x}')\phi_2(\vec{x}''')\rangle\langle \alpha_1\alpha_1\rangle \\
&\quad + \langle \alpha_1\alpha_1\rangle\langle \alpha_2\alpha_2\rangle
\end{aligned} \tag{4.6}$$

The derivation of the first term will begin with the evaluation of the three components arising from the fourth order moment of the phase. The first of these components is

$$\begin{aligned}
&\text{Comp 1} = \\
&\quad \int\int \mathrm{d}^2\vec{x}\mathrm{d}^2\vec{x}' W^s_{L_1}(\vec{x}) W^s_{L_1}(\vec{x}' - \Delta\vec{x}) \langle \phi_1(\vec{x})\phi_2(\vec{x}')\rangle \\
&\quad \times \int\int \mathrm{d}^2\vec{x}''\mathrm{d}^2\vec{x}''' W^s_{L_1}(\vec{x}'') W^s_{L_1}(\vec{x}''' - \Delta\vec{x}) \langle \phi_1(\vec{x}'')\phi_2(\vec{x}''')\rangle
\end{aligned} \tag{4.7}$$

This component consists of two terms, both of which are identical to equation 3.17. Thus, the expression for this component can be found by using the result of the evaluation of equation 3.17, which is shown in equation 3.24. Using this result, the first component is

$$\text{Comp 1} = \left[\int_0^{z_s} \mathrm{d}z'\, C_n^2(z')\, w_1(z')\right]^2 \tag{4.8}$$

where $w_1(z')$ is given in equation 3.47. The second component arising from the fourth order moment of the phase is

$$\begin{aligned}
&\text{Comp 2} = \\
&\quad \int\int \mathrm{d}^2\vec{x}\mathrm{d}^2\vec{x}'' W^s_{L_1}(\vec{x}) W^s_{L_1}(\vec{x}'') \langle \phi_1(\vec{x})\phi_1(\vec{x}'')\rangle \\
&\quad \times \int\int \mathrm{d}^2\vec{x}'\mathrm{d}^2\vec{x}''' W^s_{L_1}(\vec{x}' - \Delta\vec{x}) W^s_{L_1}(\vec{x}''' - \Delta\vec{x}) \langle \phi_2(\vec{x}')\phi_2(\vec{x}''')\rangle
\end{aligned} \tag{4.9}$$

The terms in this component consist of correlations of the wave front phase from a single source illuminating a single aperture. In this case both Δp_x and Δp_y equal zero (there is only one source), and the aperture separation also equals zero (there is only one aperture), so the appropriate expression is

$$\text{Comp 2} = \left[\int_0^{z_s} \mathrm{d}z'\, C_n^2(z')\, w_A(z')\right]^2 \tag{4.10}$$

where

$$w_A(z') = -2.92k^2 L_1^{-\frac{1}{3}} \int_{-1}^{1} \mathrm{d}u'\, \mathrm{tri}(u') \times \left\{\left\{\left[u'\left(1-\frac{z'}{z_s}\right)\right]^2\right\}^{\frac{5}{6}} - \left\{\left[1-\frac{z'}{z_s}\right]^2 + \left[u'\left(1-\frac{z'}{z_s}\right)\right]^2\right\}^{\frac{5}{6}}\right\} \tag{4.11}$$

Finally, the third component is

$$\begin{aligned}\text{Comp 3} = & \int\int \mathrm{d}^2\vec{x}\mathrm{d}^2\vec{x}'''W_{L_1}^s(\vec{x})W_{L_1}^s(\vec{x}''' - \Delta\vec{x})\langle\phi_1(\vec{x})\phi_2(\vec{x}''')\rangle \\ & \times \int\int \mathrm{d}^2\vec{x}'\mathrm{d}^2\vec{x}''W_{L_1}^s(\vec{x}' - \Delta\vec{x})W_{L_1}^s(\vec{x}'')\langle\phi_2(\vec{x}')\phi_1(\vec{x}'')\rangle\end{aligned} \tag{4.12}$$

This component is identical to the first component, the only difference being the dummy variables of integration. Thus, its result is also given by equation 4.8.

Moving on to the terms containing noise in equation 4.6, the first noise term is given by

$$\text{Noise Term 1} = \int\int \mathrm{d}^2\vec{x}\mathrm{d}^2\vec{x}''W_{L_1}^s(\vec{x})W_{L_1}^s(\vec{x}'')\langle\phi_1(\vec{x})\phi_1(\vec{x}'')\rangle\langle\alpha_2\alpha_2\rangle \tag{4.13}$$

Comparison of equation 4.13 with equation 4.9 shows that this term can be expressed as

$$\int\int \mathrm{d}^2\vec{x}\mathrm{d}^2\vec{x}''W_{L_1}^s(\vec{x})W_{L_1}^s(\vec{x}'')\langle\phi_1(\vec{x})\phi_1(\vec{x}'')\rangle\langle\alpha_2\alpha_2\rangle = \sigma_2^2 \int_0^{z_s} \mathrm{d}z'\, C_n^2(z')\, w_A(z') \tag{4.14}$$

where $\sigma_2^2 = \langle\alpha_2\alpha_2\rangle$ as given by equation 3.14. Similarly, the second term containing a noise

factor is

$$\int\int \mathrm{d}^2\vec{x}'\mathrm{d}^2\vec{x}''' W^s_{L_1}(\vec{x}'-\Delta\vec{x}) W^s_{L_1}(\vec{x}'''-\Delta\vec{x}) \langle \phi_2(\vec{x}')\phi_2(\vec{x}''')\rangle \langle \alpha_1\alpha_1\rangle = \sigma_1^2 \int_0^{z_s} \mathrm{d}z' C_n^2(z') w_A(z') \tag{4.15}$$

Finally, the first term in equation 4.3 may now be written by combining equations 4.8, 4.10, 4.14, and 4.15

$$\begin{aligned}\langle (s_1 s_2)^2\rangle = & \\ & 2\left[\int_0^{z_s} \mathrm{d}z'\, C_n^2(z')\, w_1(z')\right]^2 + \left[\int_0^{z_s} \mathrm{d}z'\, C_n^2(z')\, w_A(z')\right]^2 \\ & +\sigma_2^2\left[\int_0^{z_s} \mathrm{d}z'\, C_n^2(z')\, w_A(z')\right] + \sigma_1^2\left[\int_0^{z_s} \mathrm{d}z'\, C_n^2(z')\, w_A(z')\right] \\ & +\sigma_1^2\sigma_2^2 \end{aligned} \tag{4.16}$$

where $w_A(z')$ is given in equation 4.11.

Before results are given for the remaining terms in equation 4.3, there are two expressions which need to be presented. These expressions occur often in the remaining terms but have not been encountered before in this thesis. Therefore they are evaluated now. The first expression is the ensemble average of the slope measurement noise from two co-located slope sensors of different sizes, and is defined as

$$\langle \alpha_n \alpha_{n'}\rangle = R^2 \sigma_{n'}^2 \tag{4.17}$$

where $R = \frac{L_1}{L_2}$, α_n is the slope measurement noise of sensor n, sensor n is a square with dimension L_1, and sensor n' has dimension L_2. The variance of the slope measurement noise from sensor n' is denoted as $\sigma_{n'}^2$. As mentioned before, Wallner has shown the correlation of noise processes from separate sensors to be zero. However, in the case present in equation 4.17 the two subapertures actually overlap. In this case, the correlation yields some non-zero value which is dependent upon the amount of overlap. In practice, the two co-located apertures will each be composed of several subapertures. Because they are co-located, the two apertures will share some number of subapertures. The more subapertures they share, the more the apertures' noise processes will be correlated. Equation 4.17 reflects this fact

through the factor R^2.

The second term not encountered before is the correlation of the wave front phase of a single source illuminating two co-located apertures of different sizes. The expression for this case is

$$\int\int \mathrm{d}^2(\vec{x})\,\mathrm{d}^2(\vec{x}'')\,W^s_{L_1}(\vec{x})W^s_{L_2}(\vec{x}'')\langle\phi_1(\vec{x})\phi_1(\vec{x}'')\rangle = \int_0^{z_s} \mathrm{d}z'\,C_n^2(z')w_B(z') \tag{4.18}$$

where

$$w_B(z') = -2.92k^2R^{-2}L_2^{-\frac{1}{3}}\left[\int_{-\frac{(R+1)}{2}}^{\frac{R-1}{2}} \mathrm{d}u'\,\left(u'+\frac{1+R}{2}\right)g_B(u') + R\int_{\frac{R-1}{2}}^{\frac{1-R}{2}} \mathrm{d}u'\,g_B(u') \int_{\frac{1-R}{2}}^{\frac{R+1}{2}} \mathrm{d}u'\left(\frac{R+1}{2}-u'\right)g_B(u')\right] \tag{4.19}$$

where

$$g_B(u') = \left\{\left[\frac{1-R}{2}\left(1-\frac{z'}{z_s}\right)\right]^2 + \left[u'\left(1-\frac{z'}{z_s}\right)\right]^2\right\}^{\frac{5}{6}} - \left\{\left[\frac{1+R}{2}\left(1-\frac{z'}{z_s}\right)\right]^2 + \left[u'\left(1-\frac{z'}{z_s}\right)\right]^2\right\}^{\frac{5}{6}} \tag{4.20}$$

All results necessary to evaluate equation 4.3 are now available. Expressions for each term are presented and then combined according to equation 4.3. The first term of equation 4.3 has already been derived and is shown in equation 4.16. The second term is given by

$$\begin{aligned}\langle(s_{1'}s_{2'})^2\rangle = {} & 2\left[\int_0^{z_s} \mathrm{d}z'\,C_n^2(z')\,w_2(z')\right]^2 + \left[\int_0^{z_s} \mathrm{d}z'\,C_n^2(z')\,w_{A'}(z')\right]^2 \\ & +\sigma^2_{2'}\left[\int_0^{z_s} \mathrm{d}z'\,C_n^2(z')\,w_{A'}(z')\right] + \sigma^2_{1'}\left[\int_0^{z_s} \mathrm{d}z'\,C_n^2(z')\,w_{A'}(z')\right] \\ & +\sigma^2_{1'}\sigma^2_{2'}\end{aligned} \tag{4.21}$$

where $w_2(z')$ is given in equation 3.50 and

$$w_{A'}(z') = -2.92k^2 L_2^{-\frac{1}{3}} \int_{-1}^{1} du' \, \mathrm{tri}(u') \times \left\{ \left\{ \left[u' \left(1 - \frac{z'}{z_s} \right) \right]^2 \right\}^{\frac{5}{6}} - \left\{ \left(1 - \frac{z'}{z_s} \right)^2 + \left[u' \left(1 - \frac{z'}{z_s} \right) \right]^2 \right\}^{\frac{5}{6}} \right\} \tag{4.22}$$

The third term is

$$\begin{aligned} &\langle (s_{1'} s_2)^2 \rangle = \\ &\quad 2 \left[\int_0^{z_s} dz' \, C_n^2(z') \frac{w_3(z')}{2} \right]^2 + \int_0^{z_s} dz' C_n^2(z') w_{A'}(z') \int_0^{z_s} dz'' \, C_n^2(z'') w_A(z'') \\ &\quad + \sigma_2^2 \int_0^{z_s} dz' \, C_n^2(z') w_{A'}(z') + \sigma_{1'}^2 \int_0^{z_s} dz' \, C_n^2(z') w_A(z') \\ &\quad \sigma_{1'}^2 \sigma_2^2 \end{aligned} \tag{4.23}$$

where $w_3(z')$ is defined in equation 3.63. Next, the fourth term is

$$\begin{aligned} &\langle (s_1 s_{2'})^2 \rangle = \\ &\quad 2 \left[\int_0^{z_s} dz' \, C_n^2(z') \frac{w_3(z')}{2} \right]^2 + \int_0^{z_s} dz' C_n^2(z') w_{A'}(z') \int_0^{z_s} dz'' \, C_n^2(z'') w_A(z'') \\ &\quad + \sigma_{2'}^2 \int_0^{z_s} dz' \, C_n^2(z') w_A(z') + \sigma_1^2 \int_0^{z_s} dz' \, C_n^2(z') w_{A'}(z') \\ &\quad \sigma_1^2 \sigma_{2'}^2 \end{aligned} \tag{4.24}$$

The fifth term is

$$\begin{aligned} &\langle s_{1'} s_{2'} s_1 s_2 \rangle = \\ &\quad \int_0^{z_s} dz' \, C_n^2(z') w_1(z') \int_0^{z_s} dz'' \, C_n^2(z'') w_2(z'') + \left[\int_0^{z_s} dz' \, C_n^2(z') w_B(z') \right]^2 \\ &\quad + \left[\int_0^{z_s} dz' \, C_n^2(z') \frac{w_3(z')}{2} \right]^2 + R^2 (\sigma_{1'}^2 + \sigma_{2'}^2) \int_0^{z_s} dz' \, C_n^2(z') w_B(z') \\ &\quad + R^4 \sigma_{1'}^2 \sigma_{2'}^2 \end{aligned} \tag{4.25}$$

where $w_B(z')$ is given in equation 4.19. The sixth term in equation 4.3 is

$$\begin{aligned}\langle s_1 s_2 s_1 s_{2'} \rangle = \\ & 2\int_0^{z_s} \mathrm{d}z'\, C_n^2(z') w_1(z') \int_0^{z_s} \mathrm{d}z''\, C_n^2(z'') \frac{w_3(z'')}{2} \\ & + \int_0^{z_s} \mathrm{d}z'\, C_n^2(z') w_B(z') \int_0^{z_s} \mathrm{d}z''\, C_n^2(z'') w_A(z'') \\ & + R^2\sigma_{2'}^2 \int_0^{z_s} \mathrm{d}z'\, C_n^2(z') w_A(z') + \sigma_1^2 \int_0^{z_s} \mathrm{d}z'\, C_n^2(z') w_B(z') \\ & + R^2\sigma_1^2\sigma_{2'}^2 \end{aligned} \tag{4.26}$$

Term seven is

$$\begin{aligned}\langle s_1 s_2 s_{1'} s_2 \rangle = \\ & 2\int_0^{z_s} \mathrm{d}z'\, C_n^2(z') w_1(z') \int_0^{z_s} \mathrm{d}z''\, C_n^2(z'') \frac{w_3(z'')}{2} \\ & + \int_0^{z_s} \mathrm{d}z'\, C_n^2(z') w_B(z') \int_0^{z_s} \mathrm{d}z''\, C_n^2(z'') w_A(z'') \\ & + \sigma_2^2 \int_0^{z_s} \mathrm{d}z'\, C_n^2(z') w_B(z') + R^2\sigma_{1'}^2 \int_0^{z_s} \mathrm{d}z'\, C_n^2(z') w_A(z') \\ & + R^2\sigma_{1'}^2\sigma_2^2 \end{aligned} \tag{4.27}$$

The eighth term is

$$\begin{aligned}\langle s_1 s_{2'} s_{1'} s_{2'} \rangle = \\ & 2\int_0^{z_s} \mathrm{d}z'\, C_n^2(z') \frac{w_3(z')}{2} \int_0^{z_s} \mathrm{d}z''\, C_n^2(z'') w_2(z'') \\ & + \int_0^{z_s} \mathrm{d}z'\, C_n^2(z') w_B(z') \int_0^{z_s} \mathrm{d}z''\, C_n^2(z'') w_{A'}(z'') \\ & + \sigma_{2'}^2 \int_0^{z_s} \mathrm{d}z'\, C_n^2(z') w_B(z') + R^2\sigma_{1'}^2 \int_0^{z_s} \mathrm{d}z'\, C_n^2(z') w_{A'}(z') \\ & + R^2\sigma_{1'}^2\sigma_{2'}^2 \end{aligned} \tag{4.28}$$

Finally, the ninth term is

$$\begin{aligned}\langle s_{1'} s_{2'} s_{1'} s_2 \rangle = \\ & 2\int_0^{z_s} \mathrm{d}z'\, C_n^2(z') \frac{w_3(z')}{2} \int_0^{z_s} \mathrm{d}z''\, C_n^2(z'') w_2(z'') \end{aligned}$$

$$+\int_0^{z_s} \mathrm{d}z'\, C_n^2(z') w_B(z') \int_0^{z_s} \mathrm{d}z''\, C_n^2(z'') w_{A'}(z'')$$
$$+R^2\sigma_{2'}^2 \int_0^{z_s} \mathrm{d}z'\, C_n^2(z') w_{A'}(z') + \sigma_{1'}^2 \int_0^{z_s} \mathrm{d}z'\, C_n^2(z') w_B(z')$$
$$+R^2\sigma_{1'}^2\sigma_{2'}^2 \tag{4.29}$$

Combining the nine terms in equations 4.16 through 4.29 in accordance with equation 4.3 yields

$$\begin{aligned}
\langle C_s^2 \rangle = \\
&2\left[\int_0^{z_s} \mathrm{d}z'\, C_n^2(z') w_1(z')\right]^2 + 2\left[\int_0^{z_s} \mathrm{d}z'\, C_n^2(z') w_2(z')\right]^2 + \left[\int_0^{z_s} \mathrm{d}z' C_n^2(z') w_A(z')\right]^2 \\
&+\left[\int_0^{z_s} \mathrm{d}z' C_n^2(z') w_{A'}(z')\right]^2 + 4\left[\int_0^{z_s} \mathrm{d}z'\, C_n^2(z') w_B(z')\right]^2 + 8\left[\int_0^{z_s} \mathrm{d}z'\, C_n^2(z') \frac{w_3(z')}{2}\right]^2 \\
&+2\int_0^{z_s} \mathrm{d}z' C_n^2(z') w_A(z') \int_0^{z_s} \mathrm{d}z'' C_n^2(z'') w_{A'}(z'') \\
&+4\int_0^{z_s} \mathrm{d}z'\, C_n^2(z') w_1(z') \int_0^{z_s} \mathrm{d}z''\, C_n^2(z'') w_2(z'') \\
&-8\int_0^{z_s} \mathrm{d}z'\, C_n^2(z') w_1(z') \int_0^{z_s} \mathrm{d}z''\, C_n^2(z'') \frac{w_3(z'')}{2} \\
&-8\int_0^{z_s} \mathrm{d}z'\, C_n^2(z') w_2(z') \int_0^{z_s} \mathrm{d}z''\, C_n^2(z'') \frac{w_3(z'')}{2} \\
&-4\int_0^{z_s} \mathrm{d}z'\, C_n^2(z') w_B(z') \int_0^{z_s} \mathrm{d}z'' C_n^2(z'') w_A(z'') \\
&-4\int_0^{z_s} \mathrm{d}z'\, C_n^2(z') w_B(z') \int_0^{z_s} \mathrm{d}z'' C_n^2(z'') w_{A'}(z'') \\
&+\left[\int_0^{z_s} \mathrm{d}z' C_n^2(z') w_A(z') + \int_0^{z_s} \mathrm{d}z' C_n^2(z') w_{A'}(z')\right] \left[\sigma_1^2 + \sigma_2^2 + (\sigma_{1'}^2 + \sigma_{2'}^2)(1 - 2R^2)\right] \\
&+\left[4R^2(\sigma_{1'}^2 + \sigma_{2'}^2) - 2(\sigma_1^2 + \sigma_2^2 + \sigma_{1'}^2 + \sigma_{2'}^2)\right] \int_0^{z_s} \mathrm{d}z'\, C_n^2(z') w_B(z') \\
&+\sigma_1^2\sigma_2^2 + \sigma_{1'}^2\sigma_{2'}^2(1 + 4R^4 - 4R^2) + (\sigma_{1'}^2\sigma_2^2 + \sigma_1^2\sigma_{2'}^2)(1 - 2R^2)
\end{aligned} \tag{4.30}$$

At this point, let w_n' represent w_n with no coefficients before the integral. For example, let

$$w_A'(z) = \frac{w_A(z)}{-2.92k^2 L_1^{-\frac{1}{3}}} \tag{4.31}$$

Making such substitutions allows the coefficients to be shown in equation 4.30 without having to show all the accompanying integrals. Additionally, let $L_1 = RL_2$, and the result

is

$$
\begin{aligned}
\langle C_s^2 \rangle = \\
&4.26k^4R^{-\frac{2}{3}}L_2^{-\frac{2}{3}}\left[\int_0^{z_s} \mathrm{d}z'\, C_n^2(z')w_1'(z')\right]^2 + 4.26k^4L_2^{-\frac{2}{3}}\left[\int_0^{z_s} \mathrm{d}z'\, C_n^2(z')w_2'(z')\right]^2 \\
&+8.53k^4R^{-\frac{2}{3}}L_2^{-\frac{2}{3}}\left[\int_0^{z_s} \mathrm{d}z' C_n^2(z')w_A'(z')\right]^2 + 8.53k^4L_2^{-\frac{2}{3}}\left[\int_0^{z_s} \mathrm{d}z' C_n^2(z')w_{A'}'(z')\right]^2 \\
&+34.11k^4R^{-4}L_2^{-\frac{2}{3}}\left[\int_0^{z_s} \mathrm{d}z'\, C_n^2(z')w_B'(z')\right]^2 + 17.05k^4R^{-4}L_2^{-\frac{2}{3}}\left[\int_0^{z_s} \mathrm{d}z'\, C_n^2(z')w_3'(z')\right]^2 \\
&+17.05k^4R^{-\frac{1}{3}}L_2^{-\frac{2}{3}}\int_0^{z_s} \mathrm{d}z' C_n^2(z')w_A'(z')\int_0^{z_s} \mathrm{d}z'' C_n^2(z'')w_{A'}'(z'') \\
&+8.53k^4R^{-\frac{1}{3}}L_2^{-\frac{2}{3}}\int_0^{z_s} \mathrm{d}z'\, C_n^2(z')w_1'(z')\int_0^{z_s} \mathrm{d}z''\, C_n^2(z'')w_2'(z'') \\
&-17.05k^4R^{-\frac{7}{3}}L_2^{-\frac{2}{3}}\int_0^{z_s} \mathrm{d}z'\, C_n^2(z')w_1'(z')\int_0^{z_s} \mathrm{d}z''\, C_n^2(z'')w_3'(z'') \\
&-17.05k^4R^{-2}L_2^{-\frac{2}{3}}\int_0^{z_s} \mathrm{d}z'\, C_n^2(z')w_2'(z')\int_0^{z_s} \mathrm{d}z''\, C_n^2(z'')w_3'(z'') \\
&-34.11k^4R^{-\frac{7}{3}}L_2^{-\frac{2}{3}}\int_0^{z_s} \mathrm{d}z'\, C_n^2(z')w_B'(z')\int_0^{z_s} \mathrm{d}z'' C_n^2(z'')w_A'(z'') \\
&-34.11k^4R^{-2}L_2^{-\frac{2}{3}}\int_0^{z_s} \mathrm{d}z'\, C_n^2(z')w_B'(z')\int_0^{z_s} \mathrm{d}z'' C_n^2(z'')w_{A'}'(z'') \\
&+\left[-2.92k^2R^{-\frac{1}{3}}L_2^{-\frac{1}{3}}\int_0^{z_s} \mathrm{d}z' C_n^2(z')w_A'(z') - 2.92k^2L_2^{-\frac{1}{3}}\int_0^{z_s} \mathrm{d}z' C_n^2(z')w_{A'}'(z')\right] \\
&\qquad\qquad \times\left[\sigma_1^2+\sigma_2^2+(\sigma_{1'}^2+\sigma_{2'}^2)(1-2R^2)\right] \\
&-\left[4R^2(\sigma_{1'}^2+\sigma_{2'}^2) - 2(\sigma_1^2+\sigma_2^2+\sigma_{1'}^2+\sigma_{2'}^2)\right]2.92k^2R^{-2}L_2^{-\frac{1}{3}}\int_0^{z_s} \mathrm{d}z'\, C_n^2(z')w_B'(z') \\
&+\sigma_1^2\sigma_2^2+\sigma_{1'}^2\sigma_{2'}^2(1+4R^4-4R^2)+(\sigma_{1'}^2\sigma_2^2+\sigma_1^2\sigma_{2'}^2)(1-2R^2) \qquad (4.32)
\end{aligned}
$$

4.2.3 Reduction of Mean Squared Expression The resolution of an optical system operating in the presence of atmospheric turbulence increases with aperture size until a limiting value of resolution is reached beyond which aperture size increases have no effect. This limiting value is called the atmospheric coherence diameter, r_0, and is considered a measure of the quality of "seeing" (6). It is convenient to relate the SNR to r_0. The expression for r_0 is

$$r_0 = 0.185\left[\frac{\lambda^2}{\int C_n^2(z')\mathrm{d}z'}\right]^{\frac{3}{5}} \qquad (4.33)$$

where $\lambda = \frac{2\pi}{k}$. This allows k^4 to be written as

$$k^4 = \frac{5.612}{\left[\int C_n^2(z')\mathrm{d}z'\right]^2} r_0^{-\frac{10}{3}} \tag{4.34}$$

Use of equation 4.34 in equation 4.32 results in

$$\begin{aligned}
\langle C_s^2 \rangle = \;& 23.91\left(\frac{L_2}{r_0}\right)^{\frac{10}{3}} \frac{L_2^{-4}}{\left[\int C_n^2(z')\mathrm{d}z'\right]^2} R^{-\frac{2}{3}} \left[\int_0^{z_s} \mathrm{d}z'\, C_n^2(z') w_1'(z')\right]^2 \\
& + 23.91\left(\frac{L_2}{r_0}\right)^{\frac{10}{3}} \frac{L_2^{-4}}{\left[\int C_n^2(z')\mathrm{d}z'\right]^2} \left[\int_0^{z_s} \mathrm{d}z'\, C_n^2(z') w_2'(z')\right]^2 \\
& + 47.87\left(\frac{L_2}{r_0}\right)^{\frac{10}{3}} \frac{L_2^{-4}}{\left[\int C_n^2(z')\mathrm{d}z'\right]^2} R^{-\frac{2}{3}} \left[\int_0^{z_s} \mathrm{d}z' C_n^2(z') w_A'(z')\right]^2 \\
& + 47.87\left(\frac{L_2}{r_0}\right)^{\frac{10}{3}} \frac{L_2^{-4}}{\left[\int C_n^2(z')\mathrm{d}z'\right]^2} \left[\int_0^{z_s} \mathrm{d}z' C_n^2(z') w_{A'}'(z')\right]^2 \\
& + 191.43\left(\frac{L_2}{r_0}\right)^{\frac{10}{3}} \frac{L_2^{-4}}{\left[\int C_n^2(z')\mathrm{d}z'\right]^2} R^{-4} \left[\int_0^{z_s} \mathrm{d}z'\, C_n^2(z') w_B'(z')\right]^2 \\
& + 95.68\left(\frac{L_2}{r_0}\right)^{\frac{10}{3}} \frac{L_2^{-4}}{\left[\int C_n^2(z')\mathrm{d}z'\right]^2} R^{-4} \left[\int_0^{z_s} \mathrm{d}z'\, C_n^2(z') w_3'(z')\right]^2 \\
& + 95.68\left(\frac{L_2}{r_0}\right)^{\frac{10}{3}} \frac{L_2^{-4}}{\left[\int C_n^2(z')\mathrm{d}z'\right]^2} R^{-\frac{1}{3}} \int_0^{z_s} \mathrm{d}z' C_n^2(z') w_A'(z') \int_0^{z_s} \mathrm{d}z'' C_n^2(z'') w_{A'}'(z'') \\
& + 47.87\left(\frac{L_2}{r_0}\right)^{\frac{10}{3}} \frac{L_2^{-4}}{\left[\int C_n^2(z')\mathrm{d}z'\right]^2} R^{-\frac{1}{3}} \int_0^{z_s} \mathrm{d}z'\, C_n^2(z') w_1'(z') \int_0^{z_s} \mathrm{d}z''\, C_n^2(z'') w_2'(z'') \\
& - 95.68\left(\frac{L_2}{r_0}\right)^{\frac{10}{3}} \frac{L_2^{-4}}{\left[\int C_n^2(z')\mathrm{d}z'\right]^2} R^{-\frac{7}{3}} \int_0^{z_s} \mathrm{d}z'\, C_n^2(z') w_1'(z') \int_0^{z_s} \mathrm{d}z''\, C_n^2(z'') w_3'(z'') \\
& - 95.68\left(\frac{L_2}{r_0}\right)^{\frac{10}{3}} \frac{L_2^{-4}}{\left[\int C_n^2(z')\mathrm{d}z'\right]^2} R^{-2} \int_0^{z_s} \mathrm{d}z'\, C_n^2(z') w_2'(z') \int_0^{z_s} \mathrm{d}z''\, C_n^2(z'') w_3'(z'') \\
& - 191.43\left(\frac{L_2}{r_0}\right)^{\frac{10}{3}} \frac{L_2^{-4}}{\left[\int C_n^2(z')\mathrm{d}z'\right]^2} R^{-\frac{7}{3}} \int_0^{z_s} \mathrm{d}z'\, C_n^2(z') w_B'(z') \int_0^{z_s} \mathrm{d}z'' C_n^2(z'') w_A'(z'') \\
& - 191.43\left(\frac{L_2}{r_0}\right)^{\frac{10}{3}} \frac{L_2^{-4}}{\left[\int C_n^2(z')\mathrm{d}z'\right]^2} R^{-2} \int_0^{z_s} \mathrm{d}z'\, C_n^2(z') w_B'(z') \int_0^{z_s} \mathrm{d}z'' C_n^2(z'') w_{A'}'(z'') \\
& + \left[-6.92\left(\frac{L_2}{r_0}\right)^{\frac{5}{3}} \frac{L_2^{-2}}{\int C_n^2(z')\mathrm{d}z'} R^{-\frac{1}{3}} \int_0^{z_s} \mathrm{d}z' C_n^2(z') w_A'(z') \right. \\
& \qquad \left. -6.92\left(\frac{L_2}{r_0}\right)^{\frac{5}{3}} \frac{L_2^{-2}}{\int C_n^2(z')\mathrm{d}z'} \int_0^{z_s} \mathrm{d}z' C_n^2(z') w_{A'}'(z')\right] \\
& \qquad \times \left[\sigma_1'^2 + \sigma_2'^2 + (\sigma_{1'}'^2 + \sigma_{2'}'^2)(1 - 2R^2)\right]
\end{aligned}$$

$$- \left[4R^2(\sigma_{1'}'^2 + \sigma_{2'}'^2) - 2(\sigma_1'^2 + \sigma_2'^2 + \sigma_{1'}'^2 + \sigma_{2'}'^2)\right]$$
$$\times 6.92 \left(\frac{L_2}{r_0}\right)^{\frac{5}{3}} \frac{L_2^{-2}}{\int C_n^2(z')\mathrm{d}z'} R^{-2} \int_0^{z_s} \mathrm{d}z'\, C_n^2(z') w_B'(z')$$
$$+\sigma_1'^2\sigma_2'^2 + \sigma_{1'}'^2\sigma_{2'}'^2(1 + 4R^4 - 4R^2) + (\sigma_{1'}'^2\sigma_2'^2 + \sigma_1'^2\sigma_{2'}'^2)(1 - 2R^2) \tag{4.35}$$

where $\sigma_n'^2 = \sigma_n^2 L_2^2$.

The mean of C_s can also be written in terms of r_0 using equation 3.69

$$\langle C_s \rangle = -3.46 \left(\frac{L_2}{r_0}\right)^{\frac{5}{3}} \frac{L_2^{-2}}{\int C_n^2(z')\mathrm{d}z'} \int_0^{z_s} \mathrm{d}z' C_n^2(z') \left[R^{-\frac{1}{3}} w_1'(z') + w_2'(z') - 2R^{-2} w_3'(z')\right] \tag{4.36}$$

Notice that the factor $\left(\frac{L_2}{r_0}\right)^{\frac{5}{3}} \frac{L_2^{-2}}{\int C_n^2(z')\mathrm{d}z'}$ is common to equation 4.36 and the square root of equation 4.35. Also, recall that equation 4.36 is in the numerator of the SNR expression, while the square root of equation 4.35 is in the denominator. Therefore, the common terms will cancel in the SNR expression.

All that remains is to relate the slope measurement error, σ_n, to the slope sensor photon count, N. This will allow an examination of the light intensity necessary for useful results. Welsh and Gardner give an expression for the slope measurement error as (23)

$$\sigma = \frac{0.86\pi\eta}{N^{\frac{1}{2}} r_0} \qquad L > r_0 \tag{4.37}$$

where η is a parameter which accounts for detector imperfections and N is the total subaperture photon count.

Equation 4.37 allows σ_n to be related to $\sigma_{n'}$. Recall that $\sigma_{n'}$ is the slope measurement error for an aperture of length L_2 and σ_n is the slope measurement error for an aperture of length L_1. If the photon count for an aperture of dimension L_2 is N, then the photon count, N', for a smaller, co-located aperture of dimension L_1 is

$$N' = \frac{L_1^2}{L_2^2} N = R^2 N \tag{4.38}$$

Thus,

$$\sigma_n = R^{-1} \sigma_{n'} \tag{4.39}$$

Recall that $\sigma_{n'}'^2 = \sigma_{n'}^2 L_2^2$.

It is possible to relate $\sigma_{n'}'^2$ to the photon noise count through equation 4.37. The resulting equation is

$$\frac{N}{\left(\frac{L_2}{r_0}\right)^{\frac{1}{3}}} = \frac{(0.86\pi\eta)^2}{\sigma_{n'}'^2 \left(\frac{L_2}{r_0}\right)^{-\frac{5}{3}}} \tag{4.40}$$

Apertures $s_{1'}$ and $s_{2'}$ are identical, therefore it is reasonable to assume that $\sigma_{1'}'^2 = \sigma_{2'}'^2$. Likewise, it is reasonable to assume that $\sigma_1'^2 = \sigma_2'^2$. Making these assumptions and using equations 4.38 and 4.40, the mean square value of C_s is

$$\begin{aligned}
\langle C_s^2 \rangle = \\
&23.91R^{-\frac{2}{3}} \left[\int_0^{z_s} \mathrm{d}z'\, C_n^2(z') w_1'(z')\right]^2 + 23.91 \left[\int_0^{z_s} \mathrm{d}z'\, C_n^2(z') w_2'(z')\right]^2 \\
&+47.87R^{-\frac{2}{3}} \left[\int_0^{z_s} \mathrm{d}z' C_n^2(z') w_A'(z')\right]^2 + 11.95 \left[\int_0^{z_s} \mathrm{d}z' C_n^2(z') w_{A'}'(z')\right]^2 \\
&+191.43R^{-4} \left[\int_0^{z_s} \mathrm{d}z'\, C_n^2(z') w_B'(z')\right]^2 + 95.68R^{-4} \left[\int_0^{z_s} \mathrm{d}z'\, C_n^2(z') w_3'(z')\right]^2 \\
&+95.68R^{-\frac{1}{3}} \int_0^{z_s} \mathrm{d}z' C_n^2(z') w_A'(z') \int_0^{z_s} \mathrm{d}z'' C_n^2(z'') w_{A'}'(z'') \\
&+47.87R^{-\frac{1}{3}} \int_0^{z_s} \mathrm{d}z'\, C_n^2(z') w_1'(z') \int_0^{z_s} \mathrm{d}z''\, C_n^2(z'') w_2'(z'') \\
&-95.68R^{-\frac{7}{3}} \int_0^{z_s} \mathrm{d}z'\, C_n^2(z') w_1'(z') \int_0^{z_s} \mathrm{d}z''\, C_n^2(z'') w_3'(z'') \\
&-95.68R^{-2} \int_0^{z_s} \mathrm{d}z'\, C_n^2(z') w_2'(z') \int_0^{z_s} \mathrm{d}z''\, C_n^2(z'') w_3'(z'') \\
&-191.43R^{-\frac{7}{3}} \int_0^{z_s} \mathrm{d}z'\, C_n^2(z') w_B'(z') \int_0^{z_s} \mathrm{d}z'' C_n^2(z'') w_A'(z'') \\
&-191.43R^{-2} \int_0^{z_s} \mathrm{d}z'\, C_n^2(z') w_B'(z') \int_0^{z_s} \mathrm{d}z'' C_n^2(z'') w_{A'}'(z'') \\
&-13.84(0.86\pi\eta)^2 \left(\frac{N}{\left(\frac{L_2}{r_0}\right)^{\frac{1}{3}}}\right)^{-1} (1 - 2R^2 + R^{-2}) \int C_n^2(z')\, \mathrm{d}z' \\
&\qquad \times \left[R^{-\frac{1}{3}} \int_0^{z_s} \mathrm{d}z'\, C_n^2(z') w_A'(z') + \int_0^{z_s} \mathrm{d}z'\, C_n^2(z') w_{A'}'(z')\right] \\
&-27.68(0.86\pi\eta)^2 \left(\frac{N}{\left(\frac{L_2}{r_0}\right)^{\frac{1}{3}}}\right)^{-1} \int C_n^2(z')\, \mathrm{d}z' R^{-2}(2R^2 - R^{-1} - 1) \int_0^{z_s} \mathrm{d}z'\, C_n^2(z') w_B'(z')
\end{aligned}$$

$$+\left[(0.86\pi\eta)^2\left(\frac{N}{\left(\frac{L_2}{r_0}\right)^{\frac{1}{3}}}\right)^{-1}\int C_n^2(z')\,dz'\right]^2(4R^4-4R^2-4R+2R^{-1}+R^{-2}+1)$$

(4.41)

4.2.4 Simplification of SNR Expression The SNR expression can be simplified by making the assumption that $1-\frac{z'}{z_s}\approx 1$. Such an assumption simplifies both the mean and the mean square expressions. The expression for the mean square value of C_s becomes

$$\begin{aligned}
\langle C_s^2\rangle = \\
&23.91R^{-\frac{2}{3}}\left[\int_0^{z_s} dz'\,C_n^2(z')w_1''(z')\right]^2+23.91\left[\int_0^{z_s} dz'\,C_n^2(z')w_2''(z')\right]^2\\
&+47.87(R^{-\frac{2}{3}}+1)A^2\left[\int_0^{z_s} dz' C_n^2(z')\right]^2\\
&+191.43R^{-4}B^2\left[\int_0^{z_s} dz'\,C_n^2(z')\right]^2+95.68R^{-4}\left[\int_0^{z_s} dz'\,C_n^2(z')w_3''(z')\right]^2\\
&+95.68R^{-\frac{1}{3}}A^2\left[\int_0^{z_s} dz' C_n^2(z')\right]^2\\
&+47.87R^{-\frac{1}{3}}\int_0^{z_s} dz'\,C_n^2(z')w_1''(z')\int_0^{z_s} dz''\,C_n^2(z'')w_2''(z'')\\
&-95.68R^{-\frac{7}{3}}\int_0^{z_s} dz'\,C_n^2(z')w_1''(z')\int_0^{z_s} dz''\,C_n^2(z'')w_3''(z'')\\
&-95.68R^{-2}\int_0^{z_s} dz'\,C_n^2(z')w_2''(z')\int_0^{z_s} dz''\,C_n^2(z'')w_3(z'')\\
&-191.43(R^{-\frac{7}{3}}+R^{-2})A\,B\left[\int_0^{z_s} dz' C_n^2(z')\right]^2\\
&-13.84(0.86\pi\eta)^2\left(\frac{N}{\left(\frac{L_2}{r_0}\right)^{\frac{1}{3}}}\right)^{-1}A(1-2R^2+R^{-\frac{1}{3}}+R^{-\frac{7}{3}}+R^{-2}-2R^{\frac{5}{3}})\int C_n^2(z')\,dz'\\
&-27.68(0.86\pi\eta)^2\left(\frac{N}{\left(\frac{L_2}{r_0}\right)^{\frac{1}{3}}}\right)^{-1}R^{-2}(2R^2-R^{-1}-1)B\int C_n^2(z')\,dz'\\
&+\left[(0.86\pi\eta)^2\left(\frac{N}{\left(\frac{L_2}{r_0}\right)^{\frac{1}{3}}}\right)^{-1}\int C_n^2(z')\,dz'\right]^2(4R^4-4R^2-4R+2R^{-1}+R^{-2}+1)
\end{aligned}$$

(4.42)

where

$$w_1''(z') = \int_{-1}^{1} \mathrm{tri}(u') \left\{ 2\left[\left(\frac{\gamma}{RL_2}\right)^2 + u'^2\right]^{\frac{5}{6}} - \left[\left(\frac{\gamma}{RL_2} - 1\right)^2 + u'^2\right]^{\frac{5}{6}} - \left[\left(\frac{\gamma}{RL_2} + 1\right)^2 + u'^2\right]^{\frac{5}{6}} \right\} \tag{4.43}$$

and

$$w_2''(z') = \int_{-1}^{1} \mathrm{tri}(u') \left\{ 2\left[\left(\frac{\gamma}{L_2}\right)^2 + u'^2\right]^{\frac{5}{6}} - \left[\left(\frac{\gamma}{L_2} - 1\right)^2 + u'^2\right]^{\frac{5}{6}} - \left[\left(\frac{\gamma}{L_2} + 1\right)^2 + u'^2\right]^{\frac{5}{6}} \right\} \tag{4.44}$$

and

$$w_3''(z') = \int_{-\left(\frac{R+1}{2}\right)}^{\frac{R-1}{2}} \mathrm{d}u' \left(u' + \frac{1+R}{2}\right) g_3''(u') + R\int_{\frac{R-1}{2}}^{\frac{1-R}{2}} \mathrm{d}u'\, g_3''(u') + \int_{\frac{1-R}{2}}^{\frac{R+1}{2}} \left(\frac{R+1}{2} - u'\right) g_3''(u') \tag{4.45}$$

where

$$g_3''(u') = \left\{\left[\frac{\gamma}{L_2} + \frac{1-R}{2}\right]^2 + [u']^2\right\}^{\frac{5}{6}} - \left\{\left[\frac{\gamma}{L_2} - \frac{R+1}{2}\right]^2 + [u']^2\right\}^{\frac{5}{6}} - \left\{\left[\frac{\gamma}{L_2} + \frac{R+1}{2}\right]^2 + [u']^2\right\}^{\frac{5}{6}} + \left\{\left[\frac{\gamma}{L_2} + \frac{R-1}{2}\right]^2 + [u']^2\right\}^{\frac{5}{6}} \tag{4.46}$$

The two constants, A and B, found in equation 4.42 are given by

$$A = \int_{-1}^{1} \mathrm{tri}(u') \left[u'^{\frac{10}{6}} - (u'^2 + 1)^{\frac{5}{6}}\right] \tag{4.47}$$

and

$$B = \int_{-\left(\frac{R+1}{2}\right)}^{\frac{R-1}{2}} \mathrm{d}u' \left(u' + \frac{1+R}{2}\right) g_B(u') + R \int_{\frac{R-1}{2}}^{\frac{1-R}{2}} \mathrm{d}u'\, g_B(u') + \int_{\frac{1-R}{2}}^{\frac{R+1}{2}} \left(\frac{R+1}{2} - u'\right) g_B(u') \tag{4.48}$$

where

$$g_B(u') = \left[\left(\frac{1-R}{2}\right)^2 + u'^2\right]^{\frac{5}{6}} - \left[\left(\frac{1+R}{2}\right)^2 + u'^2\right]^{\frac{5}{6}} \tag{4.49}$$

The simplified form of the mean value of C_s is

$$\langle C_s \rangle = -3.46 \int_0^{z_s} \mathrm{d}z' C_n^2(z') \left[R^{-\frac{1}{3}} w_1''(z') + w_2''(z') - 2R^{-2} w_3''(z')\right] \tag{4.50}$$

where expressions for $w_1''(z')$, $w_2''(z')$ and $w_3''(z')$ are given in equations 4.43, 4.44, and 4.45 above.

The signal-to-noise ratio may now be evaluated using equations 4.42 and 4.50 in equation 4.1.

4.3 Signal-to-Noise Ratio Results

The signal-to-noise ratio gives an indication of the ability of the measurement methods presented in this thesis to provide useful estimates of C_n^2. In order to evaluate the SNR expression derived in the previous section, it was necessary to choose values for several parameters. After choosing the necessary parameters, the SNR without any slope measurement noise present (i.e. $N \rightarrow \infty$) was calculated for various ratios of $\frac{L_1}{L_2}$. Next, the total photon count, N, was allowed to vary in order to observe the effect of slope measurement noise on the SNR.

The model used for the $C_n^2(z')$ profile was the Hufnagel-Valley model shown in Chapter 2. The guide stars were placed at $z_s = 100$ km and the C_n^2 vertical profile was only measured to an altitude of $z' = 15$ km. This allowed use of the approximation $1 - \frac{z'}{z_s} \approx 1$. The guide star separation was $\Delta p_x = 1$ km (corresponding to an angular separation of

0.001 radians) and the aperture separation was allowed to vary in order to control the intersection altitude.

4.3.1 SNR Without Measurement Error Figures 4.1 through 4.3 show the calculated signal-to-noise ratios when no slope measurement noise is present. The SNR im-

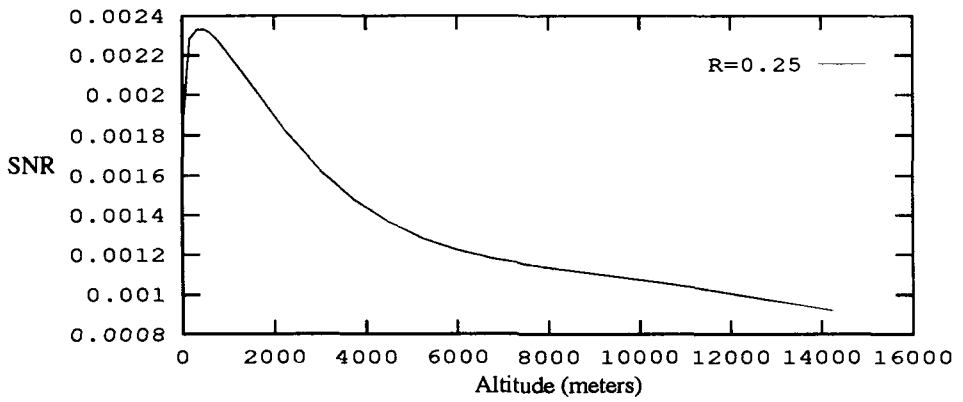

Figure 4.1. SNR Without Measurement Noise, $R = 0.25$

proves as R approaches one. This behavior indicates that the variance of the measurement correlations is approaching zero faster than the mean approaches zero. Another way of looking at it is that the weighting function is becoming more sharply peaked as $R \rightarrow 1$, thus correlations due to turbulent eddies not at the intersection altitude (noise) are receiving less weight.

4.3.2 Measurement Noise Effects on SNR As equation 4.37 shows, the slope measurement error is related to the photon count. Figure 4.4 demonstrates the effect of changes in total photon count, N, on the SNR. In obtaining this data, a value of $\eta = 1.5$ was assumed. This is a typical value of η for wave front phase slope sensors (23). The y axis of the plot is normalized by the SNR value when no slope measurement noise is present, i.e. the SNR for $N \rightarrow \infty$. The figure shows that the lower ratio of $\frac{L_1}{L_2}$ allows near noiseless performance at a lower photon count value than required by the higher ratio. This is due to less correlation of the two co-located apertures' measurement errors for smaller values of $\frac{L_1}{L_2}$. Note that while Figure 4.4 presents the SNR as a function of noise for one particular

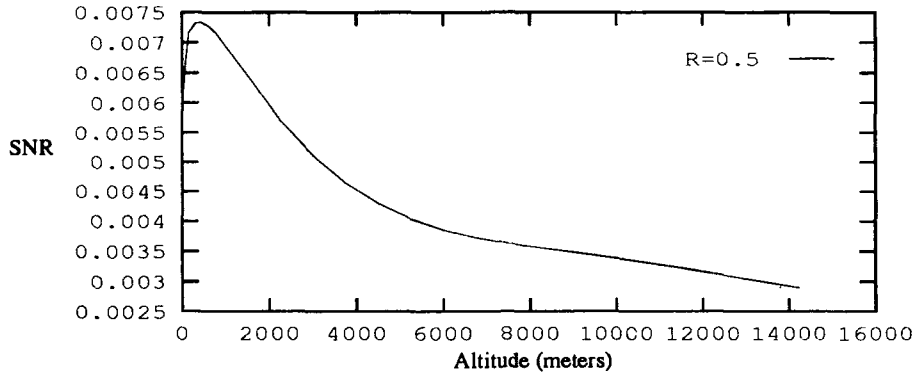

Figure 4.2. SNR Without Measurement Noise, $R = 0.5$

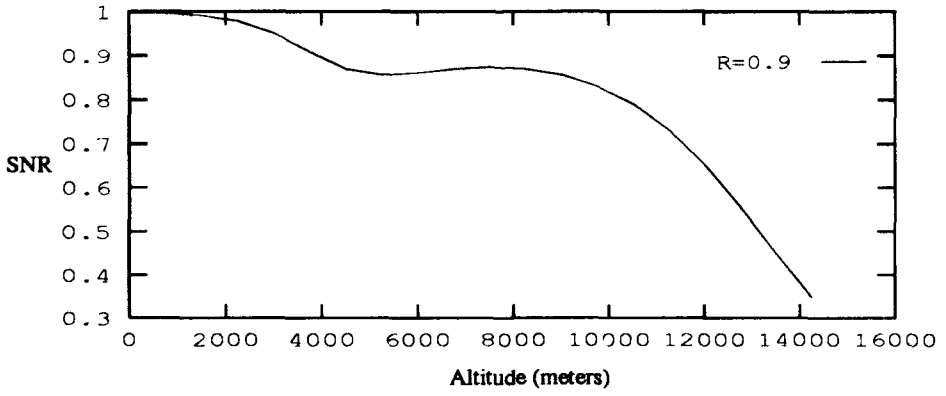

Figure 4.3. SNR Without Measurement Noise, $R = 0.9$

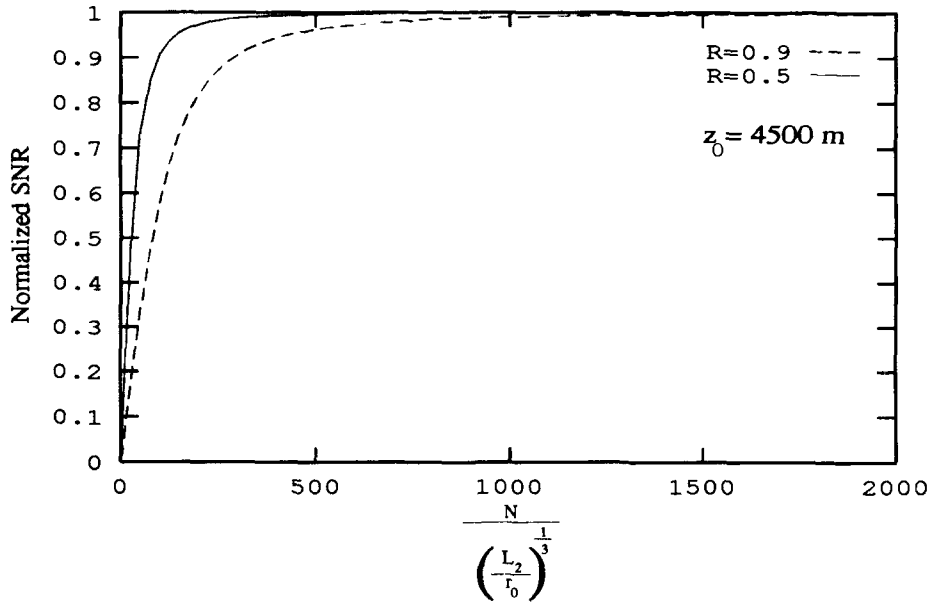

Figure 4.4. SNR as a Function of Noise

altitude, the shape of the curves would be the same for any altitude because the slope measurement noise is independent of altitude.

4.4 Derivation of SNR Expression for $\langle C_s'(0)\rangle$

4.4.1 Definition of $\langle C_s'(0)\rangle$ *SNR* The wind velocity $\vec{V}$ is estimated from the slope evaluated at zero time lag of the time-lagged measurement correlations. Therefore the SNR of the estimate of C_s' is found using the mean and variance of C_s' at $\tau = 0$. The definition of the SNR of the slope measurement at $\tau = 0$ is

$$\text{SNR} = \lim_{\tau \to 0} \frac{\left\langle \left[\frac{C_s(\tau) - C_s(0)}{\tau} \right] \right\rangle}{\left\{ \left\langle \left[\frac{C_s(\tau) - C_s(0)}{\tau} \right]^2 \right\rangle - \left[\left\langle \frac{C_s(\tau) - C_s(0)}{\tau} \right\rangle \right]^2 \right\}^{\frac{1}{2}}} \tag{4.51}$$

or

$$\text{SNR} = \lim_{\tau \to 0} \frac{\langle C_s(\tau)\rangle - \langle C_s(0)\rangle}{\{\langle C_s^2(\tau)\rangle + \langle C_s^2(0)\rangle - 2\langle C_s^2(\tau) C_s^2(0)\rangle - [\langle C_s(\tau)\rangle - \langle C_s(0)\rangle]^2\}^{\frac{1}{2}}} \tag{4.52}$$

Expressions for the mean and mean square values of the measurement correlations evaluated at $\tau = 0$ have already been derived in the first part of this chapter. However, equation 4.52 also contains the mean and mean square values of C_s as a function of τ, as well as the time-lagged correlation of the measurements. Expressions for these terms must be developed. However, the derivation of these remaining terms is almost identical to previous derivations and thus is not presented here. Instead, only the final results are shown.

4.4.2 Mean Value as a Function of τ The expression for the mean value of C_s as a function of τ is

$$
\begin{aligned}
&\langle C_s(\tau)\rangle = \\
&\quad -3.46R^{-\frac{1}{3}}\int_0^{z_s} \mathrm{d}z'\, C_n^2(z')\int \mathrm{d}u'\,\mathrm{tri}\left(u'-\frac{\Delta y}{RL_2}\right) \\
&\quad \times\left\{2\left\{\left[\frac{\gamma}{RL_2}+\frac{z'\Delta x}{z_sRL_2}\right]^2+\left[u'\left(1-\frac{z'}{z_s}\right)\right]^2+\frac{V^2(z')}{R^2L_2^2}\tau^2\right.\right. \\
&\qquad \left.\left.-2\tau\cos(\theta)\frac{V(z')}{RL_2}\left[\left(\frac{\gamma}{RL_2}+\frac{\Delta x\, z'}{RL_2z_s}\right)^2+u'^2\left(1-\frac{z'}{z_s}\right)^2\right]^{\frac{1}{2}}\right\}^{\frac{5}{6}} \\
&\quad -\left\{\left[\frac{\gamma}{RL_2}-1+\frac{z'}{z_s}\left(\frac{\Delta x}{RL_2}+1\right)\right]^2+\left[u'\left(1-\frac{z'}{z_s}\right)\right]^2+\frac{V^2(z')}{R^2L_2^2}\tau^2\right. \\
&\qquad \left.-2\tau\cos(\theta)\frac{V(z')}{RL_2}\left[\left(\frac{\gamma}{RL_2}-1+\frac{z'}{z_s}\left(\frac{\Delta x}{RL_2}+1\right)\right)^2+u'^2\left(1-\frac{z'}{z_s}\right)^2\right]^{\frac{1}{2}}\right\}^{\frac{5}{6}} \\
&\quad -\left\{\left[\frac{\gamma}{RL_2}+1+\frac{z'}{z_s}\left(\frac{\Delta x}{RL_2}-1\right)\right]^2+\left[u'\left(1-\frac{z'}{z_s}\right)\right]^2+\frac{V^2(z')}{R^2L_2^2}\tau^2\right. \\
&\qquad \left.\left.-2\tau\cos(\theta)\frac{V(z')}{RL_2}\left[\left(\frac{\gamma}{RL_2}+1+\frac{z'}{z_s}\left(\frac{\Delta x}{RL_2}-1\right)\right)^2+u'^2\left(1-\frac{z'}{z_s}\right)^2\right]^{\frac{1}{2}}\right\}^{\frac{5}{6}}\right\} \\
&\quad -3.46\int_0^{z_s} \mathrm{d}z'\, C_n^2(z')\int \mathrm{d}u'\,\mathrm{tri}\left(u'-\frac{\Delta y}{L_2}\right) \\
&\quad \times\left\{2\left\{\left[\frac{\gamma}{L_2}+\frac{z'\Delta x}{z_sL_2}\right]^2+\left[u'\left(1-\frac{z'}{z_s}\right)\right]^2+\frac{V^2(z')}{L_2^2}\tau^2\right.\right. \\
&\qquad \left.\left.-2\tau\cos(\theta)\frac{V(z')}{L_2}\left[\left(\frac{\gamma}{L_2}+\frac{\Delta x\, z'}{L_2z_s}\right)^2+u'^2\left(1-\frac{z'}{z_s}\right)^2\right]^{\frac{1}{2}}\right\}^{\frac{5}{6}}
\end{aligned}
$$

$$
\begin{aligned}
&-\left\{\left[\frac{\gamma}{L_2}-1+\frac{z'}{z_s}\left(\frac{\Delta x}{L_2}+1\right)\right]^2+\left[u'\left(1-\frac{z'}{z_s}\right)\right]^2+\frac{V^2(z')}{L_2^2}\tau^2\right.\\
&\qquad\left.-2\tau\cos(\theta)\frac{V(z')}{L_2}\left[\left(\frac{\gamma}{L_2}-1+\frac{z'}{z_s}\left(\frac{\Delta x}{L_2}+1\right)\right)^2+u'^2\left(1-\frac{z'}{z_s}\right)^2\right]^{\frac{1}{2}}\right\}^{\frac{5}{6}}\\
&-\left\{\left[\frac{\gamma}{L_2}+1+\frac{z'}{z_s}\left(\frac{\Delta x}{L_2}11\right)\right]^2+\left[u'\left(1-\frac{z'}{z_s}\right)\right]^2+\frac{V^2(z')}{L_2^2}\tau^2\right.\\
&\qquad\left.-2\tau\cos(\theta)\frac{V(z')}{L_2}\left[\left(\frac{\gamma}{L_2}+1+\frac{z'}{z_s}\left(\frac{\Delta x}{L_2}-1\right)\right)^2+u'^2\left(1-\frac{z'}{z_s}\right)^2\right]^{\frac{1}{2}}\right\}^{\frac{5}{6}}\Bigg\}\\
&+6.92R^{-2}\int_0^{z_s}\mathrm{d}z'\,C_n^2(z')\\
&\times\left\{\int_{-\left(\frac{R+1}{2}\right)+\frac{\Delta y}{L_2}}^{\frac{R-1}{2}+\frac{\Delta y}{L_2}}\mathrm{d}u'\left(u'+\frac{1+R}{2}-\frac{\Delta y}{L_2}\right)fw_3(u')+R\int_{\frac{R-1}{2}+\frac{\Delta y}{L_2}}^{\frac{1-R}{2}+\frac{\Delta y}{L_2}}\mathrm{d}u'\,fw_3(u')\right.\\
&\qquad\left.+\int_{\frac{1-R}{2}+\frac{\Delta y}{L_2}}^{\frac{R+1}{2}+\frac{\Delta y}{L_2}}\left(\frac{R+1}{2}-u'+\frac{\Delta y}{L_2}\right)fw_3(u')\right\}
\end{aligned}
\tag{4.53}
$$

where θ is the angle between $\vec{V}$ and the vector $\vec{r}$ defined by $\vec{r}=\Delta\vec{p}\frac{z'}{z_s}+(\vec{x}-\vec{x}')\left(1-\frac{z'}{z_s}\right)$ and

$$
\begin{aligned}
&fw_3(u')=\\
&\left\{\left[\frac{\gamma}{L_2}+\frac{1-R}{2}+\frac{z'}{z_s}\left(\frac{\Delta x}{L_2}-\frac{1-R}{2}\right)\right]^2+\left[u'\left(1-\frac{z'}{z_s}\right)\right]^2+\frac{V^2(z')}{L_2^2}\tau^2\right.\\
&\left.-2\frac{V(z')}{L_2}\tau\cos(\theta)\left\{\left[\frac{\gamma}{L_2}+\frac{1-R}{2}+\frac{z'}{z_s}\left(\frac{\Delta x}{L_2}-\frac{1-R}{2}\right)\right]^2+\left[u'\left(1-\frac{z'}{z_s}\right)\right]^2\right\}^{\frac{1}{2}}\right\}^{\frac{5}{6}}\\
&-\left\{\left[\frac{\gamma}{L_2}-\frac{R+1}{2}+\frac{z'}{z_s}\left(\frac{\Delta x}{L_2}+\frac{R+1}{2}\right)\right]^2+\left[u'\left(1-\frac{z'}{z_s}\right)\right]^2+\frac{V^2(z')}{L_2^2}\tau^2\right.\\
&\left.-2\frac{V(z')}{L_2}\tau\cos(\theta)\left\{\left[\frac{\gamma}{L_2}-\frac{R+1}{2}+\frac{z'}{z_s}\left(\frac{\Delta x}{L_2}+\frac{R+1}{2}\right)\right]^2+\left[u'\left(1-\frac{z'}{z_s}\right)\right]^2\right\}^{\frac{1}{2}}\right\}^{\frac{5}{6}}\\
&-\left\{\left[\frac{\gamma}{L_2}+\frac{R+1}{2}+\frac{z'}{z_s}\left(\frac{\Delta x}{L_2}-\frac{R+1}{2}\right)\right]^2+\left[u'\left(1-\frac{z'}{z_s}\right)\right]^2+\frac{V^2(z')}{L_2^2}\tau^2\right.\\
&\left.-2\frac{V(z')}{L_2}\tau\cos(\theta)\left\{\left[\frac{\gamma}{L_2}+\frac{R+1}{2}+\frac{z'}{z_s}\left(\frac{\Delta x}{L_2}-\frac{R+1}{2}\right)\right]^2+\left[u'\left(1-\frac{z'}{z_s}\right)\right]^2\right\}^{\frac{1}{2}}\right\}^{\frac{5}{6}}\\
&\left\{\left[\frac{\gamma}{L_2}+\frac{R-1}{2}+\frac{z'}{z_s}\left(\frac{\Delta x}{L_2}-\frac{R-1}{2}\right)\right]^2+\left[u'\left(1-\frac{z'}{z_s}\right)\right]^2+\frac{V^2(z')}{L_2^2}\tau^2\right.
\end{aligned}
$$

$$-2\frac{V(z')}{L_2}\tau\cos(\theta)\left\{\left[\frac{\gamma}{L_2}+\frac{R-1}{2}+\frac{z'}{z_s}\left(\frac{\Delta x}{L_2}-\frac{R-1}{2}\right)\right]^2+\left[u'\left(1-\frac{z'}{z_s}\right)\right]^2\right\}^{\frac{1}{2}}\Bigg\}^{\frac{5}{6}} \tag{4.54}$$

where $\gamma = \Delta p_x \frac{z'}{z_s} - \Delta x$.

4.4.3 Expression for Mean Square Value Terms The denominator of equation 4.52 contains the sum of $\langle C_s^2(\tau)\rangle$ and $\langle C_s^2(0)\rangle$. $\langle C_s^2(0)\rangle$ has already been calculated, and adding $\langle C_s^2(\tau)\rangle$ yields

$$\begin{aligned}
&\langle C_s^2(0)\rangle + \langle C_s^2(\tau)\rangle = \\
&\quad 23.91R^{-\frac{2}{3}}\left[\int_0^{z_s} \mathrm{d}z'\, C_n^2(z')ww_1'(z')\right]^2 + 23.91\left[\int_0^{z_s} \mathrm{d}z'\, C_n^2(z')ww_2'(z')\right]^2 \\
&\quad +95.68R^{-4}\left[\int_0^{z_s} \mathrm{d}z'\, C_n^2(z')ww_3'(z')\right]^2 \\
&\quad +47.87R^{-\frac{1}{3}}\int_0^{z_s} \mathrm{d}z'\, C_n^2(z')ww_1'(z')\int_0^{z_s} \mathrm{d}z''\, C_n^2(z'')ww_2'(z'') \\
&\quad +23.91R^{-\frac{2}{3}}\left[\int_0^{z_s} \mathrm{d}z'\, C_n^2(z')w_1'(z')\right]^2 + 23.91\left[\int_0^{z_s} \mathrm{d}z'\, C_n^2(z')w_2'(z')\right]^2 \\
&\quad +95.68R^{-\frac{2}{3}}\left[\int_0^{z_s} \mathrm{d}z' C_n^2(z')w_A'(z')\right]^2 + 95.68\left[\int_0^{z_s} \mathrm{d}z' C_n^2(z')w_A'(z')\right]^2 \\
&\quad +382.86R^{-4}\left[\int_0^{z_s} \mathrm{d}z'\, C_n^2(z')w_B'(z')\right]^2 + 95.68R^{-4}\left[\int_0^{z_s} \mathrm{d}z'\, C_n^2(z')w_3'(z')\right]^2 \\
&\quad +191.43R^{-\frac{1}{3}}\left[\int_0^{z_s} \mathrm{d}z' C_n^2(z')w_A'(z')\right]^2 \\
&\quad +47.87R^{-\frac{1}{3}}\int_0^{z_s} \mathrm{d}z'\, C_n^2(z')w_1'(z')\int_0^{z_s} \mathrm{d}z''\, C_n^2(z'')w_2'(z'') \\
&\quad -95.68R^{-\frac{7}{3}}\int_0^{z_s} \mathrm{d}z'\, C_n^2(z')ww_1'(z')\int_0^{z_s} \mathrm{d}z''\, C_n^2(z'')ww_3'(z'') \\
&\quad -95.68R^{-2}\int_0^{z_s} \mathrm{d}z'\, C_n^2(z')ww_2'(z')\int_0^{z_s} \mathrm{d}z''\, C_n^2(z'')ww_3'(z'') \\
&\quad -95.68R^{-\frac{7}{3}}\int_0^{z_s} \mathrm{d}z'\, C_n^2(z')w_1'(z')\int_0^{z_s} \mathrm{d}z''\, C_n^2(z'')w_3'(z'') \\
&\quad -95.68R^{-2}\int_0^{z_s} \mathrm{d}z'\, C_n^2(z')w_2'(z')\int_0^{z_s} \mathrm{d}z''\, C_n^2(z'')w_3(z'') \\
&\quad -382.86R^{-\frac{7}{3}}\int_0^{z_s} \mathrm{d}z'\, C_n^2(z')w_B'(z')\int_0^{z_s} \mathrm{d}z'' C_n^2(z'')w_A'(z'') \\
&\quad -382.86R^{-2}\int_0^{z_s} \mathrm{d}z'\, C_n^2(z')w_B'(z')\int_0^{z_s} \mathrm{d}z'' C_n^2(z'')w_{A'}'(z'')
\end{aligned}$$

$$
\begin{aligned}
&-27.68(0.86\pi\eta)^2\left(\frac{N}{\left(\frac{L_2}{r_0}\right)^{\frac{1}{3}}}\right)^{-1}(1-2R^2+R^{-2})\int C_n^2(z')\,\mathrm{d}z' \\
&\qquad\times\left[R^{-\frac{1}{3}}\int_0^{z_s}\mathrm{d}z'\,C_n^2(z')w'_A(z')+\int_0^{z_s}\mathrm{d}z'\,C_n^2(z')w'_{A'}(z')\right] \\
&-55.36(0.86\pi\eta)^2\left(\frac{N}{\left(\frac{L_2}{r_0}\right)^{\frac{1}{3}}}\right)^{-1}\int C_n^2(z')\,\mathrm{d}z'R^{-2}(2R^2-R^{-1}-1)\int_0^{z_s}\mathrm{d}z'\,C_n^2(z')w'_B(z') \\
&+2\left[(0.86\pi\eta)^2\left(\frac{N}{\left(\frac{L_2}{r_0}\right)^{\frac{1}{3}}}\right)^{-1}\int C_n^2(z')\,\mathrm{d}z'\right]^2(4R^4-4R^2-4R+2R^{-1}+R^{-2}+1)
\end{aligned}
\tag{4.55}
$$

where

$$
\begin{aligned}
&ww'_1(z')= \\
&\quad\int \mathrm{d}u'\,\mathrm{tri}(u'-\frac{\Delta y}{RL_2}) \\
&\quad\times\left\{2\left\{\left[\frac{\gamma}{RL_2}+\frac{z'\Delta x}{z_sRL_2}\right]^2+\left[u'\left(1-\frac{z'}{z_s}\right)\right]^2+\frac{V^2(z')}{R^2L_2^2}\tau^2\right.\right. \\
&\qquad\left.\left.-2\tau\cos(\theta)\frac{V(z')}{RL_2}\left[\left(\frac{\gamma}{RL_2}+\frac{\Delta x\,z'}{RL_2z_s}\right)^2+u'^2\left(1-\frac{z'}{z_s}\right)^2\right]^{\frac{1}{2}}\right\}^{\frac{5}{6}} \\
&\quad-\left\{\left[\frac{\gamma}{RL_2}-1+\frac{z'}{z_s}\left(\frac{\Delta x}{RL_2}+1\right)\right]^2+\left[u'\left(1-\frac{z'}{z_s}\right)\right]^2+\frac{V^2(z')}{R^2L_2^2}\tau^2\right. \\
&\qquad\left.-2\tau\cos(\theta)\frac{V(z')}{RL_2}\left[\left(\frac{\gamma}{RL_2}-1+\frac{z'}{z_s}\left(\frac{\Delta x}{RL_2}+1\right)\right)^2+u'^2\left(1-\frac{z'}{z_s}\right)^2\right]^{\frac{1}{2}}\right\}^{\frac{5}{6}} \\
&\quad-\left\{\left[\frac{\gamma}{RL_2}+1+\frac{z'}{z_s}\left(\frac{\Delta x}{RL_2}11\right)\right]^2+\left[u'\left(1-\frac{z'}{z_s}\right)\right]^2+\frac{V^2(z')}{R^2L_2^2}\tau^2\right. \\
&\qquad\left.\left.-2\tau\cos(\theta)\frac{V(z')}{RL_2}\left[\left(\frac{\gamma}{RL_2}+1+\frac{z'}{z_s}\left(\frac{\Delta x}{RL_2}-1\right)\right)^2+u'^2\left(1-\frac{z'}{z_s}\right)^2\right]^{\frac{1}{2}}\right\}^{\frac{5}{6}}\right\}
\end{aligned}
\tag{4.56}
$$

and

$$
\begin{aligned}
ww_2'(z') = & \\
& \int \mathrm{d}u' \,\mathrm{tri}(u' - \frac{\Delta y}{L_2}) \\
& \times \left\{ 2 \left\{ \left[\frac{\gamma}{L_2} + \frac{z' \Delta x}{z_s L_2} \right]^2 + \left[u' \left(1 - \frac{z'}{z_s} \right) \right]^2 + \frac{V^2(z')}{L_2^2} \tau^2 \right. \right. \\
& \qquad \left. \left. -2\tau \cos(\theta) \frac{V(z')}{L_2} \left[\left(\frac{\gamma}{L_2} + \frac{\Delta x \, z'}{L_2 z_s} \right)^2 + u'^2 \left(1 - \frac{z'}{z_s} \right)^2 \right]^{\frac{1}{2}} \right\}^{\frac{5}{6}} \right. \\
& \quad - \left\{ \left[\frac{\gamma}{L_2} - 1 + \frac{z'}{z_s} \left(\frac{\Delta x}{L_2} + 1 \right) \right]^2 + \left[u' \left(1 - \frac{z'}{z_s} \right) \right]^2 + \frac{V^2(z')}{L_2^2} \tau^2 \right. \\
& \qquad \left. -2\tau \cos(\theta) \frac{V(z')}{L_2} \left[\left(\frac{\gamma}{L_2} - 1 + \frac{z'}{z_s} \left(\frac{\Delta x}{L_2} + 1 \right) \right)^2 + u'^2 \left(1 - \frac{z'}{z_s} \right)^2 \right]^{\frac{1}{2}} \right\}^{\frac{5}{6}} \\
& \quad - \left\{ \left[\frac{\gamma}{L_2} + 1 + \frac{z'}{z_s} \left(\frac{\Delta x}{L_2} 11 \right) \right]^2 + \left[u' \left(1 - \frac{z'}{z_s} \right) \right]^2 + \frac{V^2(z')}{L_2^2} \tau^2 \right. \\
& \qquad \left. \left. -2\tau \cos(\theta) \frac{V(z')}{L_2} \left[\left(\frac{\gamma}{L_2} + 1 + \frac{z'}{z_s} \left(\frac{\Delta x}{L_2} - 1 \right) \right)^2 + u'^2 \left(1 - \frac{z'}{z_s} \right)^2 \right]^{\frac{1}{2}} \right\}^{\frac{5}{6}} \right\}
\end{aligned}
\tag{4.57}
$$

and

$$
\begin{aligned}
ww_3'(z') = & \\
& \int_{-\left(\frac{R+1}{2}\right) + \frac{\Delta y}{L_2}}^{\frac{R-1}{2} + \frac{\Delta y}{L_2}} \mathrm{d}u' \left(u' + \frac{1+R}{2} - \frac{\Delta y}{L_2} \right) fw_3(u') + R \int_{\frac{R-1}{2} + \frac{\Delta y}{L_2}}^{\frac{1-R}{2} + \frac{\Delta y}{L_2}} \mathrm{d}u' \, fw_3(u') \\
& \qquad + \int_{\frac{1-R}{2} + \frac{\Delta y}{L_2}}^{\frac{R+1}{2} + \frac{\Delta y}{L_2}} \left(\frac{R+1}{2} - u' + \frac{\Delta y}{L_2} \right) fw_3(u')
\end{aligned}
\tag{4.58}
$$

where $fw_3(u')$ is defined in equation 4.54. The weighting functions $w_1'(z')$, $w_2'(z')$, $w_3'(z')$ and $w_B'(z')$ are defined as they were in section 4.2.2. Also,

$$
w_A' = \int_{-1}^{1} \mathrm{d}u' \,\mathrm{tri}(u') \left\{ \left\{ \left[u' \left(1 - \frac{z'}{z_s} \right) \right]^2 \right\}^{\frac{5}{6}} - \left\{ \left[1 - \frac{z'}{z_s} \right]^2 + \left[u' \left(1 - \frac{z'}{z_s} \right) \right]^2 \right\}^{\frac{5}{6}} \right\} \tag{4.59}
$$

As always, $\gamma = \Delta p_x \frac{z'}{z_s} - \Delta x$. The only expression remaining to be evaluated in equation 4.52 is the time-lagged correlation.

4.4.4 Expression for Time-lagged Term Before the SNR can be evaluated, an expression is necessary for the time-lagged correlation contained in equation 4.52. The expression is

$$
\begin{aligned}
&\langle C_s(\tau)C_s(0)\rangle = \\
&\quad 23.91R^{-\frac{2}{3}}\int_0^{z_s} \mathrm{d}z'\, C_n^2(z')ww_1'(z')\int_0^{z_s} \mathrm{d}z''C_n^2(z'')w_1'(z'') \\
&\quad +23.91R^{-\frac{1}{3}}\int_0^{z_s} \mathrm{d}z'\, C_n^2(z')ww_1'(z')\int_0^{z_s} \mathrm{d}z''\, C_n^2(z'')w_2'(z'') \\
&\quad +23.91R^{-\frac{1}{3}}\int_0^{z_s} \mathrm{d}z'\, C_n^2(z')ww_2'(z')\int_0^{z_s} \mathrm{d}z''C_n^2(z'')w_1'(z'') \\
&\quad +23.91\int_0^{z_s} \mathrm{d}z'\, C_n^2(z')ww_2'(z')\int_0^{z_s} \mathrm{d}z''\, C_n^2(z'')w_2'(z'') \\
&\quad +95.68R^{-4}\int_0^{z_s} \mathrm{d}z'\, C_n^2(z')ww_3'(z')\int_0^{z_s} \mathrm{d}z''\, C_n^2(z'')w_3'(z'') \\
&\quad -47.87R^{-\frac{7}{3}}\int_0^{z_s} \mathrm{d}z'\, C_n^2(z')ww_1'(z')\int_0^{z_s} \mathrm{d}z''\, C_n^2(z'')w_3'(z'') \\
&\quad -47.87R^{-2}\int_0^{z_s} \mathrm{d}z'\, C_n^2(z')ww_2'(z')\int_0^{z_s} \mathrm{d}z''\, C_n^2(z'')w_3'(z'') \\
&\quad -47.87R^{-\frac{7}{3}}\int_0^{z_s} \mathrm{d}z'\, C_n^2(z')ww_3'(z')\int_0^{z_s} \mathrm{d}z''C_n^2(z'')w_1'(z'') \\
&\quad -47.87R^{-2}\int_0^{z_s} \mathrm{d}z'\, C_n^2(z')ww_3'(z')\int_0^{z_s} \mathrm{d}z''\, C_n^2(z'')w_2'(z'') \\
&\quad +47.87R^{-\frac{2}{3}}\int_0^{z_s} \mathrm{d}z'\, C_n^2(z')w_m'(z')\int_0^{z_s} \mathrm{d}z''\, C_n^2(z'')w_A'(z'') \\
&\quad +47.87R^{-\frac{1}{3}}\int_0^{z_s} \mathrm{d}z'\, C_n^2(z')w_m'(z')\int_0^{z_s} \mathrm{d}z''\, C_n^2(z'')w_A'(z'') \\
&\quad +191.43R^{-4}\int_0^{z_s} \mathrm{d}z'\, C_n^2(z')w_P'(z')\int_0^{z_s} \mathrm{d}z''\, C_n^2(z'')w_B'(z'') \\
&\quad +47.87\int_0^{z_s} \mathrm{d}z'\, C_n^2(z')w_A'(z')\int_0^{z_s} \mathrm{d}z''\, C_n^2(z'')w_n'(z'') \\
&\quad +47.87R^{-\frac{1}{3}}\int_0^{z_s} \mathrm{d}z'\, C_n^2(z')w_A'(z')\int_0^{z_s} \mathrm{d}z''\, C_n^2(z'')w_n'(z'') \\
&\quad -95.68R^{-\frac{7}{3}}\int_0^{z_s} \mathrm{d}z'\, C_n^2(z')w_B'(z')\int_0^{z_s} \mathrm{d}z''\, C_n^2(z'')w_m'(z'') \\
&\quad -95.68R^{-2}\int_0^{z_s} \mathrm{d}z'\, C_n^2(z')w_B'(z')\int_0^{z_s} \mathrm{d}z''\, C_n^2(z'')w_n'(z'') \\
&\quad -95.68R^{-\frac{7}{3}}\int_0^{z_s} \mathrm{d}z'\, C_n^2(z')w_A'(z')\int_0^{z_s} \mathrm{d}z''\, C_n^2(z'')w_P'(z'') \\
&\quad -95.68R^{-2}\int_0^{z_s} \mathrm{d}z'\, C_n^2(z')w_A'(z')\int_0^{z_s} \mathrm{d}z''\, C_n^2(z'')w_P'(z'')
\end{aligned}
\tag{4.60}
$$

where $w_1'(z')$, $w_2'(z')$, $w_3'(z')$, $ww_1'(z')$, $ww_2'(z')$, $ww_3'(z')$, $w_A'(z')$ and $w_B'(z')$ have all been defined previously. The other weighting functions present in equation 4.60 are defined as

$$w_m'(z') = \int_{-1}^{1} \mathrm{d}u' \, \mathrm{tri}(u') \times \left\{ \left\{ \left[u' \left(1 - \frac{z'}{z_s} \right) \right]^2 + \frac{V^2(z')}{R^2 L_2^2} \tau^2 - 2\tau \cos(\theta) \frac{V(z')}{RL_2} u' \left(1 - \frac{z'}{z_s} \right) \right\}^{\frac{5}{6}} - \left\{ \left(1 - \frac{z'}{z_s} \right)^2 + \left[u' \left(1 - \frac{z'}{z_s} \right) \right]^2 + \frac{V^2(z')}{R^2 L_2^2} \tau^2 - 2\tau \cos(\theta) \frac{V(z')}{RL_2} \left\{ \left(1 - \frac{z'}{z_s} \right)^2 + \left[u' \left(1 - \frac{z'}{z_s} \right) \right]^2 \right\}^{\frac{1}{2}} \right\}^{\frac{5}{6}} \right\} \tag{4.61}$$

and

$$w_n'(z') = \int_{-1}^{1} \mathrm{d}u' \, \mathrm{tri}(u') \times \left\{ \left\{ \left[u' \left(1 - \frac{z'}{z_s} \right) \right]^2 + \frac{V^2(z')}{L_2^2} \tau^2 - 2\tau \cos(\theta) \frac{V(z')}{L_2} u' \left(1 - \frac{z'}{z_s} \right) \right\}^{\frac{5}{6}} - \left\{ \left(1 - \frac{z'}{z_s} \right)^2 + \left[u' \left(1 - \frac{z'}{z_s} \right) \right]^2 + \frac{V^2(z')}{L_2^2} \tau^2 - 2\tau \cos(\theta) \frac{V(z')}{L_2} \left\{ \left(1 - \frac{z'}{z_s} \right)^2 + \left[u' \left(1 - \frac{z'}{z_s} \right) \right]^2 \right\}^{\frac{1}{2}} \right\}^{\frac{5}{6}} \right\} \tag{4.62}$$

and

$$w_p'(z') = \int_{-\left(\frac{R+1}{2}\right)+\frac{\Delta y}{L_2}}^{\frac{R-1}{2}+\frac{\Delta y}{L_2}} \mathrm{d}u' \left(u' + \frac{1+R}{2} - \frac{\Delta y}{L_2} \right) f w_p'(u') + R \int_{\frac{R-1}{2}+\frac{\Delta y}{L_2}}^{\frac{1-R}{2}+\frac{\Delta y}{L_2}} \mathrm{d}u' \, f w_p'(u') + \int_{\frac{1-R}{2}+\frac{\Delta y}{L_2}}^{\frac{R+1}{2}+\frac{\Delta y}{L_2}} \left(\frac{R+1}{2} - u' + \frac{\Delta y}{L_2} \right) f w_p'(u') \tag{4.63}$$

where

$$
\begin{aligned}
& fw_p'(u') = \\
& \quad \left\{ \left[\left(1 - \frac{z'}{z_s}\right) \frac{1-R}{2} \right]^2 + \left[u' \left(1 - \frac{z'}{z_s}\right) \right]^2 + \frac{V^2(z')}{L_2^2} \tau^2 \right. \\
& \qquad \left. -2 \frac{V(z')}{L_2} \tau \cos(\theta) \left\{ \left[\left(1 - \frac{z'}{z_s}\right) \frac{1-R}{2} \right]^2 + \left[u' \left(1 - \frac{z'}{z_s}\right) \right]^2 \right\}^{\frac{1}{2}} \right\}^{\frac{5}{6}} \\
& \quad \left\{ \left[\left(1 - \frac{z'}{z_s}\right) \frac{1+R}{2} \right]^2 + \left[u' \left(1 - \frac{z'}{z_s}\right) \right]^2 + \frac{V^2(z')}{L_2^2} \tau^2 \right. \\
& \qquad \left. -2 \frac{V(z')}{L_2} \tau \cos(\theta) \left\{ \left[\left(1 - \frac{z'}{z_s}\right) \frac{1+R}{2} \right]^2 + \left[u' \left(1 - \frac{z'}{z_s}\right) \right]^2 \right\}^{\frac{1}{2}} \right\}^{\frac{5}{6}}
\end{aligned}
\tag{4.64}
$$

Coefficients common to equations 4.53, 4.55, and 4.60 are not shown because the common coefficients will cancel when these equations are placed in the signal-to-noise ratio expression given by equation 4.52. It is now possible to calculate SNR values using equations 4.53, 4.55, and 4.60. Before doing so, however, these equations are simplified by assuming $1 - \frac{z'}{z_s} \approx 1$.

4.4.5 Simplification of SNR Terms Before presenting SNR results, the terms which comprise the SNR expression are simplified by assuming $1 - \frac{z'}{z_s} \approx 1$. As mentioned in Chapter 3, such an approximation is often valid and reduces the complexity of the calculations which must be performed to obtain estimates of C_n^2 and $\vec{V}$. The resulting simplified expression for the mean value as a function of τ is

$$
\langle C_s(\tau) \rangle = -3.46 \int_0^{z_s} \mathrm{d}z' \, C_n^2(z') \left[R^{-\frac{1}{3}} w w_1''(z') + w w_2''(z') - 2 w w_3''(z') \right] \tag{4.65}
$$

The simplified form of the sum of the mean square value terms is

$$
\begin{aligned}
& \langle C_s^2(0) \rangle + \langle C_s^2(\tau) \rangle = \\
& \quad 23.91 R^{-\frac{2}{3}} \left[\int_0^{z_s} \mathrm{d}z' \, C_n^2(z') w w_1''(z') \right]^2 + 23.91 \left[\int_0^{z_s} \mathrm{d}z' \, C_n^2(z') w w_2''(z') \right]^2 \\
& \quad + 95.68 R^{-4} \left[\int_0^{z_s} \mathrm{d}z' \, C_n^2(z') w w_3''(z') \right]^2
\end{aligned}
$$

$$
\begin{aligned}
&+47.87R^{-\frac{1}{3}}\int_0^{z_s} \mathrm{d}z'\, C_n^2(z')ww_1''(z')\int_0^{z_s} \mathrm{d}z''\, C_n^2(z'')ww_2''(z'')\\
&+23.91R^{-\frac{2}{3}}\left[\int_0^{z_s} \mathrm{d}z'\, C_n^2(z')w_1''(z')\right]^2+23.91\left[\int_0^{z_s} \mathrm{d}z'\, C_n^2(z')w_2''(z')\right]^2\\
&+95.68A^2(1+R^{-\frac{2}{3}}+2R^{-\frac{1}{3}})\left[\int_0^{z_s} C_n^2(z')\,\mathrm{d}z'\right]^2\\
&+382.86R^{-4}B^2\left[\int_0^{z_s} \mathrm{d}z'\, C_n^2(z')\right]^2+95.68R^{-4}\left[\int_0^{z_s} \mathrm{d}z'\, C_n^2(z')w_3''(z')\right]^2\\
&+47.87R^{-\frac{1}{3}}\int_0^{z_s} \mathrm{d}z'\, C_n^2(z')w_1''(z')\int_0^{z_s} \mathrm{d}z''\, C_n^2(z'')w_2''(z'')\\
&-95.68R^{-\frac{7}{3}}\int_0^{z_s} \mathrm{d}z'\, C_n^2(z')ww_1''(z')\int_0^{z_s} \mathrm{d}z''\, C_n^2(z'')ww_3''(z'')\\
&-95.68R^{-2}\int_0^{z_s} \mathrm{d}z'\, C_n^2(z')ww_2''(z')\int_0^{z_s} \mathrm{d}z''\, C_n^2(z'')ww_3''(z'')\\
&-95.68R^{-\frac{7}{3}}\int_0^{z_s} \mathrm{d}z'\, C_n^2(z')w_1''(z')\int_0^{z_s} \mathrm{d}z''\, C_n^2(z'')w_3''(z'')\\
&-95.68R^{-2}\int_0^{z_s} \mathrm{d}z'\, C_n^2(z')w_2''(z')\int_0^{z_s} \mathrm{d}z''\, C_n^2(z'')w_3(z'')\\
&-382.86AB(R^{-2}+R^{-\frac{7}{3}})\left[\int_0^{z_s} C_n^2(z')\,\mathrm{d}z'\right]^2\\
&-27.68(0.86\pi\eta)^2\left(\frac{N}{\left(\frac{L_2}{r_0}\right)^{\frac{1}{3}}}\right)^{-1}A(1-2R^2+R^{-\frac{1}{3}}+R^{-\frac{7}{3}}+R^{-2}-2R^{\frac{5}{3}})\int C_n^2(z')\,\mathrm{d}z'\\
&-55.36(0.86\pi\eta)^2\left(\frac{N}{\left(\frac{L_2}{r_0}\right)^{\frac{1}{3}}}\right)^{-1}R^{-2}(2R^2-R^{-1}-1)B\int C_n^2(z')\,\mathrm{d}z'\\
&+2\left[(0.86\pi\eta)^2\left(\frac{N}{\left(\frac{L_2}{r_0}\right)^{\frac{1}{3}}}\right)^{-1}\int C_n^2(z')\,\mathrm{d}z'\right]^2(4R^4-4R^2-4R+2R^{-1}+R^{-2}+1)
\end{aligned}
\tag{4.66}
$$

The simplified form of the time-lagged correlation is

$$
\begin{aligned}
&\langle C_s(\tau)C_s(0)\rangle =\\
&\quad 23.91R^{-\frac{2}{3}}\int_0^{z_s} \mathrm{d}z'\, C_n^2(z')ww_1''(z')\int_0^{z_s} \mathrm{d}z''C_n^2(z'')w_1''(z'')\\
&\quad +23.91R^{-\frac{1}{3}}\int_0^{z_s} \mathrm{d}z'\, C_n^2(z')ww_1''(z')\int_0^{z_s} \mathrm{d}z''\, C_n^2(z'')w_2''(z'')\\
&\quad +23.91R^{-\frac{1}{3}}\int_0^{z_s} \mathrm{d}z'\, C_n^2(z')ww_2''(z')\int_0^{z_s} \mathrm{d}z''C_n^2(z'')w_1''(z'')
\end{aligned}
$$

$$
\begin{aligned}
&+23.91 \int_0^{z_s} \mathrm{d}z'\, C_n^2(z') w w_2''(z') \int_0^{z_s} \mathrm{d}z''\, C_n^2(z'') w_2''(z'') \\
&+95.68 R^{-4} \int_0^{z_s} \mathrm{d}z'\, C_n^2(z') w w_3''(z') \int_0^{z_s} \mathrm{d}z''\, C_n^2(z'') w_3''(z'') \\
&-47.87 R^{-\frac{7}{3}} \int_0^{z_s} \mathrm{d}z'\, C_n^2(z') w w_1''(z') \int_0^{z_s} \mathrm{d}z''\, C_n^2(z'') w_3''(z'') \\
&-47.87 R^{-2} \int_0^{z_s} \mathrm{d}z'\, C_n^2(z') w w_2''(z') \int_0^{z_s} \mathrm{d}z''\, C_n^2(z'') w_3''(z'') \\
&-47.87 R^{-\frac{7}{3}} \int_0^{z_s} \mathrm{d}z'\, C_n^2(z') w w_3''(z') \int_0^{z_s} \mathrm{d}z''\, C_n^2(z'') w_1''(z'') \\
&-47.87 R^{-2} \int_0^{z_s} \mathrm{d}z'\, C_n^2(z') w w_3''(z') \int_0^{z_s} \mathrm{d}z''\, C_n^2(z'') w_2''(z'') \\
&+47.87 AM(R^{-\frac{2}{3}} + R^{-\frac{1}{3}}) \left[\int_0^{z_s} \mathrm{d}z'\, C_n^2(z') \right]^2 \\
&+191.43 R^{-4} BP \left[\int_0^{z_s} \mathrm{d}z'\, C_n^2(z') \right]^2 \\
&+47.87\, A\, N(1 + R^{-\frac{1}{3}}) \left[\int_0^{z_s} \mathrm{d}z'\, C_n^2(z') \right]^2 \\
&-95.68\, B(R^{-\frac{7}{3}} M + R^2 N) \left[\int_0^{z_s} \mathrm{d}z'\, C_n^2(z') \right]^2 \\
&-95.68\, A\, P(R^{-\frac{7}{3}} + R^{-2}) \left[\int_0^{z_s} \mathrm{d}z'\, C_n^2(z') \right]^2
\end{aligned}
\tag{4.67}
$$

where $w_1''(z')$, $w_2''(z')$, and $w_3''(z')$ are defined in equations 4.43, 4.44, and 4.45. The constants A and B are defined in equations 4.47 and 4.48. The other weighting functions present in equations 4.65, 4.66, and 4.67 are defined as

$$
\begin{aligned}
w w_1''(z') = &\int \mathrm{d}u'\, \mathrm{tri}\left(u' - \frac{\Delta y}{RL_2}\right) \\
&\times \left\{ 2 \left\{ \left(\frac{\gamma}{RL_2}\right)^2 + u'^2 + \frac{V^2(z')}{R^2 L_2^2}\tau^2 - 2\tau \cos(\theta) \frac{V(z')}{RL_2} \left[\left(\frac{\gamma}{RL_2}\right)^2 + u'^2 \right]^{\frac{1}{2}} \right\}^{\frac{5}{6}} \right. \\
&- \left\{ \left(\frac{\gamma}{RL_2} - 1\right)^2 + u'^2 + \frac{V^2(z')}{R^2 L_2^2}\tau^2 - 2\tau \cos(\theta) \frac{V(z')}{RL_2} \left[\left(\frac{\gamma}{RL_2} - 1\right)^2 + u'^2 \right]^{\frac{1}{2}} \right\}^{\frac{5}{6}} \\
&\left. - \left\{ \left(\frac{\gamma}{RL_2} + 1\right)^2 + u'^2 + \frac{V^2(z')}{R^2 L_2^2}\tau^2 - 2\tau \cos(\theta) \frac{V(z')}{RL_2} \left[\left(\frac{\gamma}{RL_2} + 1\right)^2 + u'^2 \right]^{\frac{1}{2}} \right\}^{\frac{5}{6}} \right\}
\end{aligned}
\tag{4.68}
$$

and

$$ww_2''(z') = \int \mathrm{d}u' \,\mathrm{tri}\left(u' - \frac{\Delta y}{L_2}\right)$$
$$\times \left\{ 2\left\{ \left(\frac{\gamma}{L_2}\right)^2 + u'^2 + \frac{V^2(z')}{L_2^2}\tau^2 - 2\tau\cos(\theta)\frac{V(z')}{L_2}\left[\left(\frac{\gamma}{L_2}\right)^2 + u'^2\right]^{\frac{1}{2}} \right\}^{\frac{5}{6}} \right.$$
$$- \left\{ \left(\frac{\gamma}{L_2} - 1\right)^2 + u'^2 + \frac{V^2(z')}{L_2^2}\tau^2 - 2\tau\cos(\theta)\frac{V(z')}{L_2}\left[\left(\frac{\gamma}{L_2} - 1\right)^2 + u'^2\right]^{\frac{1}{2}} \right\}^{\frac{5}{6}}$$
$$\left. - \left\{ \left(\frac{\gamma}{L_2} + 1\right)^2 + u'^2 + \frac{V^2(z')}{L_2^2}\tau^2 - 2\tau\cos(\theta)\frac{V(z')}{L_2}\left[\left(\frac{\gamma}{L_2} + 1\right)^2 + u'^2\right]^{\frac{1}{2}} \right\}^{\frac{5}{6}} \right\} \tag{4.69}$$

and

$$ww_3''(z') =$$
$$\int_{-\left(\frac{R+1}{2}\right)+\frac{\Delta y}{L_2}}^{\frac{R-1}{2}+\frac{\Delta y}{L_2}} \mathrm{d}u' \left(u' + \frac{1+R}{2} - \frac{\Delta y}{L_2}\right) fw_3'(u') + R\int_{\frac{R-1}{2}+\frac{\Delta y}{L_2}}^{\frac{1-R}{2}+\frac{\Delta y}{L_2}} \mathrm{d}u'\, fw_3'(u')$$
$$+ \int_{\frac{1-R}{2}+\frac{\Delta y}{L_2}}^{\frac{R+1}{2}+\frac{\Delta y}{L_2}} \left(\frac{R+1}{2} - u' + \frac{\Delta y}{L_2}\right) fw_3'(u') \tag{4.70}$$

where

$$fw_3'(u') =$$
$$\left\{ \left[\frac{\gamma}{L_2} + \frac{1-R}{2}\right]^2 + u'^2 + \frac{V^2(z')}{L_2^2}\tau^2 - 2\frac{V(z')}{L_2}\tau\cos(\theta)\left\{\left[\frac{\gamma}{L_2} + \frac{1-R}{2}\right]^2 + u'^2\right\}^{\frac{1}{2}} \right\}^{\frac{5}{6}}$$
$$- \left\{ \left[\frac{\gamma}{L_2} - \frac{R+1}{2}\right]^2 + u'^2 + \frac{V^2(z')}{L_2^2}\tau^2 - 2\frac{V(z')}{L_2}\tau\cos(\theta)\left\{\left[\frac{\gamma}{L_2} - \frac{R+1}{2}\right]^2 + u'^2\right\}^{\frac{1}{2}} \right\}^{\frac{5}{6}}$$
$$- \left\{ \left[\frac{\gamma}{L_2} + \frac{R+1}{2}\right]^2 + u'^2 + \frac{V^2(z')}{L_2^2}\tau^2 - 2\frac{V(z')}{L_2}\tau\cos(\theta)\left\{\left[\frac{\gamma}{L_2} + \frac{R+1}{2}\right]^2 + u'^2\right\}^{\frac{1}{2}} \right\}^{\frac{5}{6}}$$
$$\left\{ \left[\frac{\gamma}{L_2} + \frac{R-1}{2}\right]^2 + u'^2 + \frac{V^2(z')}{L_2^2}\tau^2 - 2\frac{V(z')}{L_2}\tau\cos(\theta)\left\{\left[\frac{\gamma}{L_2} + \frac{R-1}{2}\right]^2 + u'^2\right\}^{\frac{1}{2}} \right\}^{\frac{5}{6}} \tag{4.71}$$

Finally, the constants M, N, and P are given by

$$M = \int_{-1}^{1} \mathrm{d}u' \, \mathrm{tri}(u') \left\{ \left\{ u'^2 + \frac{V^2(z')}{R^2 L_2^2}\tau^2 - 2\tau \cos(\theta)\frac{V(z')}{RL_2}u' \right\}^{\frac{5}{6}} - \left\{ 1 + u'^2 + \frac{V^2(z')}{R^2 L_2^2}\tau^2 - 2\tau \cos(\theta)\frac{V(z')}{RL_2}\left\{1 + u'^2\right\}^{\frac{1}{2}} \right\}^{\frac{5}{6}} \right\} \tag{4.72}$$

and

$$N = \int_{-1}^{1} \mathrm{d}u' \, \mathrm{tri}(u') \left\{ \left\{ u'^2 + \frac{V^2(z')}{L_2^2}\tau^2 - 2\tau \cos(\theta)\frac{V(z')}{L_2}u' \right\}^{\frac{5}{6}} - \left\{ 1 + u'^2 + \frac{V^2(z')}{L_2^2}\tau^2 - 2\tau \cos(\theta)\frac{V(z')}{L_2}\left\{1 + u'^2\right\}^{\frac{1}{2}} \right\}^{\frac{5}{6}} \right\} \tag{4.73}$$

and

$$P = \int_{-\left(\frac{R+1}{2}\right)+\frac{\Delta y}{L_2}}^{\frac{R-1}{2}+\frac{\Delta y}{L_2}} \mathrm{d}u' \left(u' + \frac{1+R}{2} - \frac{\Delta y}{L_2} \right) fw_p''(u') + R \int_{\frac{R-1}{2}+\frac{\Delta y}{L_2}}^{\frac{1-R}{2}+\frac{\Delta y}{L_2}} \mathrm{d}u' \, fw_p''(u') + \int_{\frac{1-R}{2}+\frac{\Delta y}{L_2}}^{\frac{R+1}{2}+\frac{\Delta y}{L_2}} \left(\frac{R+1}{2} - u' + \frac{\Delta y}{L_2} \right) fw_p''(u') \tag{4.74}$$

where

$$fw_p''(u') = \left\{ \left(\frac{1-R}{2}\right)^2 + u'^2 + \frac{V^2(z')}{L_2^2}\tau^2 - 2\frac{V(z')}{L_2}\tau \cos(\theta) \left[\left(\frac{1-R}{2}\right)^2 + u'^2 \right]^{\frac{1}{2}} \right\}^{\frac{5}{6}} - \left\{ \left(\frac{1+R}{2}\right)^2 + u'^2 + \frac{V^2(z')}{L_2^2}\tau^2 - 2\frac{V(z')}{L_2}\tau \cos(\theta) \left[\left(\frac{1+R}{2}\right)^2 + u'^2 \right]^{\frac{1}{2}} \right\}^{\frac{5}{6}} \tag{4.75}$$

Reiterating, θ is the angle between $\vec{V}$ and $\Delta\vec{p}_{z_s}^{z'} + \vec{x} - \vec{x}''$.

4.5 $\langle C_s'(0) \rangle$ *Signal-to-Noise Ratio Results*

The previous section has presented the expressions needed to evaluate the SNR of the wind sensing technique proposed in this thesis. In order to evaluate the SNR, values had to be selected for several parameters. The Bufton wind profile presented in Chapter 2 was used for $\vec{V}(z')$, and the Hufnagel-Valley turbulence model was used for $C_n^2(z')$. The assumed measurement geometry was the same as when evaluating the C_s SNR. The guide stars were placed at $z_s = 100$ km and the $\vec{V}$ vertical profile was only measured to $z' = 15$ km. This allowed use of the approximation $1 - \frac{z'}{z_s} \approx 1$. The guide star separation was $\Delta p_x = 1$ km and the aperture separation was allowed to vary in order to control the intersection altitude. The limit as $\tau \rightarrow 0$ of equation 4.52 was then evaluated numerically.

4.5.1 $\langle C_s'(0) \rangle$ *SNR Without Measurement Error* Figures 4.5 and 4.6 show the calculated signal-to-noise ratios when no slope measurement noise is present. Like the SNR

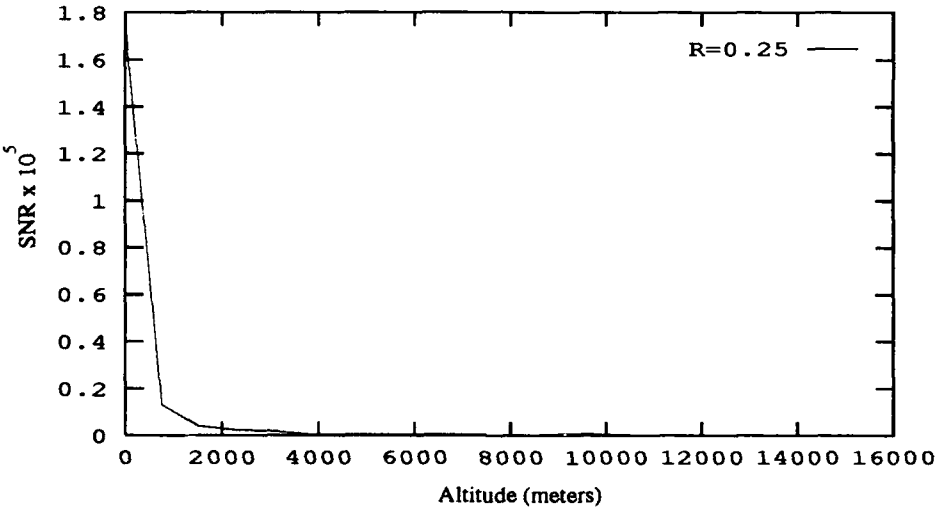

Figure 4.5. $\langle C_s'(0) \rangle$ SNR Without Measurement Noise, $R = 0.25$

of the C_s estimates, the SNR of the $C_s'(0)$ estimates improves as R approaches one. The results in Figures 4.5 and 4.6 were computed using $\cos\theta = 1$.

4.5.2 Measurement Noise Effects on $\langle C_s'(0) \rangle$ *SNR* Figure 4.7 shows the the effect of changes in total photon count, N, on the SNR. The value selected for η was $\eta = 1.5$.

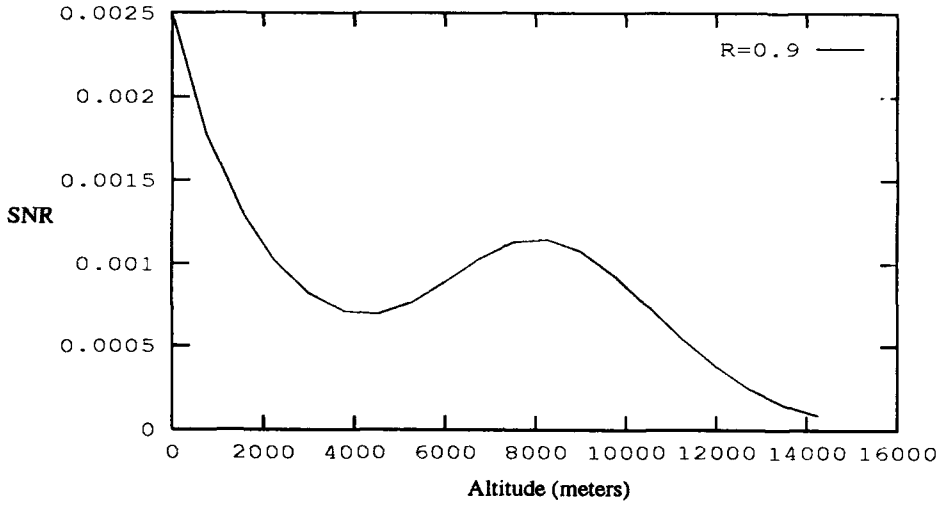

Figure 4.6. $\langle C_s'(0) \rangle$ SNR Without Measurement Noise, $R = 0.9$

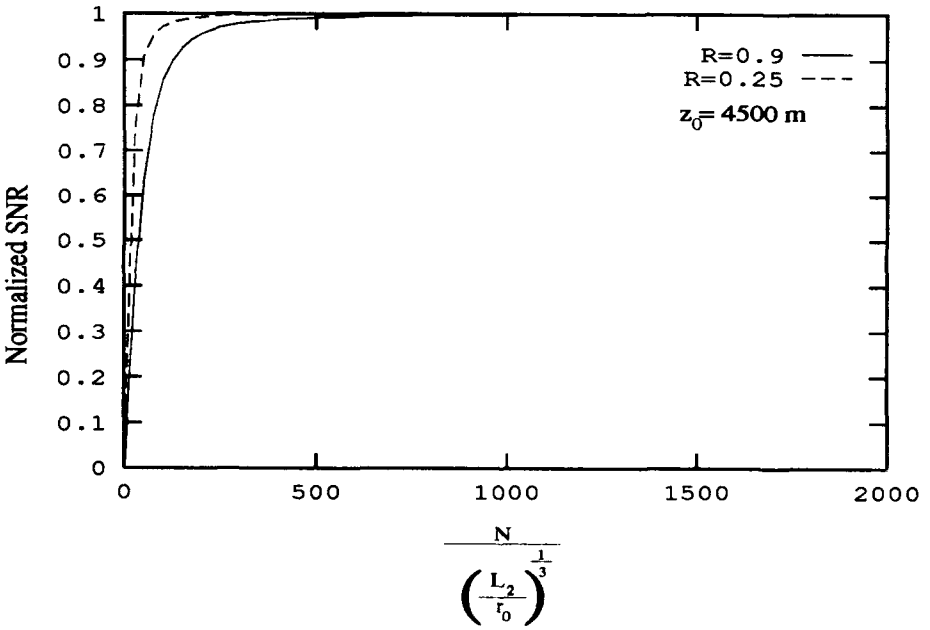

Figure 4.7. $\langle C_s'(0) \rangle$ SNR as a Function of Measurement Noise

The plot is normalized so that an SNR value of one is the normalized SNR value when no slope measurement error is present. These results indicate that as the ratio of $\frac{L_1}{L_2}$ becomes smaller, less photons are needed to achieve near noiseless performance. This trend is due to less correlation between the noise processes of the co-located apertures. Like Figure 4.4, Figure 4.7 presents the SNR as a function of noise for one particular altitude, but the shape of the curves would be the same for any altitude because the noise value is independent of altitude.

4.6 Improving SNR

The signal-to-noise ratio never exceeded one in any of the results presented thus far. However, these results were all for a single correlation measurement on one aperture. As mentioned before, slope sensors normally consist of multiple subapertures. Thus, it may be possible to make more than one measurement at a time. Also, several independent measurements could be taken on the same aperture over a period of time. Either method of increasing the number of independent estimates available will increase the SNR by decreasing the variance of the estimate.

4.7 Conclusion

This chapter presented the SNR expressions and results for the estimates of the measurement correlations used to derive C_n^2 and $\vec{V}$. These expressions are sufficiently general that any desired model for the vertical profiles of C_n^2 and $\vec{V}$ may be included. These SNR expressions provide important information for the determination of the number of independent measurements necessary to obtain accurate estimates of the quantities of interest. Additionally, the slope measurement noise was related to total photon count and the effects of photon count on the SNR quantified.

V. *Implementation Issues*

5.1 Introduction

The results shown in previous chapters have been obtained neglecting certain effects present in a practical implementation of the proposed measurement technique. As a result, the performance of a remote sensing system based upon the method examined in this thesis will likely be less than the theoretical performance presented in Chapters III and IV.

This chapter discusses the effects some of the implementation issues may have on system performance. The chapter begins with a presentation of weighting functions calculated for a representative measurement geometry. The weighting functions are calculated using the results of Chapter 3. There is then a discussion of some effects which will alter the shapes of the weighting functions and hence alter the performance of the system. Possible methods for dealing with these effects are also discussed.

5.2 Example Measurement Geometry

A practical measurement geometry is presented in Figure 5.1. In this example, the guide stars are placed at an altitude of $10 - 20$ km and are separated by $1 - 3$ m. In this case, the approximation $1 - \frac{z'}{z_s} \approx 1$ is not valid. The aperture in the sensor plane is assumed to be either a 1.5 m $\times$ 1.5 m aperture constructed of 16 subapertures, or a 3.5 m $\times$ 3.5 m aperture constructed of 32 subapertures. The subapertures are assumed to be square.

Figure 5.2 displays the C_n^2 path weighting function, $w_C(z')$, resulting from three different sensor separations. In this case $z_s = 10$ km, $\Delta p_x = 1$ m, and $L_1 = 18.8$ cm, where L_1 is found from $L_1 = 2\left(\frac{1.5\text{ m}}{16}\right)$. Figure 5.3 shows the y-directed wind weighting function $\vec{w}_V(z')$ for the same conditions. The figures clearly demonstrate that the resolution of the weighting functions decreases at lower altitudes. Recall from Section 3.5 that the resolution is inversely proportional to the angle at which the optical beams intersect. This angle decreases as the intersection altitude decreases. Increasing the altitude of the guide stars would help mitigate this effect.

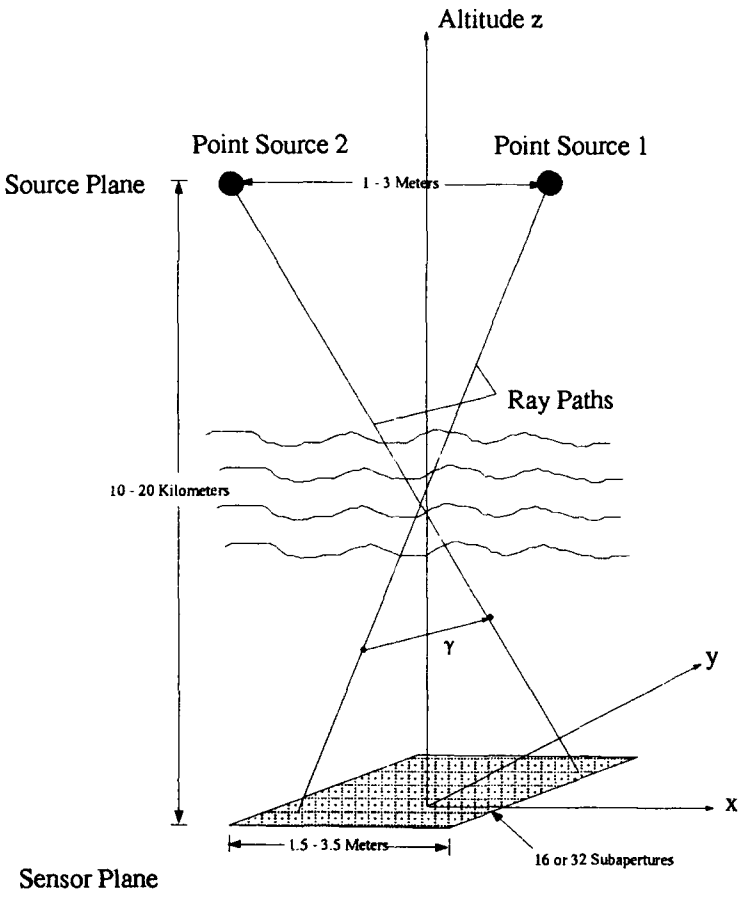

Figure 5.1. A Representative Measurement Geometry

Figures 5.4 and 5.5 present the weighting functions when $z_s = 20$ km, $\Delta p_x = 3$ m, and $L_1 = 2\left(\frac{3.5 \text{ m}}{32}\right) = 22$ cm. Once again the resolution of the weighting functions decreases with decreasing intersection altitude.

The weighting functions in Figures 5.2 through 5.5 were calculated assuming stationary guide star images in the image plane and deterministic guide star locations within the atmosphere. In a real implementation of this measurement technique, neither of these assumptions is true. Thus, the effects of image dance and beam wander must be discussed.

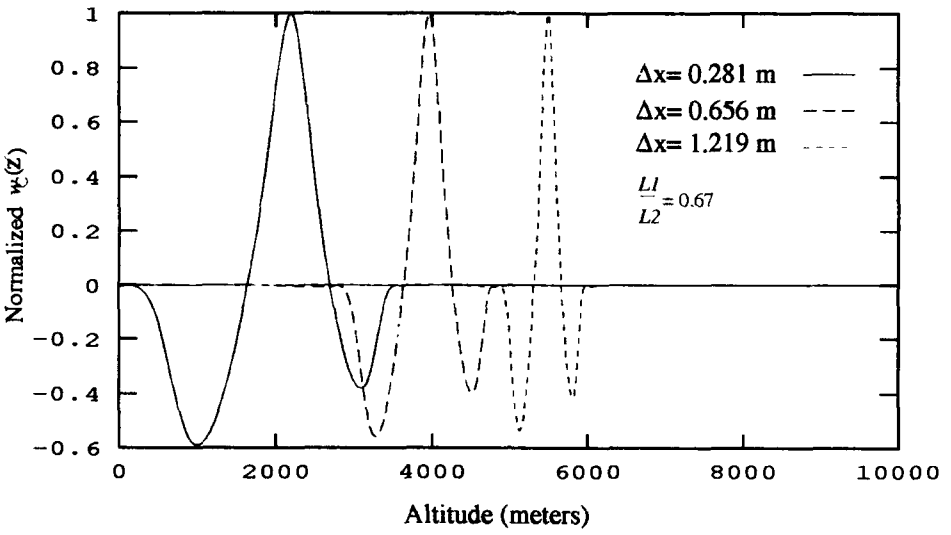

Figure 5.2. First Example of $w_C(z')$ for Three Values of Δx

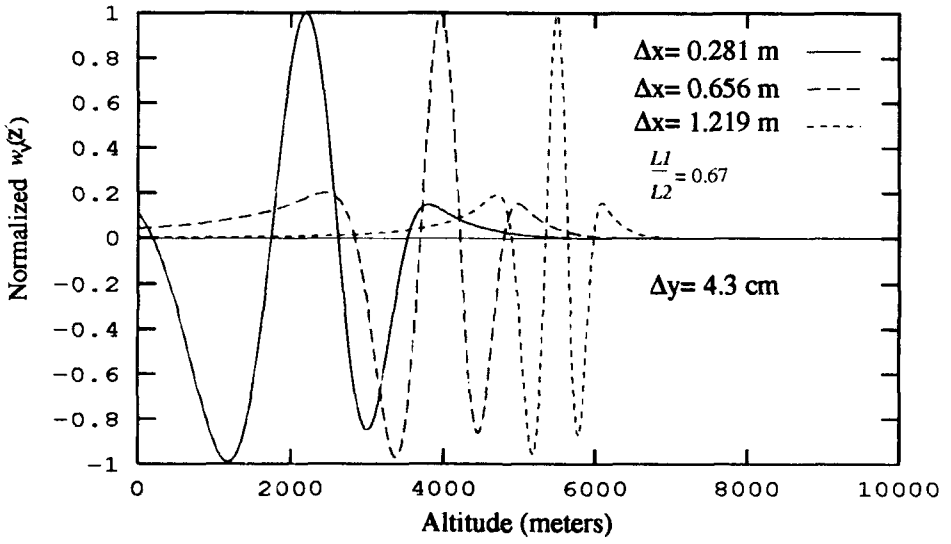

Figure 5.3. First Example of $\vec{w}_V(z') \cdot \hat{y}$ for Three Values of Δx

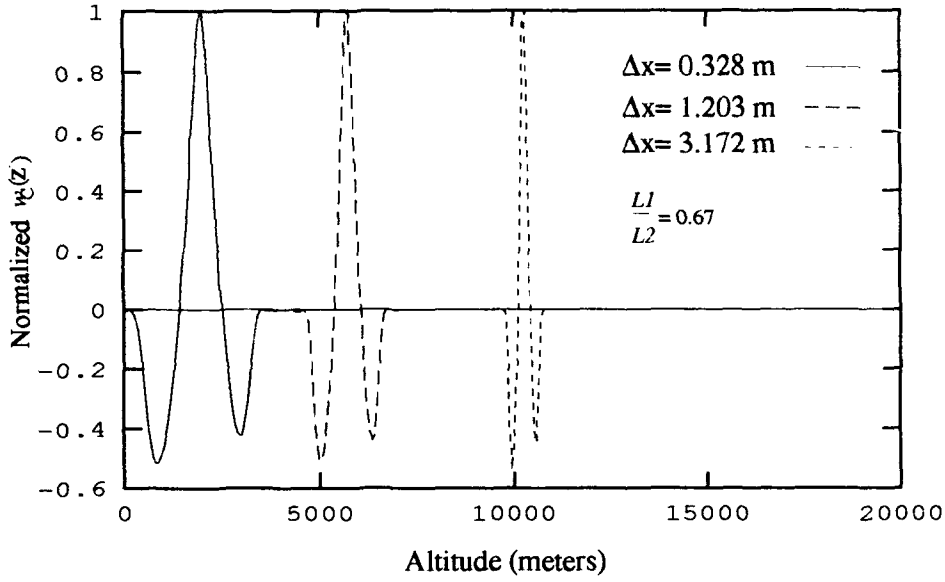

Figure 5.4. Second Example of $w_C(z')$ for Three Values of Δx

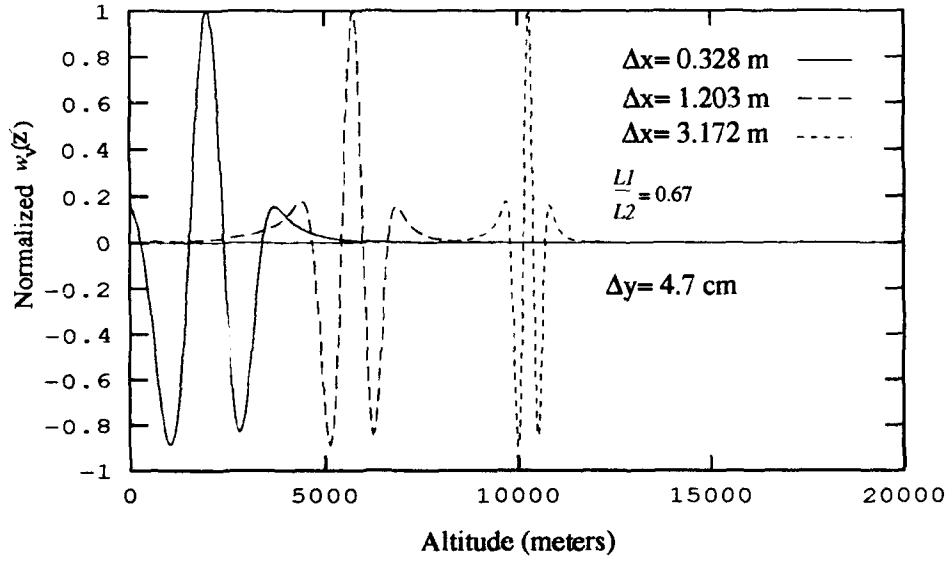

Figure 5.5. Second Example of $\vec{w}_V(z') \cdot \hat{y}$ for Three Values of Δx

5.3 *Tilt Correction*

The turbulence induces random changes in the overall wave front phase slope, or tilt, which causes the guide star images to move, or dance, about the image plane. Removing the low order distortions of the wave front phase yields a pseudo-stationary image in the image plane. In most measurement schemes incorporating artificial guide stars, this compensation is usually accomplished with a tip-tilt correction system. The system is composed of a wave front tilt sensor, a tip-tilt correction mirror, and a control algorithm.

The band pass filtering approach adopted in this thesis does not require such a system, however. The low order phase distortions are common to both co-located sensors and are removed when the larger sensor's output is subtracted from the smaller sensor's output. Thus the low frequency components of the phase distortions do not contribute to the measurement correlations.

5.4 *Beam Wander*

The artificial guide stars are generated by ground based lasers. As a laser beam propagates through the atmosphere, turbulent eddies which are large with respect to the beam's diameter, D, deflect the beam. This causes random movement of each guide star's location. Thus, the guide star separation, $\Delta\vec{p}$, becomes a random variable and therefore the crossing altitude of the beams also becomes a random variable.

If the uplinks are separated by a distance much greater than the beam diameter, then the movements of the guide stars are uncorrelated because the beams are affected by unrelated turbulent eddies. The movements may be correlated at some time lag due to motion of the turbulent eddies. The amount of correlation would depend upon the time lag and the vertical wind profile.

Fante (2) shows that the variance of the guide star position is dependent upon the ratio of $\frac{D}{\rho_0}$, where ρ_0 is called the spherical wave coherence length. Beland and Krause-Postorff (1) show that $\rho_0 = \frac{r_0}{2}$, where r_0 is defined in equation 4.33.

To examine the effect of beam wander on the example measurement geometry of Figure 5.1, let $r_0 = 10$ cm, which represents moderately good seeing conditions, and let

the laser beam have a diameter of 5 cm and wavelength of $\lambda = 0.5\mu$m. Assuming the guide stars are generated at $z_s = 10$ km and the crossing altitude is 5 km, application of Fante's equations gives the variance of each guidestar's movement as 0.5 cm, and the RMS value of the intersection altitude deviation is 22 m. A larger ratio of $\frac{D}{\rho_0}$ would yield a greater crossing altitude deviation. Obviously, this movement of the intersection altitude will reduce the vertical resolution by flattening and broadening the peaks of the weighting functions.

A method for reducing beam wander is to use an adaptive optics system to shape the wave front so the beam focuses to the same point in space at all times. Such an approach requires knowledge of the quantity being measured, therefore the variance of the intersection will only be reduced to some limiting value beyond which further reduction is not possible. The amount of reduction in the variance of the intersection altitude would depend upon the capabilities of the adaptive optics system employed.

5.5 Conclusion

This chapter presented an example measurement geometry and showed the resulting weighting functions as calculated from the expressions in chapter three. This chapter also discussed the effects of guide star motion upon the performance of a practical system implementing the proposed measurement technique. Methods which may mitigate these effects so that the performance approximates that shown in the example were suggested.

VI. Conclusions and Recommendations

6.1 Conclusions

This research has demonstrated that the spatial correlations of band pass filtered wave front slope measurements may be used to calculate the value of the atmospheric structure constant. The spatial correlations are related to C_n^2 through an integral expression containing C_n^2 and a path weighting function. An expression for the path weighting function was developed, and it was found that the shape of the path weighting function is determined by the measurement geometry and by the width of the filter pass band. As the pass band becomes more narrow, the path weighting function becomes more sharply peaked.

This research has also shown that the temporal correlations of band pass filtered wave front slope measurements may be used to obtain the transverse atmospheric wind velocity profile. Evaluation of the slope of the temporal correlation function at zero time lag yields an integral expression containing C_n^2, $\vec{V}$, and a wind path weighting function. An expression for the wind path weighting function was developed, and again it was found that the shape of the path weighting function is determined by the measurement geometry and by the width of the filter pass band, with the wind path weighting function becoming more sharply peaked as the filter pass band becomes more narrow. This method measures the wind in one direction only, therefore the measurement geometry must be properly aligned to obtain the wind speed in the direction of interest.

The measurement technique presented in this thesis has not been experimentally implemented. However, signal-to-noise ratio calculations for commonly accepted C_n^2 and $\vec{V}$ profile models indicate that multiple measurements will be necessary to obtain accurate estimates of the quantities being sensed. The number of measurements required will likely not be so great as to render this method impractical for measurement of $C_n^2(z)$. However, low signal-to-noise ratios for the estimate of the slope of the temporal correlation function at zero time lag indicates that this technique may not be practical for the remote sensing of transverse atmospheric wind profiles.

6.2 Recommendations

The following additional research is suggested.

1. Using accepted models for atmospheric turbulence and wind velocities, this measurement technique should be computer simulated. The spatial and temporal correlations of filtered wave front slope measurements should be calculated by the simulation, and the results used to determine C_n^2 and $\vec{V}$. The values of C_n^2 and $\vec{V}$ found in this manner should then be compared to known results to determine the accuracy of this method.

2. The shapes of the path weighting functions as modified due to laser propagation effects should be determined.

3. This optical remote sensing technique should be experimentally implemented and the results compared to those obtained from existing methods.

6.3 Summary

The spatial correlations of band pass filtered wave front slope measurements may be used to calculate the value of the atmospheric structure constant. Additionally, the temporal correlations of band pass filtered wave front slope measurements may be used to obtain the transverse atmospheric wind velocity profile. Experimental implementation and verification of this technique is necessary before its use in an adaptive optics system.

Bibliography

1. Beland, Robert R. and J. Krause-Polstorff. *Lidar Measurement of Optical Turbulence: Theory of Crossed Path Technique*. Technical Report PL-TR-91-2139, Phillips Laboratory, Directorate of Geophysics, Hanscom AFB, MA, July 1991.
2. Fante, R.L. "Electromagnetic Beam Propagation in a Turbulent Media," *Proceedings of the IEEE*, *63*:1669–1692 (December 1975).
3. Fried, David L. "Remote Sensing of the Optical Strength of Atmospheric Turbulence and Wind Velocity," *Proceedings of the IEEE*, *57*:415–420 (October 1969).
4. Fugate, Robert Q. et al. "Measurement of Atmospheric Wavefront Distortion Using Scattered Light from a Laser Guide-star," *Nature*, *353*:144–146 (September 1991).
5. Gaskill, Jack D. *Linear Systems, Fourier Transforms, and Optics*. New York: John Wiley and Sons, 1978.
6. Goodman, Joseph W. *Statistical Optics*. New York: John Wiley and Sons, 1985.
7. Halliday, David and Robert Resnick. *Physics*. New York: John Wiley and Sons, 1978.
8. Hardy, J.W. "Active Optics: A New Technology for the Control of Light," *Proceedings of the IEEE*, *66*:651–697 (June 1978).
9. Kolmogoroff, A. N. "The Local Structure of Turbulence in Incompressible Viscous Fluids for Very Large Reynolds Numbers." *Turbulence: Classic Papers on Statistical Theory* edited by Sheldon K. Friedlander and Leonard Topper, 151–155, New York: Interscience Publishers, 1961.
10. Lawrence, R. S., et al. "Use of Scintillations to Measure Average Wind Across a Light Beam," *Applied Optics*, *11*:239–243 (February 1972).
11. Lee, R.W. and J. C. Harp. "Weak scattering in random media, with applications to remote probing," *Proc. IEEE*, *57*:375–406 (1969).
12. Lutomirski, R.F. and R.G. Buser. "Mutual Coherence Function of a Finite Optical Beam and Application to Coherent Detection," *Applied Optics*, *12*:2159–2160 (September 1973).
13. Mahapatra, Pravas R. "Modern Aviation Weather Systems for Efficient Flight Management," *IEEE Position, Location, and Navigation Symposium*, 457–463 (1990).
14. Merkle, Fritz. "Adaptive Optics," *Physics World*, *66*:33–38 (January 1991).
15. National Bureau of Standards. *Handbook of Mathematical Functions with Formula, Graphs, and Mathematical Tables*. Washington: Government Printing Office, 1965.
16. Parenti, R.R. "Recent Advances in Adaptive Optics Methods and Technology," *SPIE Vol. 1000—Laser Wavefront Control*, 101–109 (1988).
17. Rejack, Michael D. *Sensing Refractive Turbulence Profiles Using Wave Front Slope Measurements from Two Reference Sources*. MS thesis, AFIT/GE/ENG/91D-46, School of Engineering, Air Force Institute of Technology (AU), Wright-Patterson AFB OH, December 1991. DTIC Number AD-A243696.

18. Tatarski, V.I. *Wave Propagation in a Turbulent Medium*. New York: McGraw-Hill Book Company, 1961. Translated from the Russian by R.A. Silverman.

19. Taylor, G.I. "Statistical Theory of Turbulence," *Proceedings of the Royal Society of London*, *151*:421–478 (1935).

20. Wallner, Edward P. "Optical Wave-Front Correction Using Slope Measurements," *Journal of the Optical Society of America*, *12*:1771–1776 (December 1983).

21. Wang, Ting-i., et al. "Wind and Refractive Turbulence Sensing Using Crossed Laser Beams," *Applied Optics*, *13*:2602–2608 (November 1974).

22. Welsh, B.M. "Sensing refractive–turbulence profiles using wave front phase measurements from multiple reference sources." Accepted for publication in *Applied Optics*, July 1992.

23. Welsh, Byron M. and Chester S. Gardner. "Performance Analysis of Adaptive-Optics Systems Using Laser Guide Stars and Slope Sensors," *Journal of the Optical Society of America*, *6*:1913–1923 (December 1989).

24. Whalen, Anthony D. *Detection of Signals in Noise*. New York: Academic Press, 1971.

25. Yura, H. T. "An Elementary Derivation of Phase Fluctuations of an Optical Wave in the Atmosphere," *SPIE Proceedings*, *75*:9–15 (January 1976).

Vita

Steven Carl Koeffler was born in Kearney, Nebraska on 21 October 1964. He graduated from Mountlake Terrace Senior High School in Mountlake Terrace, Washington in 1983. Captain Koeffler received a Bachelor of Science degree in Electrical Engineering, with honors, from Seattle University, Seattle, Washington in June 1987. Upon graduation, he was commissioned as a lieutenant in the United States Air Force Reserve. After being ordered to active duty in February 1988, he was assigned as an avionics engineer with the Advanced Cruise Missile test team, Strategic Air Command, Edwards Air Force Base, California. He entered the School of Engineering, Air Force Institute of Technology, in May 1991.

Permanent Address: 2414 204th St. SW # 9
Lynnwood, WA 98036

REPORT DOCUMENTATION PAGE

Form Approved
OMB No. 0704-0188

1. AGENCY USE ONLY (Leave blank)	2. REPORT DATE	3. REPORT TYPE AND DATES COVERED
	December 1992	Master's Thesis

4. TITLE AND SUBTITLE
REMOTE SENSING OF TURBULENCE AND TRANSVERSE ATMOSPHERIC WIND PROFILES USING OPTICAL REFERENCE SOURCES

5. FUNDING NUMBERS

6. AUTHOR(S)
Captain Steven C. Koeffler, USAF

7. PERFORMING ORGANIZATION NAME(S) AND ADDRESS(ES)
Air Force Institute of Technology, WPAFB OH 45433-6583

8. PERFORMING ORGANIZATION REPORT NUMBER
AFIT/GE/ENG/92D-22

9. SPONSORING / MONITORING AGENCY NAME(S) AND ADDRESS(ES)
Captain Mike Roggemann
PL/LIMI
Kirtland AFB, NM 87117

10. SPONSORING / MONITORING AGENCY REPORT NUMBER

11. SUPPLEMENTARY NOTES

12a. DISTRIBUTION / AVAILABILITY STATEMENT
Distribution Unlimited

12b. DISTRIBUTION CODE

13. ABSTRACT *(Maximum 200 words)*

This thesis examines a remote sensing technique for measuring the atmospheric structure constant and the transverse atmospheric wind velocity as a function of altitude by performing temporal and spatial correlations of band pass filtered wave front slope sensor measurements. Two point sources are used to illuminate two pairs of co-located wave front slope sensors. The sources and sensors are arranged to give rise to crossed optical paths. For each pair of wave front slope sensors, the output of the larger sensor is subtracted from the output of the smaller sensor. This band pass filters the smaller sensor's output. The filtered outputs are then correlated. The spatial correlation is related to the structure constant by an integral containing a path weighting function. The path weighting function is sharply peaked at the intersection altitude and decays rapidly to zero. The temporal correlation is related to the wind velocity through an integral containing a wind path weighting function which is sharply peaked at the intersection altitude and decays rapidly to zero. The vertical resolution of each path weighting function is calculated. Also, signal-to-noise ratios are calculated using generally accepted models for the structure constant and atmospheric wind profiles.

14. SUBJECT TERMS
Atmospheric Optics, Atmospheric Motion, Adaptive Optics, Phase Detectors, Correlation, Atmospheric Refraction

15. NUMBER OF PAGES
116

16. PRICE CODE

17. SECURITY CLASSIFICATION OF REPORT	18. SECURITY CLASSIFICATION OF THIS PAGE	19. SECURITY CLASSIFICATION OF ABSTRACT	20. LIMITATION OF ABSTRACT
UNCLASSIFIED	UNCLASSIFIED	UNCLASSIFIED	UL